Physico-chemical properties of South African shales and siltstones in the context of geological CO$_2$ storage

By

Ngqondi Songezo Nxokwana

Thesis submitted in

fulfilment of the requirements for the degree

of

Master of Science in Geology

in the

Department of Geology at the University of Pretoria

Supervised by

Prof. W. Altermann, Department of Geology, University of Pretoria

Co-supervised by

Dr L. Van Der Merwe, Department of Chemistry, University of Pretoria

Dr F.J. Doucet, Council for Geoscience

January 2020

DECLARATION OF ORIGINALITY

I, **Ngqondi Songezo Nxokwana** declare that the thesis/dissertation, which I hereby submit for the degree **Masters of Science (MSc)** at the University of Pretoria, is my own work and has not previously been submitted by me for a degree at this or any other tertiary institution.

1. I understand what plagiarism is and am aware of the University's policy in this regard.

2. I declare that this **thesis** (e.g. essay, report, project, assignment, dissertation, thesis, etc.) is my own original work. Where other people's work has been used (either from a printed source, internet or any other source), this has been properly acknowledged and referenced in accordance with departmental requirements.

3. I have not used work previously produced by another student or any other person to hand in as my own.

4. I have not allowed, and will not allow, anyone to copy my work with the intention of passing it off as his or her work.

Signature: _____

Date: _____

ABSTRACT

Shale is normally impermeable and has a low porosity; it was therefore not considered by the project on geological storage of CO_2 in South Africa (the "Atlas" project) as a potential storage reservoir. However, research in other parts of the world such as the United States of America (USA) on carbonaceous shales similar to those of the Central Karoo Basin of South Africa has proved that shales store significant amounts of CO_2 in an adsorbed state within their organic matter, also known as kerogen. The paucity of conventional storage reservoirs for the geo-sequestration of CO_2 in the interior of South Africa, where most sources of the anthropogenic CO_2 are situated, has prompted this study, which focuses on the carbonaceous shales and siltstones of the Karoo Basin of South Africa and their potential for CO_2 adsorption. Six samples from five old Soekor boreholes were selected for the study and their physico-chemical properties were studied through parameters such as petrography, mineralogy, elemental composition, bulk density, maturity (vitrinite reflectance), kerogen, total organic content (TOC), low pressure adsorption and high pressure adsorption.

In terms of TOC, which is one of the important parameters for gas adsorption onto shales, the studied carbonaceous shale samples compare quite favourably to those from other parts of the world that have been found to successfully store significant amounts of CO_2. These include the Barnett Shale of the USA which measures 4.00 wt.% of TOC and the famous Marcellus shale (USA) with 1–10 wt.%. The Irati and the Rio Bonito formations of Brazil have the highest TOC values found in the literature, measuring 2.3–26.30 wt.% and 1.7–43.90 wt.%, respectively. The Whitehill Formation of the Karoo Basin of South Africa has values of 0.5–14.70 wt.% TOC as described in the literature. In this study a sample from the Whitehill Formation from borehole G39974 gave a measured value of 4.52 wt.%, while a sample from the underlying Prince Albert Formation, from borehole KL 1-65, measured a value of 1.17 wt.% TOC. In the north-eastern part of the Karoo Basin, two samples from the Pietermaritzburg Formation, a north-eastern stratigraphic equivalent of the Whitehill Formation which pinches out in this part of the basin intersected by boreholes SW 1-67 and LA 1-68, measured 2.50 wt.% and 0.77 wt.% TOC, respectively. Sample

1124.5 from the Volksrust Formation intersected by borehole BE 1-67 measured 0.21 wt.% TOC. For maturity studies, all the six samples measured reflectance values above 1.4%Ro and are therefore classified as overmature. A plot on the HI vs OI index plot revealed that these samples plot predominantly below the gas prone Type III kerogen curve.

The samples exhibit a specific surface area of 17.40–21.88 m^2/g, with an average of 19.66 m^2/g. This compares quite favourably with the gas-bearing Silurian shales in the Sichuan Basin (China) which exhibit a specific surface area of 17.83–29.49 m^2/g, with an average of 22.18 m^2/g. There is also a trend of increasing surface area with TOC content, affirming the influence of organic matter on the surface area.

The high pressure adsorption experiments on the samples exhibited anomalous behaviour which affected the credibility of the results. Most experiments showed an unprecedented increase in pressure instead of the expected decrease due to the CO_2 being adsorbed onto the shale samples. The samples are from the old Soekor drill cores which have been exposed to the atmosphere for over 40 years and have undergone severe weathering during that period. The weathering and the degree of oxidation and break-down of pyrite are strongly suspected to be the cause of the anomalous behaviour.

Based on the content of organic matter and kerogen, these samples have potential to store CO_2. However, maturity studies have revealed that these shales and siltstones are in fact overmature and at this stage are likely to have less gas generating capacity and thus less affinity to adsorb CO_2. This could be argued also in favour of storage capacity as the gas does not disturb contact of CO_2 to rock, however, the high tightness as a consequence of over-maturity will have a higher negative effect on adsorption potential. Further studies on freshly drilled core samples are recommended to ascertain these findings given the limitations posed by the condition of the current samples, especially in studying the adsorption behaviour. Only then can we conclusively deduce whether or not the shales and siltstones of the Karoo Supergroup have a role to play in South Africa's anthropogenic CO_2 geo-sequestration endeavours.

ACKNOWLEDGEMENTS

ACADEMIC OUTPUTS

Annual technical reports:

N.S. Nxokwana, W. Altermann, D. Cole, M. Cloete, F.J. Doucet, E.M van der Merwe. (2013). Physico-chemical Properties of South African Shales in the Context of Geological CO_2 Storage. Annual Progress Report No (2013-0132), Council for Geoscience.

Conference proceedings:

N.S. Nxokwana, W. Altermann, D. Cole, M. Cloete, F.J. Doucet, E.M van der Merwe. (2011). Physico-chemical Properties of South African Shales in the Context of Geological CO_2 Storage. Abstract Book Geosynthesis 2011; Abstract No 3.33, pp. 183.

N.S. Nxokwana, W. Altermann, D. Cole, M. Cloete, F.J. Doucet, E.M van der Merwe. (2011). Physico-chemical Properties of South African Shales in the Context of Geological CO_2 Storage. Oral presentation at the Second South African Carbon Capture and Storage Conference. Johannesburg, South Africa, 24–28 October 2011.

N.S. Nxokwana, W. Altermann, D. Cole, M. Cloete, F.J. Doucet, E.M van der Merwe. (2012). Physico-chemical Properties of South African Shales in the Context of Geological CO_2 Storage. Oral presentation at the 17th Fossil Fuel Foundation Coal Science and Technology Indaba, Johannesburg, South Africa, 13–14 November 2012.

N.S. Nxokwana, W. Altermann, D. Cole, M. Cloete, F.J. Doucet, E.M van der Merwe. (2013). Physico-chemical Properties of South African Shales in the Context of Geological CO_2 Storage. Oral presentation at the Third South African Carbon Capture and Storage Conference, Johannesburg, South Africa, 03–04 October 2013.

N.S. Nxokwana, W. Altermann, D. Cole, M. Cloete, F.J. Doucet, E.M van der Merwe. (2013). Physico-chemical Properties of South African Shales in the Context of Geological CO_2 Storage. Oral presentation at the 18th Coal Science and Technology Indaba, Parys, South Africa, 13–14 November 2013.

N.S. Nxokwana, W. Altermann, D. Cole, M. Cloete, F.J. Doucet, E.M van der Merwe. (2013). Physico-chemical Properties of South African Shales in the Context of Geological CO_2 Storage. Poster presentation at the Fourth South African Carbon Capture and Storage Conference, Johannesburg, South Africa, 20–21 October 2015.

N.S. Nxokwana, W. Altermann, D. Cole, M. Cloete, F.J. Doucet, E.M van der Merwe. (2015). Physico-chemical Properties of South African Shales in the Context of Geological CO_2 Storage. Oral and poster presentation at the Cape Karoo Imbizo, Port Elizabeth, South Africa, 23–30 November 2015.

N.S. Nxokwana, W. Altermann, D. Cole, M. Cloete, F.J. Doucet, E.M van der Merwe. (2015). Physico-chemical Properties of South African Shales in the Context of Geological CO_2 Storage. Poster presentation at the Council for Geoscience Annual Conference, Pretoria, South Africa, 04–05 February 2016.

-

Table of Contents

LIST OF FIGURES

LIST OF TABLES

NOMENCLATURE

atm   atmosphere

BAU   Business as Usual

BET   Brunauer-Emmett-Teller Method

CBM   Coal Bed Methane

CCS   Carbon Capture and Storage

CDM   Clean Development Mechanism

CGS   Council for Geoscience

CFCs   Chlorofluorocarbons

CH4   Methane

CIMERA Centre of Excellence for Integrated Mineral and Energy Resource Analysis

CO_2   Carbon Dioxide

C&S   Carbon and Sulphur

CSIR   Council for Scientific and Industrial Research

ECBM   Enhanced Coal Bed Methane

EOR   Enhanced Oil Recovery

Gt   Gigatons

GHG   Green House Gas

JI   Joint Implementation

IRGC   International Risk Government Council

IPCC   Intergovernmental Panel on Climate Change

ISGS   Illinois State Geological Survey

KARIN   Karoo Research Initiative

LLGHGs   Long-lived Green House Gases

m^2   Square metres

m^3   Cubic metres

PASA   Petroleum Agency South Africa

ppm   Parts per million

SACCCS   South African Centre for Carbon Capture and Storage

SEM   Scanning Electron Microscopy

SF_6   Sulphur hexafluoride

Soekor   Southern Oil Exploration Corporation (now PetroSA)

VAS   Volumetric Adsorption System

XRD   X-Ray Diffraction

XRF   X-Ray fluorescence

TOC   Total Organic Carbon

%   Percentage

VAS   Volumetric Adsorption System

WP   Work Package

wt   Weight

wt.%   Weight per cent

GLOSSARY

Adsorption: a process that occurs when a gas or liquid solute accumulates on the surface of a solid or, more rarely, a liquid (absorbent), forming a molecular or atomic film (the absorbate). It is different from absorption, in which a substance diffuses into a liquid or solid to form a solution. The term sorption encompasses both processes, while desorption is a reverse process.

Anthropogenic: effects, processes, objects or materials are those that are derived from human activities, as opposed to those occurring in natural environments without human influences.

Carbon capture: the separation and entrapment of CO_2 from large stationary sources.

Carbon sequestration: the capture and secure storage of carbon that would otherwise be emitted to or remain in the atmosphere.

Climate change: means a change of climate which is attributed directly or indirectly to human activity that alters the composition of the global atmosphere and which is in addition to natural climate variability observed over comparable time periods.

CO_2 storage: a process of retaining captured CO_2 into geological formations or oceanic reservoirs for time scales of centuries or longer so that it does not reach the atmosphere.

Drill core: a cylindrical sample of earth, mineral or rock extracted from the ground by means of a corer so that the strata are undisturbed in the sample.

Emissions: means the release of greenhouse gases and/or their precursors into the atmosphere over a specified area and period of time.

Facies: distinctive conditions of rock formation, reflecting a particular process or environment. Facies based on petrological characteristics such as grain size and mineralogy are called lithofacies, whereas facies based on fossil content are called biofacies.

Fluvial: of or pertaining to a river or stream.

Geological formation: the basic or fundamental rock-stratigraphic unit in the local classification of rocks, consisting of a body of rock (usually a sedimentary stratum or strata, but also in igneous and metamorphic rocks) generally characterised by some degree of internal lithological homogeneity of distinctive lithological features such as chemical composition, structures, textures or gross aspect of fossils. Formations are of regional extent within which they have similar character, petrographically and mineralogically, but also in terms of facies.

Geothermal gradient: rate of increase of temperature in the earth with depth; the thermal gradient of the earth. The gradient near the surface of the earth varies from place to place depending upon the heat flow in the region and on the conductivity of the rocks. The approximate average geothermal gradient in the earth's crust is about 25 °C/km.

Greenhouse gases: means those gaseous constituents of the atmosphere, both natural and anthropogenic that absorb and re-emit infrared radiation. These are: Carbon dioxide (CO_2), Methane (CH_4), Nitrous Oxide (N_2O), Hydrofluorocarbons (HFCs), Perfluorocarbons (PFCs) and sulphur hexafluoride (SF6).

Group: a stratigraphic term used for a grouping of geological formations.

Isotherm: refers to the volume of gas adsorbed on a solid surface as a function of pressure for a specific temperature, gas and solid material.

Natural gas: Natural gas is a mixture of gases which are enriched in hydrocarbons. All these gases (methane, nitrogen, carbon dioxide, etc.) are naturally occurring in the atmosphere. Natural gas reserves are found deep inside the earth's interior near other solid and liquid hydrocarbon beds such as coal and crude oil.

Methane (CH_4): a colourless, odourless, flammable gas and the main constituent of natural gas (used as a fuel); the lightest component of crude oil and also an important component of marsh gas formed by the decomposition of organic material in the absence of air.

Munsell chart: A colour identification system for sediment, soil, chert, pottery and rock; an aid used in the physical examination and recording of objects where colour is an essential or at least a significant aspect of the analysis.

Kerogen: is a mixture of fossilised organic material found in oil shales and other sedimentary rocks. It is insoluble in normal organic solvents because of the high molecular weight of its component compounds and yields petroleum products upon burning.

Lacustrine: referring to a lake.

Long-lived Green House Gases (LLGHGs): simply defined as a greenhouse gas that stays in the atmosphere long enough to cause warming.

Organic matter: is matter composed of organic compounds that has come from the remains of dead organisms such as plants and animals and their waste products in the environment. Basic structures are created from cellulose, tannin, cutin and lignin, along with other various proteins, lipids and carbohydrates.

Permeability: the property or capacity of a porous rock, sediment or soil for transmitting a fluid.

Physico-chemical properties: relating to both physical and chemical properties.

Porosity: a measure of the void spaces in a material, expressed as a fraction of the volume of voids over the total volume, between 0 and 1, or a percentage between 1 and 100%.

Radiative forcing: is a perturbation of the energy balance of the earth-atmosphere system following, for example, a change in the concentration of carbon dioxide or a change in the output of the sun. The climate system responds to the radiative forcing so as to re-establish the energy balance.

Reservoir: a body of rock or sediment that is sufficiently porous and permeable to host and store CO_2. Sandstone and limestone are the most common reservoir rocks.

Saline aquifers: bodies of porous, permeable rock that hold unusable brine.

Seal: an impermeable rock that forms a barrier above and around a reservoir such that fluids are held in the reservoir.

Sedimentary basin: any geographical feature exhibiting subsidence and consequent infilling by sedimentation.

Shale: is a fine-grained, indurated, detrital sedimentary rock formed by the consolidation (as by compression or cementation) of clay, silt or mud and characterised by finely laminated (laminae 0.1–0.4 mm thick) structure and/or fissility approximately parallel to bedding (along which the rock breaks readily into thin layers).

Source of greenhouse gas(es): means any process or activity or mechanism which releases a greenhouse gas, an aerosol or precursor of a greenhouse gas into the atmosphere.

Supercritical state: at temperature and pressure above the critical temperature and pressure of the substance concerned. The critical point represents the highest temperature and pressure at which the substance can exist as a vapour and liquid in equilibrium.

Supergroup: the largest lithostratigraphic subdivision, comprising a series of groups, or groups and formations.

Vitrinite reflectance: a method for identifying the maximum temperature history of sediments in sedimentary basins and can also be an indicator of hydrocarbon resources. It can be calibrated to indicate the maturity of hydrocarbon source rocks and indicates whether a rock has been heated enough to produce oil, oil and gas or gas only. Vitrinite reflectance measures the percentage of incident light reflected from a polished surface of vitrinite and is presented in units %Ro, the measured percentage of reflected light from a sample which is immersed in oil (%Ro = % reflectance in oil).

Well: man-made hole drilled into the earth to produce liquids or gases, or to allow the injection of fluids.

Total Organic Carbon (TOC): This is the total amount of organic carbon in the rock; this relates to the adsorptive capacity of a shale to hold gas in a matrix, independent of porosity.

Transportation of CO_2: The movement of the captured anthropogenic CO_2 from the point source to a chosen storage site. Transportation can either be by means of

pipelines, ships, or tanker trucks depending on the distance between the point source and the storage site.

CHAPTER ONE: INTRODUCTION

1.1 Introduction

Geological storage of carbon dioxide (CO_2) is the process whereby the gas is captured and separated from the industrial source, transported and injected into deep geological formations for long-term storage and finally measured, monitored and verified to ensure that the CO_2 stays in the storage formation (Cloete, 2010). The geological formation is usually a permeable and porous sandstone reservoir overlain by an impermeable shale, also referred to as a cap-rock as its primary role is to prevent the gas from escaping from the reservoir rock (Cloete, 2010).

The CO_2 Storage Atlas on South Africa's storage capacity published by the Council for Geoscience reported that 98% of the country's storage capacity is in offshore Mesozoic Basins and only 2% is onshore (Cloete, 2010). This presents a challenge for South Africa as most of the sources of CO_2 are situated onshore, far from the coast. A significant portion of South Africa's interior is covered by the Karoo Basin, which contains widespread organic-rich shales. These shales supposedly contain significant amounts of shale gas and as a result, shale gas exploration is anticipated to take place in the Karoo Basin in the near future (United States Energy Information Administration, 2011). Studies in other parts of the world such as the United States of America (USA) have revealed that shales can store significant amounts of CO_2 in an adsorbed state (Busch et al., 2008). Indeed, bulk volumes of CO_2 concentrations are greater for shale (222–389 mol/m^3), when compared to coal and cemented sandstone (3–4 and 8–10 mol/m^3), respectively (Busch et al., 2008). This might be explained in terms of the structure of kerogen which is a nanoporous material with micropores (< 2 nm) and mesopores (2–50 nm) with molecular sieving properties allowing CO_2, a molecule with a linear molecular geometry, to reside in small pores which cannot be accessed by other naturally occurring gases (Busch et al., 2008). In anticipation of gas production in the Karoo Basin in the near future and the recent findings on the ability of carbonaceous shales to store CO_2, this study investigates the possibility of storing CO_2 in the shales after the natural gas has been harvested.

The present study targets the shales of the Prince Albert and Whitehill formations and their north-eastern stratigraphic equivalents, the Pietermaritzburg, Vryheid and Volksrust formations. The shales and siltstones will be thoroughly characterised and the sorption behaviour of CO_2 in the samples will be determined.

The overall aim of this project is to generate critical data necessary for the development of a database for the carbonaceous shales and siltstones of the Ecca Group which will inform scientists and decision-makers about the potential role these shales could play in Carbon Capture and Storage (CCS) in South Africa.

1.2 Geological background

1.2.1 Karoo stratigraphy

The Karoo Supergroup ranges in age from Late Carboniferous to Middle Jurassic and attains a total cumulative thickness of about 12 km in the south-eastern portion of the Main Karoo Basin towards the eastern end of the Karoo Trough (a linear east–west zone of maximum subsidence along the southern basin edge). The bulk of the Karoo strata occurs in the main basin, which covers an area of approximately 700 000 km^2 but was much more extensive during the Permian (Johnson et al., 2006).

This study focuses on the carbonaceous shales of the Ecca Group (see Figures 1.1 and 1.2).
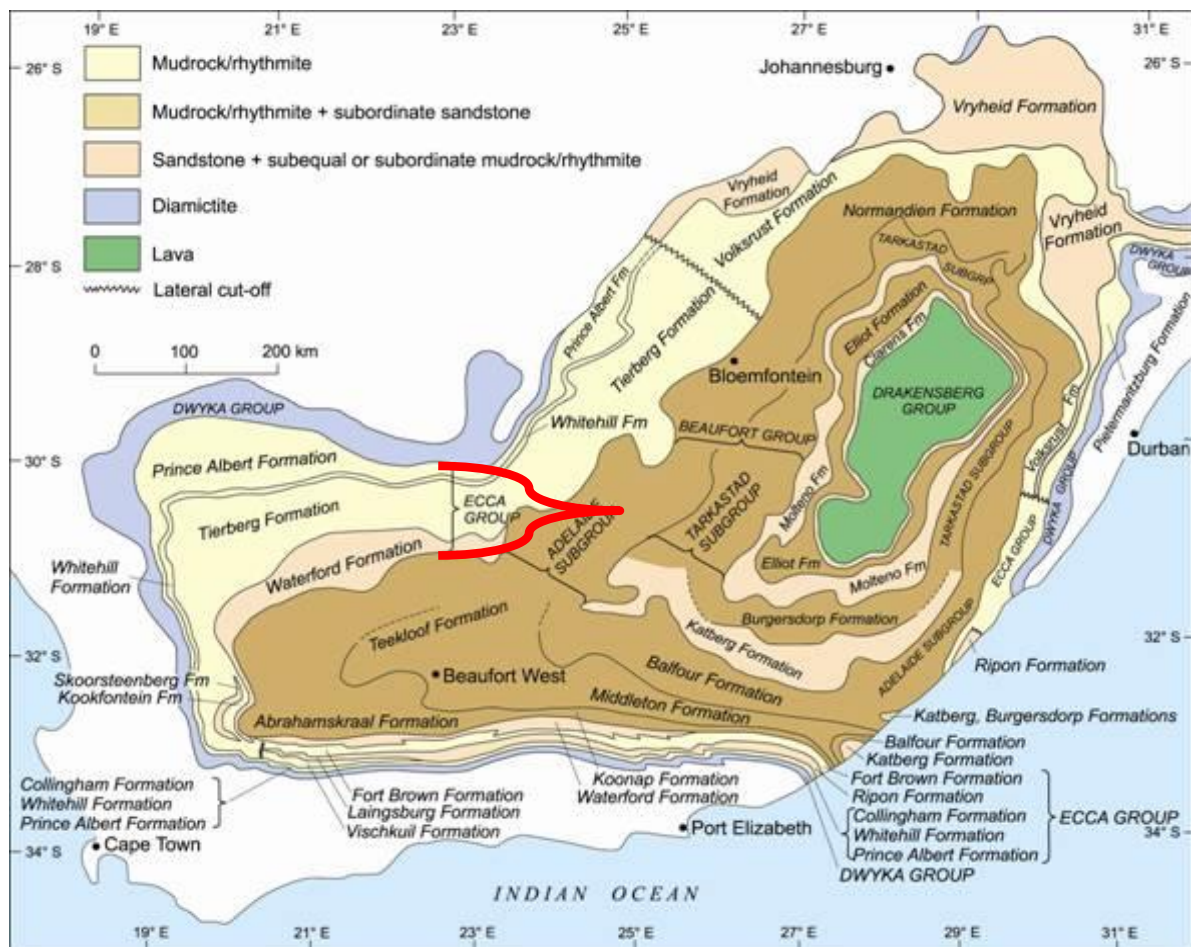
Figure 1.1. Areal distribution (schematic) of lithostratigraphic units in the Main Karoo Basin. (Source: Johnson et al., 2006).
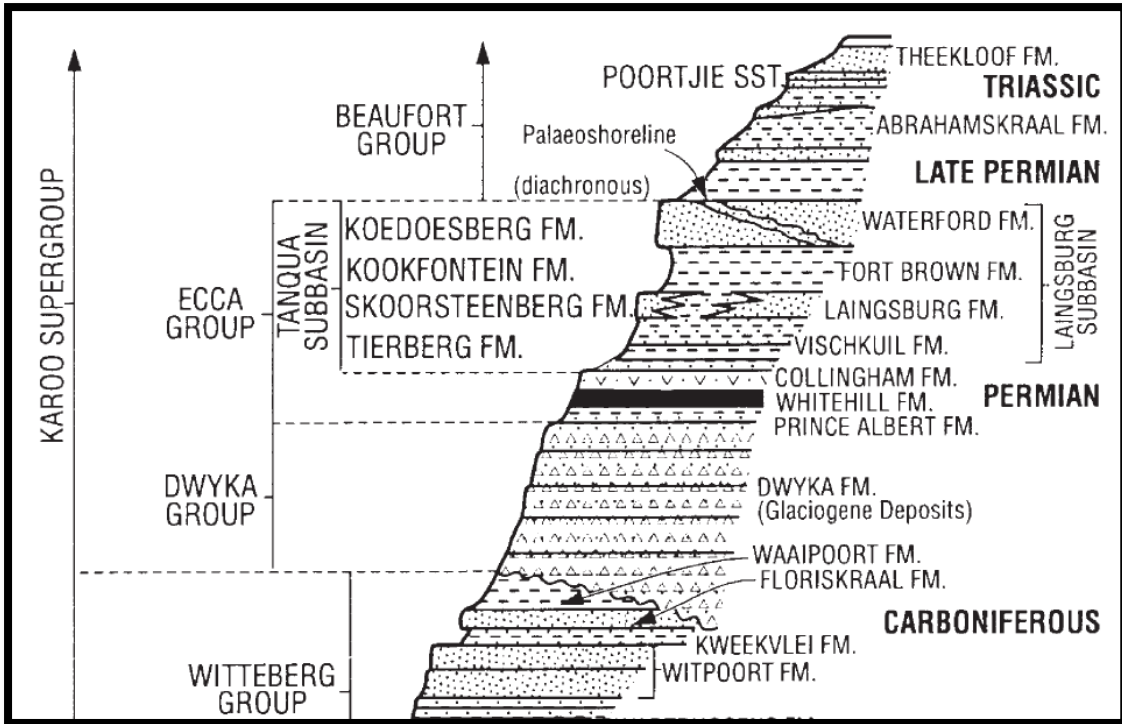
Figure 1.2. Simplified stratigraphy of the Karoo Basin. (Chesapeake Energy, 2010).

1.2.2 Ecca Group

The Ecca Group overlies the glacial deposits of the Dwyka Group of the Karoo Supergroup. It is Permian in age (Johnson et al., 2006). The shales of the Ecca Group were deposited during the flooding that resulted from the melting of the retreating glacier. The Ecca Group comprises a total of sixteen formations reflecting the lateral facies changes that characterise this succession (Johnson et al., 2006). This study focuses only on the Prince Albert, Whitehill, Collingham, Tierberg, Pietermaritzburg, Vryheid and Volksrust formations, all of which will be discussed individually in the following sub-sections.
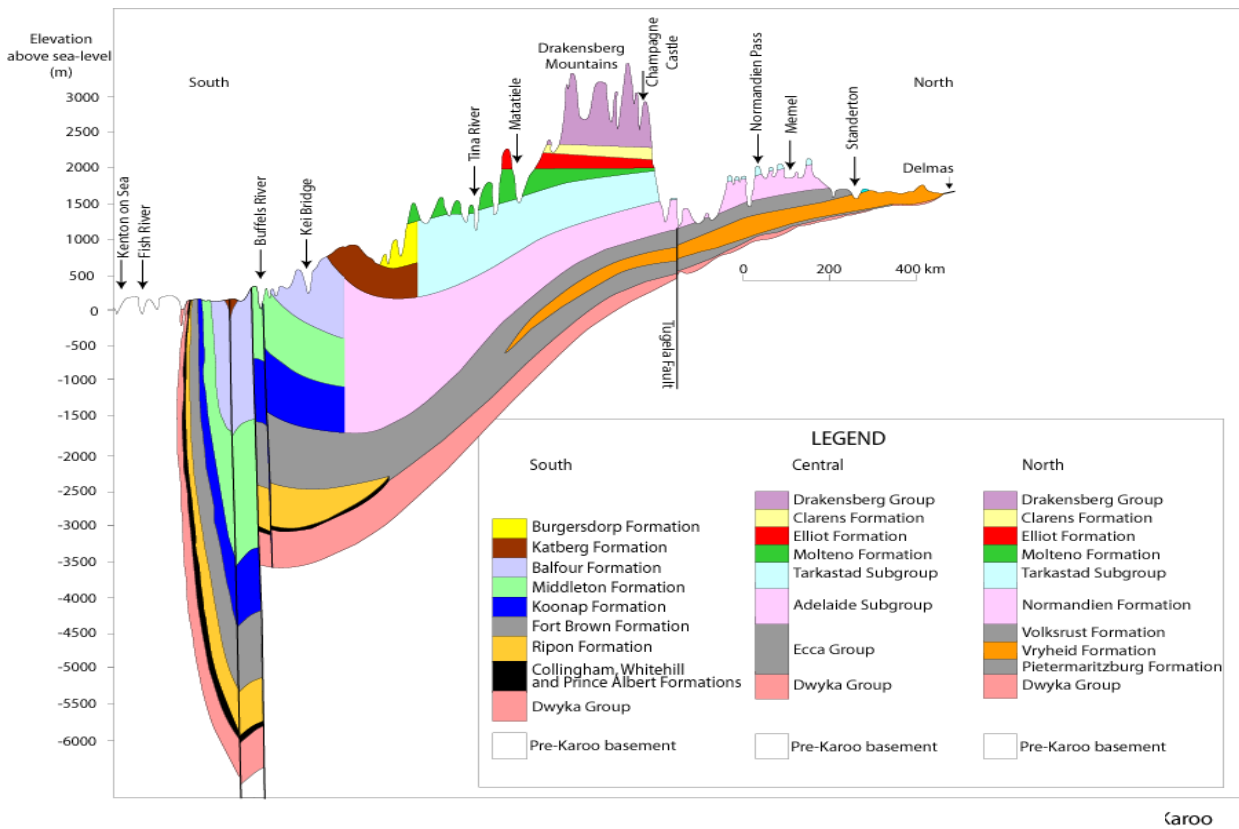
Figure 1.3. Lithostratigraphic cross-section across the Main Karoo. (Source: Cole, 2010).

i) Prince Albert Formation

The Prince Albert Formation occurs southwest of a line from Hertzogville to Bloemfontein and Coffee Bay, which is defined by pinch-out of the overlying Whitehill Formation (Cole, 2005). It conformably overlies diamictite, sandstone or rhythmite of the Dwyka Group and is conformably overlain by the carbonaceous shales of the Whitehill Formation (Cole, 1991, 2005). It mostly comprises dark-grey shale and subordinate silty rhythmites, but contains siltstone and fine-grained sandstone beds in the Boshof– Hertzogville area. The Prince Albert Formation has a variable thickness ranging between 100 and 500 m and is Asselian to Artinskian in age (Cole and McLachlan, 1991, 1994).

5

ii)   Whitehill Formation

The Whitehill Formation is present southwest of a line from Hertzogville to Bloemfontein and Coffee Bay, along which it pinches out (Cole and Basson, 1991). It conformably overlies the shales of the Prince Albert Formation with a sharp contact. It is Early Permian (Kungurian) in age (Oelofsen and Aruajo, 1987). Shales of the Whitehill Formation are high in carbon content and were deposited in a shallow epicontinental basin. Presence of pyrite and the high organic content suggest reducing (anoxic) conditions below the sediment-water interface (Cole, 2010).

iii)   Collingham Formation

The Collingham Formation is predominantly argillaceous and conformably overlies the Whitehill Formation with a sharp contact. It ranges between 30 and 70 m in thickness and is Mid-Permian (Roadian) in age (Cole, 2010). The Collingham Formation was deposited from the suspension settling of mud from a deep-water basin plain environment and has characteristic volcanic tuff and chert beds (Cole, 2010).

iv)   Tierberg Formation

The Tierberg Formation conformably overlies the Collingham Formation in the south and Whitehill Formation elsewhere where the Collingham Formation pinches out. It is up to 1 300 m in thickness and ranges from Roadian to Wuchiapingian in age (Cole, 2010). The dominant environment of deposition seems to be shallow marine with basin plain to prodelta facies (Cole, 2010).

v)   Pietermaritzburg Formation

The Pietermaritzburg Formation is the lowermost unit of the Ecca Group in the north-eastern part of the basin. It is up to 420 m thick to the east of Lesotho and is Late Sakmarian to Kungurian (Early Permian) in age (Cole, 2010). It was formed by suspension settling of muds in a cold marine environment (Cole, 2010).

vi)   Volksrust Formation

The Volksrust Formation is present in the north-eastern part of the basin where it overlies the Vryheid Formation. Its thickness varies from 0–400 m, thickening towards the south and southwest (Johnson, 2006). It ranges from Roadian to Wuchiapingian in age (Figure 1.4). Shallow marine environment is the common depositional environment (Cole, 2010).
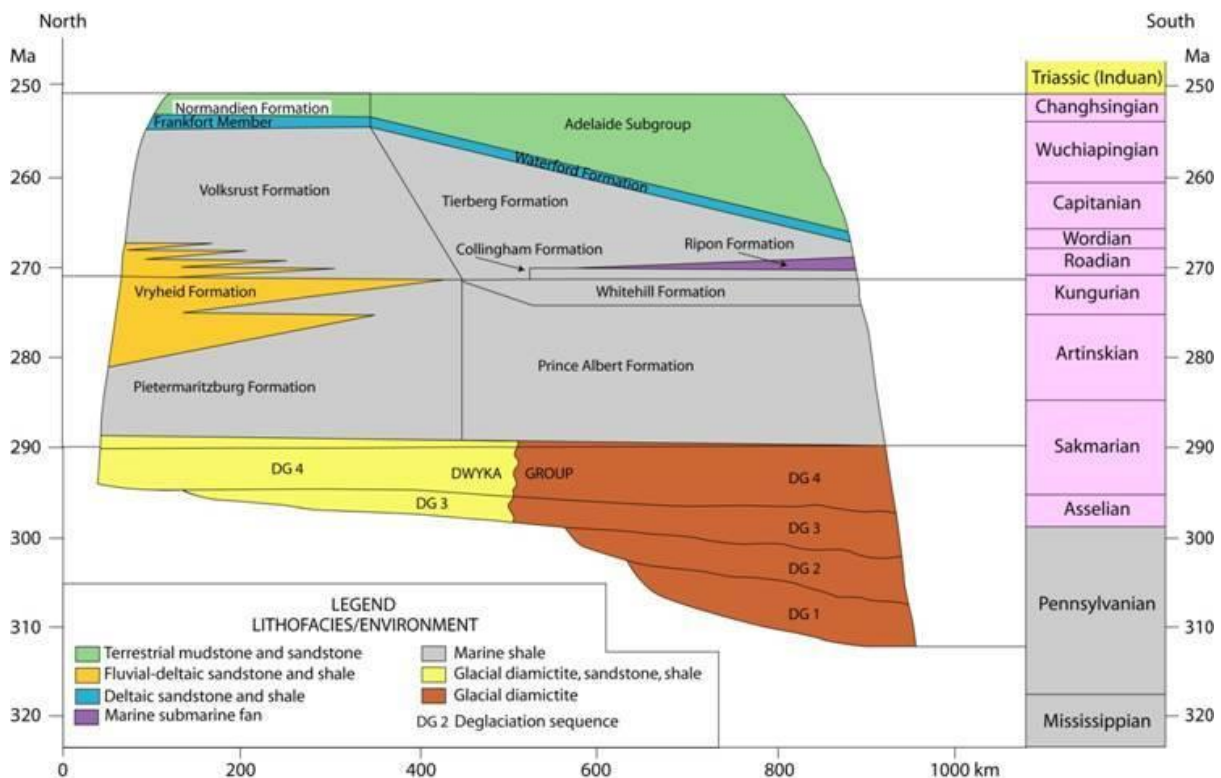
Figure 1.4. Distribution in time and space of the Dwyka, Ecca and lower Beaufort Groups. (Source: Cole, 2010).

1.3 Aim of this project

The project constitutes of two work packages (WP):

1. WP1: Identification, classification and detailed characterisation of the selected Ecca Group shales and siltstones in the Karoo Basin of South Africa.

The Council for Geoscience and Petroleum Agency South Africa (PASA) records were consulted to draw a national inventory of the South African shales and siltstones and to draw illustrated maps showing the geographic distribution of the shale formations.

Five old Soekor deep boreholes from across the Karoo Basin of South Africa namely KL 1/65, SW 1/67, BE 1/67, G39974 and LA 1/68 were logged and sampled.

The physico-chemical properties tested were:

• Elemental composition (XRF — both major and trace elements)

• Mineralogy (XRD)

• Petrography

• Scanning electron microscopy (SEM)

• Total organic carbon (TOC)

• Bulk density

• Kerogen maturation

• Low pressure CO_2 adsorption (BET), and

• High pressure adsorption isotherms.

The results from these analyses will aid in the characterisation of these shales and in developing a database necessary to inform decision-makers about the role shales and siltstones can play in CCS in South Africa.

2. WP2 — CO_2 sorption behaviour in South African shales and siltstones.

Low pressure CO_2 sorption experiments:

Low pressure CO_2 adsorption measurements were performed on a chosen set of six samples in order to characterise the micropores and measure the porosity of the shale samples. It is generally accepted that low pressure adsorption of CO_2 is useful for characterising microporosity (pore diameter < 2 nm), while low pressure adsorption of nitrogen is useful for characterising meso- and macroporosity (Clarkson et al., 2013).

High pressure sorption experiments:

In high pressure sorption experiments, the CO_2 sorption capacity (sorption isotherms) of powdered shale and siltstone sample material were determined as a function of pressure by a volumetric method, using a high pressure volumetric adsorption system. Care was taken to ensure a constant temperature in all experiments (45 °C). At these temperatures, CO_2 is either in the gaseous or, at pressures above 73.8 bar, in the supercritical state. The experimental data were evaluated in terms of excess (Gibbs) sorption isotherms. The observed reduction in gas pressure resulting from gas sorption was compared to the theoretical "non-sorption" case. The volume changes relating to the increased amount of adsorbed phase with pressure were not considered.

CHAPTER TWO: LITERATURE REVIEW

2.1   Introduction

In November 2007, the Intergovernmental Panel on Climate Change (IPCC) stated that the total emissions of anthropogenic greenhouse gases (CO_2, CH_4 and N_2O) due to human activities increased by 70% between 1970 and 2004 and that global increases in CO_2 concentrations are due primarily to fossil fuel use, with land-use change providing another significant but smaller contribution (IRGC, 2007). The latest analysis of observations from the World Meteorological Organisation's (WMO) Global Atmospheric Watch (GAW) Programme shows that the globally averaged mixing ratios of CO_2, CH_4 and N_2O reached new highs in 2010, with CO_2 at 389.0 ppm, CH_4 at 1 808 ppb and N_2O at 323.2 ppb. These values are higher than those recorded in pre-industrial times (before 1750) by 39%, 158% and 20%, respectively (WMO, 2010). Out of all the greenhouses gases CO_2 is the single most important anthropogenic greenhouse gas in the atmosphere, contributing approximately 64% to radiative forcing by Long-lived Green House Gases (LLGHG (WMO, 2010). For about 10 000 years prior to the industrial revolution, the abundance of CO_2 in the atmosphere was nearly constant at about 280 ppm (WMO, 2010). This level provided a balance in the atmosphere, the oceans and the biosphere. Owing to the burning of fossil fuels, deforestation and land-use change that came with the industrial revolution since 1750, atmospheric CO_2 has increased by 39% (WMO, 2010).

Carbon dioxide in the atmosphere acts as a blanket that envelops the planet trapping the longwave radiation which would otherwise radiate heat away from the planet. The more CO_2 in the atmosphere, the stronger will be its warming effect. This is known as the greenhouse effect (WMO, 2010).

Methane, on the other hand, contributes about 18% to radiative forcing by LLGHGs. About 40% of CH_4 released to the atmosphere comes from natural sources such as wetlands and termites, while 60% comes from anthropogenic sources such as ruminants, rice agriculture, fossil fuel exploitation, landfills and biomass burning (WMO, 2010).

The continued emission of anthropogenic CO_2 and other greenhouse gases in the atmosphere will have dire effects on the earth's natural systems and ecosystems (WMO, 2010). The warming effect of the increasing amounts of greenhouse gases in the atmosphere has a marked effect on agriculture, natural systems, and a whole host of other environmental variables (WMO, 2010). Measures and actions have to be taken globally to mitigate the amount of greenhouse gases in the atmosphere, particularly CO_2 which is the most abundant greenhouse gas in the atmosphere.

2.2 CO_2 emissions in South Africa

South Africa has a heavily coal-dependent economy with 94% of electricity and 65% of South Africa's primary energy supply coming from coal (Beck et al., 2011). In addition, 30% of South Africa's domestic fuel-oil demand is met through the conversion of coal and gas to transportation fuels by Sasol and PetroSA (Beck et al., 2011). This has resulted in South Africa being placed as the 13th largest CO_2 emitter in the world (Beck et al., 2011). Due to the continued increase in energy demand, Eskom has expanded its power generating capacity by adding two new coal-fired power stations, Medupi and Kusile. As these will be in operation for some time to come to meet South Africa's increasing energy demands, it means that, despite advances made in renewable energy and energy efficiency measures, coal usage and dependency in South Africa will continue to increase.

The main sources and the concentrations of CO_2 emissions are centred in the main urban areas as well as some mining areas as shown in the maps below (Figures 2.1 and 2.2).
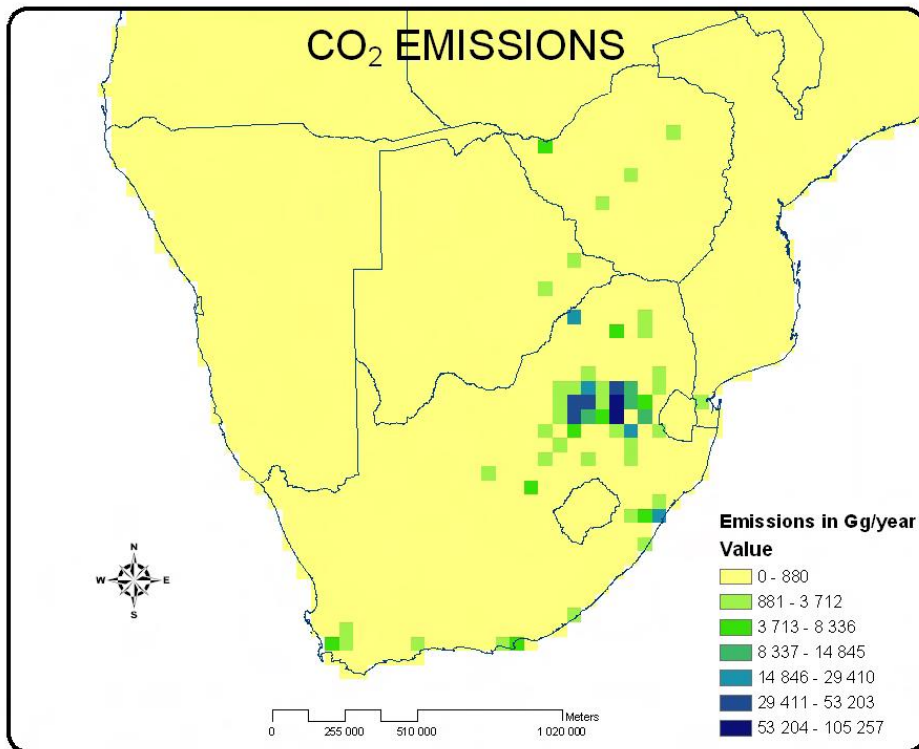
Figure 2.1. Concentrations of carbon dioxide over South Africa (Engelbrecht, 2004).
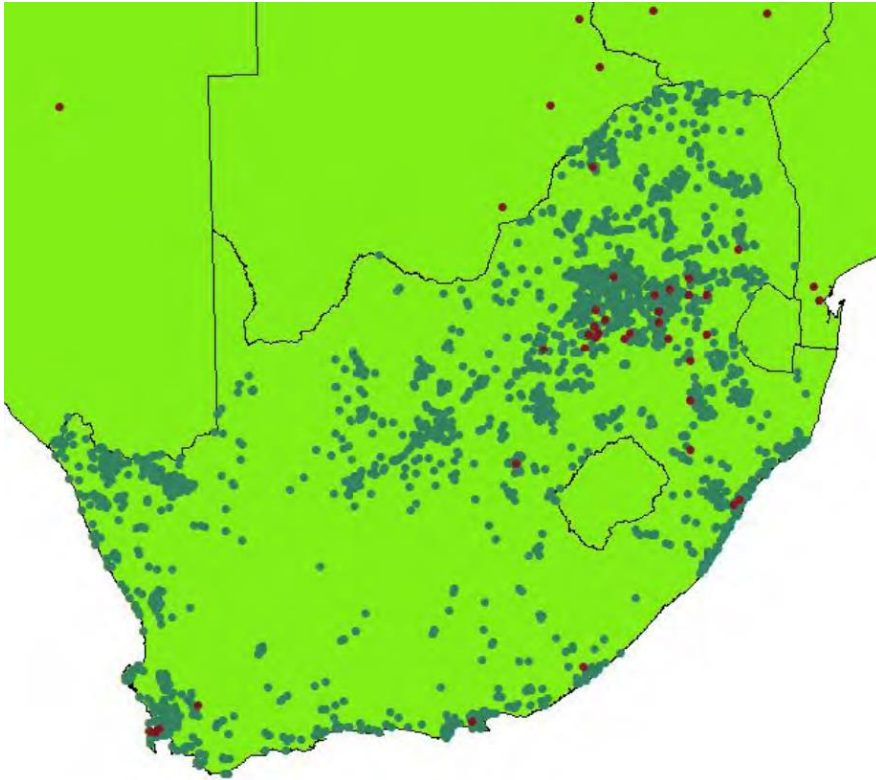
Figure 2.2. Carbon dioxide emissions from mines and industry (grey) and power stations (red) (Engelbrecht, 2004).

2.3 South African CO_2 sequestration efforts

South Africa is a signatory to the 1992 United Nations Framework on Climate Change (UNFCC) and its Kyoto Protocol (Kiratu, 2010). As South Africa is classified as a developing (Non-Annex 1) country it is exempted from the mandatory GHG emissions reduction targets that the Annex I countries are obligated to meet. However, South Africa is continuing to make serious endeavours to demonstrate a responsible approach towards reducing its CO_2 emissions profile. At the climate change negotiations in Copenhagen, South Africa announced that it would take nationally appropriate mitigation actions to enable a reduction in national GHG emissions equating to a deviation of 34% below the "Business as Usual" emissions growth trajectory by 2020 and 42% deviation below the "Business as Usual" below emissions trajectory by 2025, pended upon the provision of sufficient funding and technology support (Beck et al., 2011). In 2009, South Africa established the South African Centre for Carbon Capture and Storage (SACCCS). SACCCS was tasked with the role of creating a CCS Research and Development Roadmap for South Africa that outlines the steps towards CCS deployment in South Africa. Key milestones from the Roadmap include the development of a geological storage atlas by 2010, a CO_2 test injection by 2017 (Beck et al., 2011) and an operational demonstration project by 2020. With South Africa being a developing country, one of the critical issues in the development of this Roadmap is CCS capacity building. In addition to technical capacity, South Africa also needs to build institutional, financial, legal and human capacity, and it is likely that these capacity requirements can be met with assistance from developed countries (Beck et al., 2011).
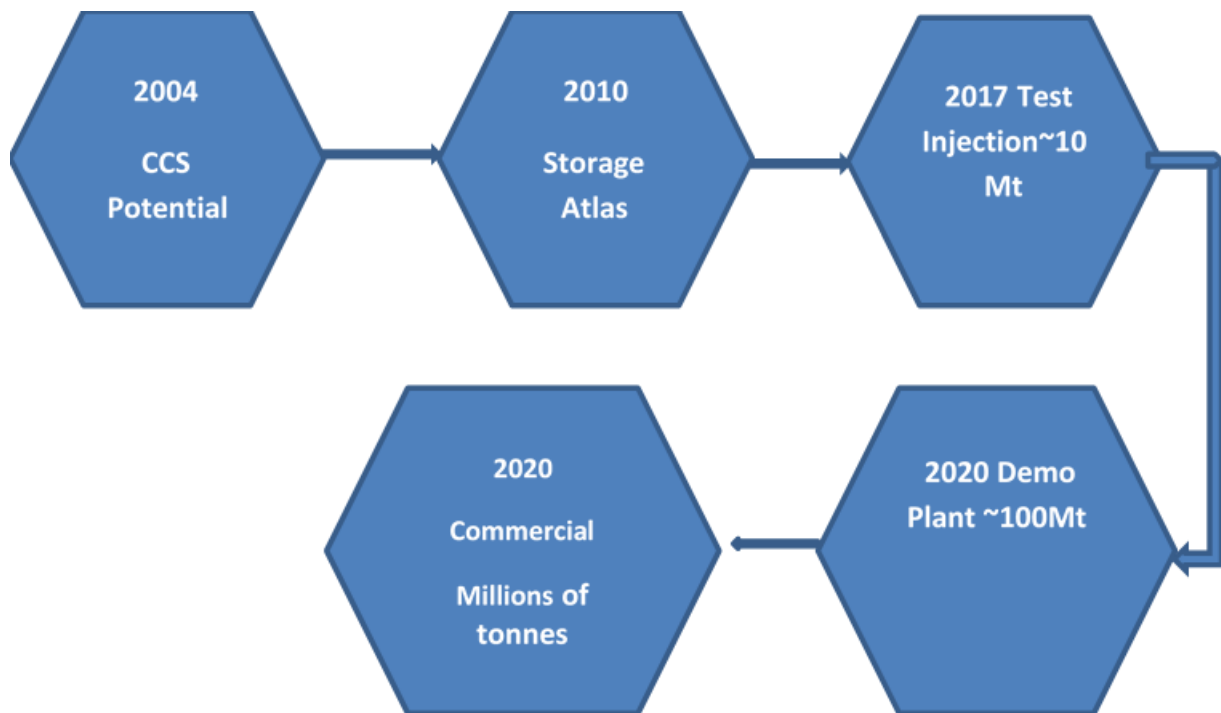
Figure 2.3. Diagram showing the South African CCS roadmap.

The then Department of Minerals and Energy commissioned an investigation into the potential for CO_2 sequestration in South Africa by the Council for Scientific and Industrial Research (CSIR), the results of which were released in 2004. The study, conducted by Engelbrecht et al. (2004) found that South Africa has the potential for sequestration of CO_2. The study revealed that, of the more than 400 million tonnes of annual CO_2 emissions, approximately 60% was sequestrable, 65% of which emanated from coal-fired electricity generating stations. On the other hand, nearly 30 million tonnes per year of ~95% concentration of CO_2 is emitted by the synthetic fuel industry (coal and gas to liquid — Sasol and gas to liquid — PetroSA) (Surridge and Cloete, 2009). In this case, the capture process has already been done, and the CO_2 merely requires pressurisation before transmission to an injection site. In summary, this study showed that South Africa has capturable emissions and potential storage sites. A geological storage atlas which undertook to assess the storage capacity of South Africa was released in 2010 (Cloete, 2010). The Atlas reported that the estimated capacity of geological storage in South Africa is around 150 Gt (150 000

Mt) of CO_2; 98% of this storage is in the offshore Mesozoic Basins along the coast of South Africa and only 2% occurs onshore (Figure 2.4). The storage potential lies mainly in the capacity of saline formations associated with oil and gas-bearing sequences in the Outeniqua, Orange and Durban/Zululand Basins. The estimated capacities are: ~48 Gt for the Outeniqua Basin, ~56 Gt for the Orange Basin and ~42 Gt for the Durban/Zululand Basin (Cloete, 2010). Onshore estimated capacities are: ~0.46 Gt for the onshore Zululand Basin, ~0.40 Gt for the onshore Algoa Basin and ~1.2 Gt for the coalfields of South Africa (Cloete, 2010). A big portion of the onshore Karoo Basin is covered by the non-porous and impermeable shales of the Ecca Group. Due to their non-porous and impermeable nature, these shales were overlooked by the Atlas study. However, the current study aims to investigate the potential that these shales might have for unconventional CCS in South Africa. Given that the shales and siltstones occur in a large part of the interior basin and major sources of anthropogenic CO_2 are situated in the interior of the country, far from the potential storage sites identified by the Atlas, prompts the need to find unconventional means of storing CO_2 in the Karoo Basin.
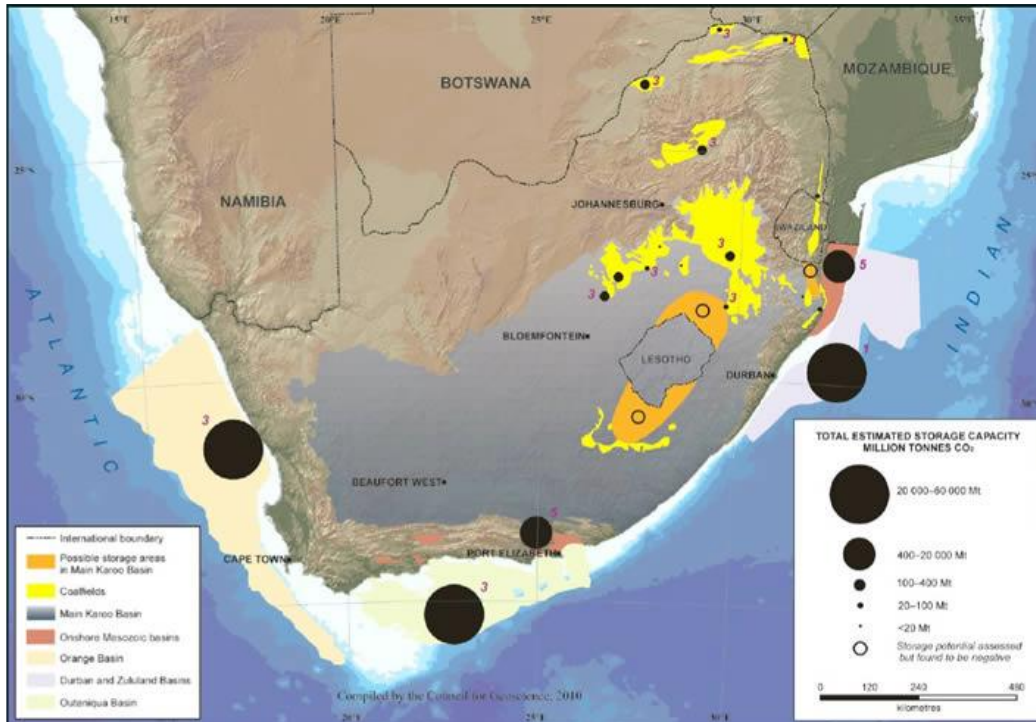
Figure 2.4. Map showing the offshore Mesozoic Basins of South Africa and their estimated CO_2 storage capacities. The black shaded circles indicate the storage capacities. (Cloete, 2010).

2.4 Carbon Capture and Storage (CCS)

CCS technology is one of the approaches for mitigating potential climate change due to emissions of anthropogenic CO_2 and other greenhouse gases. It is essentially the removal of CO_2 from industrial sources and transport to be stored in secure subsurface reservoirs. The stored CO_2 is then measured, monitored and verified to ensure long-term storage in the geological formation (Cloete, 2010). The CCS process basically consists of three stages, namely: 1) capture and separation of CO_2 from an industrial source; 2) transport to a storage site; and 3) storage in geological or oceanic reservoirs (Herzog and Golomb, 2004). Some of these stages are discussed in the sections below.

2.4.1 Capture

Carbon dioxide capture is a process that is designed to produce a concentrated stream that can readily be transported to a CO_2 capture storage site. This process is more applicable to large, centralised sources like power plants and large industries.

There are three main approaches to CO_2 for industrial and power plant applications and these include pre-combustion, oxy-fuel combustion and post-combustion (IPCC, 2005). The operating principles of these three main technologies are illustrated in Figure 2.5.
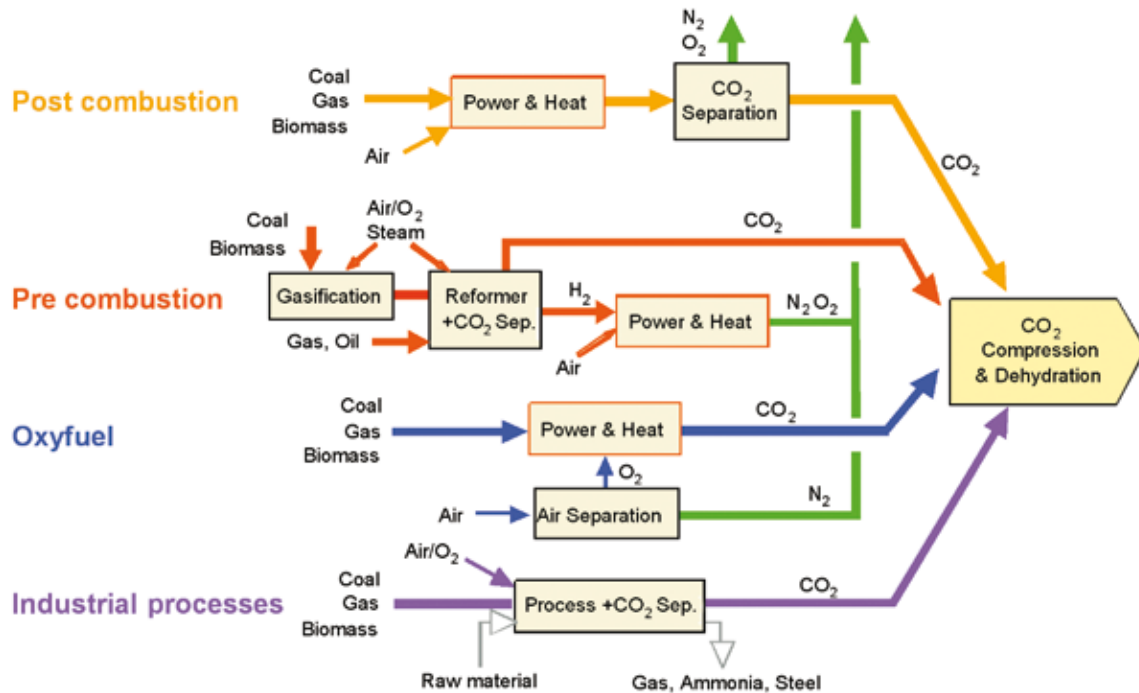
Figure 2.5. Illustration of the three main CO_2 capture processes (IPCC, 2005).

2.4.2 Storage

Following capture and transportation of CO_2 from anthropogenic sources, the third stage of CCS is storage, where CO_2 is injected into geological sinks or the deep ocean (Herzog and Golomb, 2004). Carbon dioxide can also be stored by means of a process known as mineral carbonation, which is beyond the scope of this study. The current study focuses on geological storage, which is discussed in detail in the following section.

i)   Geological storage

Subsurface geological storage can be performed both onshore and offshore, with offshore sites made accessible through pipelines from the shore or from offshore platforms (Cloete, 2010). Geological sinks for CO_2 include depleted oil and gas reservoirs, unminable coal seams and deep saline formations. Mafic rocks such as

basalt and deep oceanic waters have also been suggested as potential hostilities for geo-sequestration of CO_2. For geological storage, CO_2 must first be compressed to a dense fluid state known as 'supercritical'. Depending on the geothermal gradient, the density of CO_2 increases with increasing depth and the supercritical state is attained at a depth of 800 m below surface or greater. With increased density at greater depths, larger volumes of CO_2 can be stored at relatively small volume leading to efficient utilisation of underground storage space in the pore spaces of sedimentary rocks. Traditionally, the geological requirements for a suitable storage site for CO_2 include having a porous and permeable reservoir rock. The injected CO_2 will move into and reside in the void spaces between the loosely packed grains of the reservoir rock. These void spaces are also filled with water with high concentrations of salts and other solutes. The stored CO_2 will, over time, dissolve in these liquids and may react with the formation water and surrounding rocks to form stable minerals such as carbonates, depending on the surrounding geochemistry of the environment (Global Energy Technology Strategy Program (GTSP), 2006). The reservoir rock must be overlain by a non-porous and impermeable rock, known as a cap-rock. The cap-rock is impermeable and acts as a barrier that prevents the migration and escape of CO_2 out of the target storage formation. Other mechanisms through which CO_2 can remain trapped underground include: retention as an immobile phase trapped in the pore spaces of the storage formation; dissolution in the *in situ* formation fluids; and/or adsorption onto organic matter in coal and in shale. Additionally, it may be trapped by reacting with minerals in the storage formation and cap-rock to produce carbonate minerals (IPCC, 2005).

There are potential risks to humans and the environment associated with geological storage. These include: leaking injection wells, abandoned wells, leakage across faults and ineffective cap-rocks. Leakage of CO_2 can potentially degrade the quality of groundwater and have detrimental effects on plants and subsoil animals. Its release back to the atmosphere, on the other hand, could also create local health and safety concerns. Avoiding or mitigating these impacts will require careful site selection, effective regulatory oversight, an appropriate monitoring programme that provides early warning that the storage site is not functioning as anticipated, and implementation of remediation methods to stop or control CO_2 releases (IPCC, 2005).

ii)   Geological storage potential in South Africa

As shown in section 2.2 (Figure 2.4), South Africa's storage capacity is mainly confined in the offshore Late Mesozoic Basins (Outeniqua, Orange and Durban/ Zululand Basins) and to a less extent in the Late Palaeozoic Karoo Basin (Cloete, 2010). These basins are relatively young and largely undeformed, but their stratigraphy and depositional histories are not well studied or understood (Cloete, 2010).

The synthetic fuel industry in South Africa produces around 30 Mt of concentrated CO_2 per year, which would be a low-cost early opportunity application for CCS experimental CO_2 storage (Beck et al., 2011). As the largest CO_2 emitters in South Africa, Sasol and Eskom are located inland where storage capacity is limited; in-house expertise within these two companies will be required to construct pipelines to access storage sites offshore (Beck et al., 2011).

A large part of the South African interior is covered by the Karoo Basin, which includes widespread carbonaceous shales of the Ecca Group. As shales are generally impermeable and non-porous, they do not suit the conventional CO_2 storage requirements. Unconventional means of storing CO_2 in these shales of the Karoo Basin have to be investigated so as to supplement South Africa's onshore storage capacity.

2.5 Geology of the Karoo Basin of South Africa

The Karoo Basin has an aerial extent of some 550 000 km^2 and has its greatest sedimentary fill along the southern margin of the basin (Cadle et al., 1993). The sedimentary succession thins northwards and it pinches out along the northern margin of the basin. The basin is therefore asymmetric in cross-section and is classified as a tectonic foreland basin (Cadle et al., 1993). The predominant sedimentary transport direction was from south to north with a minor component of fill from the north. Sedimentation began in the Carboniferous Period with the deposition of the glaciogenic Dwyka Formation (Cadle et al., 1993). The Ecca Group

shales were deposited following the retreat of the glacier and the transgression of the Ecca sea. The Ecca Group normally comprises dark-coloured shales with interspersed siltstones and sandstones (course-grained and pebbly in places) and occasional coal seams, deposited subaqueously under reducing, generally moist conditions in marine, lacustrine, deltaic and fluvial environments. The Ecca Group is up to 3 000 m thick in the south (Johnson et al., 1996).

2.5.1 Karoo dolerites

Lower Jurassic sills and dykes are present throughout the Karoo sedimentary sequence, with the most extensive and thickest sills located within the Ecca Group (Aarnes et al., 2011). The Karoo dolerites intruded strata of the Ecca Group and preferentially the carbonaceous shale of the Whitehill Formation (Cole, 2010). More than a thousand exposed breccia pipes are located in the western Karoo Basin, rooted in contact metamorphic aureoles in shales. These are cylindrical pipe structures up to 150 m in diameter that cut vertically through the sedimentary strata. They are characterised by more or less *in situ* brecciation and metamorphism of organic-rich layers from the Ecca Group, with some layers of intermixed sediment and dolerite (Aarnes et al., 2011). This intrusive dolerite suite represents a shallow feeder system to the flood basalt eruptions. It as an interconnected network of dykes, sills and saucer-shaped sheets, so that it is nearly impossible to point their occurrence to any particular intrusive or tectonic event (Johnson et al., 2006).

$^{40}Ar/^{39}Ar$ dating methods indicate that these dolerites were erupted within 0.5 million years at about 183 Ma. Dolerite is present over about 390 000 km^2 of the Main Karoo Basin, but absent in the southernmost part of the basin, south of approximately latitude 32º30'S in the region where strata have been deformed by the Cape Fold Belt (Cole, 2010).

2.5.2 Economic importance of the Karoo Basin

The Karoo Basin hosts all the economic coal deposits of the subcontinent. The combined reserves are estimated to be in the order of 67 000 MT, which is nearly 10% of the world total (Johnson et al., 2006). The coals are generally inertinite rich and high in ash. With total recoverable Karoo Supergroup coal reserves of 55 333 Mt (*in situ* resources of 121 218 Mt), of which 37 625 Mt are present in the Main Karoo Basin, South Africa ranks fifth in the world (Johnson et al., 2006).

The Karoo Basin has also been explored extensively for hydrocarbons. Soekor (Southern Oil Exploration Corporation (Pty) Ltd) was established in 1965 with a mandate to prove or disprove the existence of economic accumulations of oil or gas in South Africa (Cole, 2010). Current petroleum exploration activities in the Karoo are focused on three unconventional play types: shale gas, coalbed methane and biogenic gas, although the potential for conventional hydrocarbon plays also exists (Petroleum Agency SA, 2011). The current study pays particular focus on the current shale gas exploration in the Karoo Basin of South Africa. This is due to findings from other parts of the world that comparable carbonaceous shales have a potential to store significant amounts of CO_2 in their organic matter. Extraction of CH_4 from the shales also presents an opportunity to sequester CO_2 in the spaces previously occupied by CH_4.

2.5.3 Hydrocarbon potential of the Karoo shales

The Karoo Basin has attracted a number of exploration activities for its shale gas potential. The shale gas resource of the Karoo Basin is currently unknown due to the paucity of relevant geoscientific data, but preliminary model estimates of the technically recoverable resource range from ~30 Tcf to 500 Tcf (Petroleum Agency SA, 2011). The Whitehill Formation is of particular interest as it meets all the basic requirements for a successful shale gas play; it is rich in organic matter, thermally mature, has a high silica content and is deeply buried (Petroleum Agency SA, 2011).

The Whitehill Formation was deposited by suspension settling of mud in a shallow epicontinental basin (Cole, 2010). The Whitehill Formation appears to have been deposited under reducing (anoxic) conditions below the sediment-water interface as shown by high organic content, presence of pyrite, as well as bioturbation being restricted to the middle part of the formation. Anoxic conditions are necessary for the preservation of organic matter. Following burial and lithification, the organic carbon content of the shales is usually shown by their colour, with the darkest shales (black) having the highest organic carbon content.

2.6 CO_2 Adsorption capacity of shales

2.6.1 What is shale?

Shale is a fine-grained, indurated, detrital sedimentary rock formed by the consolidation (as by compression or cementation) of clay, silt or mud and characterised by finely laminated (laminae 0.1–0.4 mm thick) structures and/or fissility approximately parallel to bedding along which the rock breaks readily into thin layers (Gary at al., 1972). Shales are compacted and well-splitting (fissile) mudstones and contain mainly clay minerals of sizes below 2 μm. Shales vary in their content of organic matter which is reflected in their level of darkness. The darkest shales have the highest content of the finely dispersed insoluble organic material, also known as kerogen. Kerogen is a non-porous material with micropores (< 2 nm) and mesopores (2–50 nm) (Kang et al., 2010).

Since shale is normally impermeable and has a low porosity, it was not considered by the Atlas project on geological storage of CO_2 in South Africa as a potential storage reservoir (Cloete, 2010). However, it has been shown that, although widely known as an impermeable sedimentary rock with low porosity, organic shale has the ability to store significant amounts of gas permanently due to trapping of the gas in an adsorbed state within the finely dispersed organic matter (kerogen), as well as in microfractures within the shale.

In order to preserve organic material from oxidation, a moderate to reducing depositional environment is required. For South African shales, these conditions are confined to the shales of the Ecca and Dwyka Groups of the Main Karoo Basin, with the Whitehill Formation preserved in the strongest reducing conditions (Cole, 2010). The Whitehill Formation consists of dark carbonaceous shale, which represents suspension sedimentation of muds under strongly anoxic redox conditions (Faure and Cole, 1999). It is overlain by transgressive marine shale with deep-water siliciclastic turbidites and tuffs being deposited in the southern part of the basin (Cairncross et al., 2005; Cole, 2010). The organic carbon content of the Ecca and Dwyka Group shales combined increases on average from 0.5 to 2.0% in the southern and central parts of the Karoo Basin and to 2 to 15% in the northern part of the basin (Rowsell and De Swardt, 1976). The higher values in the northern part were measured for carbonaceous shales adjacent to coal in the Vryheid Formation (Rowsell and De Swardt, 1976). Values for the Whitehill Formation, where reported, are relatively high, lying between 3 and 7% (Cole, 2010).

2.6.2 Adsorption on shales — studies from other parts of the world

Although it is still at a theoretical stage, CO_2 storage in gas shales is increasingly attracting a considerable amount of interest, particularly in those parts of the world that are endowed with extensive shale deposits, but limited CO_2 storage capacity in conventional porous reservoirs, such as the USA (Godec et al., 2012). Indeed, it has been shown that although widely known as an impermeable sedimentary rock with low porosity, organic shale has the ability to store significant amounts of gas permanently due to trapping of the gas in an adsorbed state within its finely dispersed organic matter also known as kerogen. Storage in organic shale has the added advantages that the organic matter acts as a molecular sieve allowing CO_2 — with linear molecular geometry — to reside in small pores that other naturally occurring gases cannot access (Kang et al., 2010). In addition, the molecular interaction energy between the organics and CO_2 molecules is different to other naturally occurring gases, which leads to its enhanced adsorption. Hence, the affinity

of shale to CO_2 is due to partly steric and thermodynamic effects similar to those of coals that are being considered for enhanced coalbed methane recovery (Kang et al., 2010). Organic-rich gas shales appear to behave similarly to coal and desorb methane while preferentially adsorbing CO_2 (Godec et al., 2012).

Nuttal et al. (2004) reported that initial estimates on the Devonian black shales in Kentucky for potential CO_2 indicate a sequestration capacity of 5.3 billion tons of CO_2 in the Lower Huron Member of the Ohio Shale of eastern Kentucky, and as much as 28 billion tons in total in the deeper and thicker parts of the Devonian shales. At Kentucky's current rate of power plant emissions, the organic-rich, black shales in the state could sequester more than 300 years' worth of the CO_2 produced, provided that they are made permeable for CO_2 injection by fracking (Nuttal et al., 2004). Total organic content determined from these Devonian shales range from 0.69 to 4.62%. Carbon dioxide adsorption capacities at 400 psi range from a low of 19 scf/ton in less organic zones to more than 86 scf/ton in the Lower Huron Member of the shale (Nuttal et al., 2004).

2.6.3 Effect of Total Organic Carbon (TOC) on the CO_2 adsorption of shales

It has been shown that organic carbon content plays a significant role in the adsorption of CO_2 in shales. A study conducted by Lu et al. (1993) on Devonian shales showed a strong linear correlation between adsorption capacities and total organic contents of shale samples, which indicates that gas solution on organic material is one of major mechanisms of adsorbed gas storage in shales. A strong correlation between CO_2 sorption capacity and TOC on the shale samples from the Paraná Basin, Brazil, has also been reported by Weigner et al. (2010) (Figure 2.6). Adsorption on shale is about an order of magnitude lower than the adsorption on coal (Chareonsuppanimit et al., 2012). This is due to the fact that coals have a much higher organic content than shales. This further illustrates the significant effect of TOC on the adsorption of CO_2 on both shales and coal. In a study by Cheng et al. (2004) the adsorption isotherms indicate that the total adsorption capacities of total hydrocarbon gases on geological material decrease successively in this order: shaly

coal, oil shale, montmorillonite and kaolinite. The effect of clay minerals is discussed in the next session.
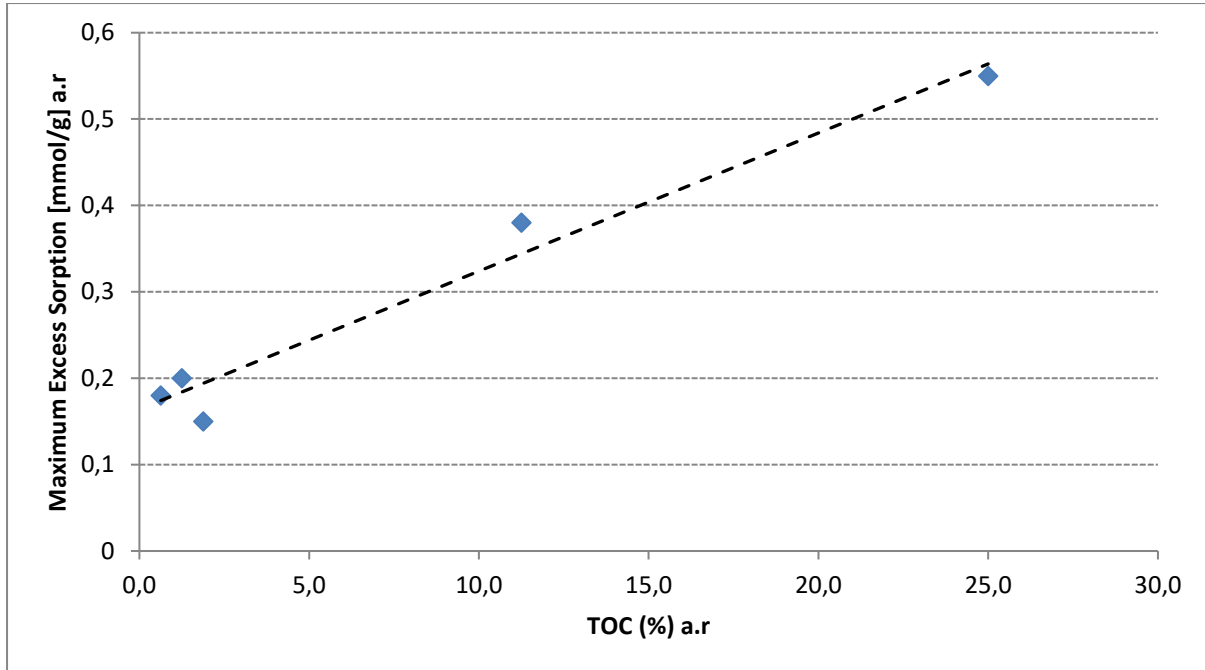
Figure 2.6. Maximum excess sorption for CO_2 (8–12 MPa pressure range, 45 ºC) vs TOC contents of shale samples from the CBM-001-ST-RS well and Permian (Irati) and Devonian (Ponta Grossa) shale samples. (Adapted from Weigner et al., 2010).

2.6.4 Effect of clay minerals on CO_2 adsorption of shales

TOC plays a significant role in the adsorption of CO_2 on shales. However, it has also been demonstrated by Lu et al. (1993) in a study on Devonian shale that shale samples with very low organic contents (less than 1% TOC) still have significant adsorbed gas storage. Since the main mineral compositions of Devonian shale are clay (mainly illite), carbonates and quartz, and since carbonates and quartz are non-absorbable for natural gas, illite may be the other factor for adsorbed gas storage; this was verified with adsorption isotherms (Lu et al., 1993). The adsorption isotherms for illite by Xiao-Chun et al. (1995) are shown in Figure 2.7.

In another study conducted by Busch et al. (2009) on Muderong shale it was observed that organic matter contents on these shales are low (0.5%) and therefore a major CO_2 uptake is most likely related to sorption on clay minerals. Looking at the individual clay minerals present in shales (e.g. smectite, illite, kaolinite, chlorite) sorption experiments were also performed on these materials and it was demonstrated that sorption capacities decrease with decreasing micropore volumes in the order smectite>illite>kaolinite>chlorite (Busch et al., 2009). Ross et al. (2009) also stated that clay minerals are capable of sorbing gas to their internal structure, the amount of which is dependent on the clay type. Furthermore, mercury porosimetry analyses show that total porosities are larger in clay-rich shales compared to silica-rich shales due to open porosity associated with the aluminosilicate fraction (Ross et al., 2009).
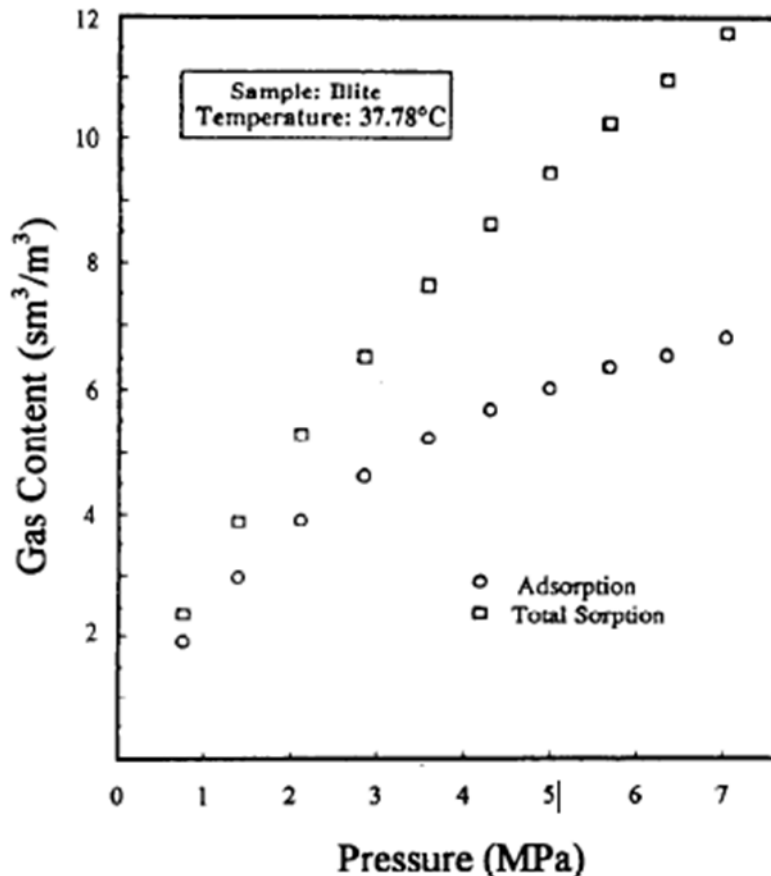
Figure 2.7. Illite adsorption and total sorption isotherms (Xiao-Chun Lu et al., 1995).

2.7 Bulk density

Bulk density in sedimentary rocks is essentially a function of the mineral composition, porosity and of the saturation. In general, the bulk density of sediment depends on the density of the mineral matrix, the pore volume (porosity) and density of fluids occupying the pore space. It indirectly provides a measure of the sediments porosity (Maillol, 2001).

Organic matter has a relatively low density and its presence therefore causes a decrease in bulk density relative to sediment with no organic matter, but the same rock matrix and porosity (Schwarzkopf, 1992).

Various studies have shown a trend of TOC content increasing with decreasing formation density. This trend has also been observed in the Ecca Group shales of the Karoo Basin, which are targeted for this study.

2.8 Kerogen maturation

Kerogen is generally defined as disseminated organic matter in sediments that is insoluble in normal petroleum solvents. It is a mixture of organic compounds (long-chain biopolymers) that contain carbon, hydrogen and oxygen with minor amounts of nitrogen and sulphur (Almashramah, 2011). The term is applied to organic matter in oil shales that yield oil upon heating and is regarded as the prime source for petroleum generation. In petroleum studies kerogen is classified into three basic types (I, II, and III) based on the ratio of C, H and O content (Almashramah, 2011). Type I kerogen is frequently associated with lacustrine organic matter, Type II can be associated with planktonic organic matter in open marine and freshwater lacustrine environments, and Type III with higher plants from a terrestrial input into lacustrine or marine settings (Vandenbroucke, 2007). Types I and II are predominantly oil-prone and Type III primarily generates gas and some waxy oil (Almashramah, 2011). Some workers state that Type II kerogen is both gas- and oil-prone.

The type of organic matter in shale samples has a significant effect on its capacity to adsorb hydrocarbon gases. In a study by Cheng (2004) it was observed that the gas retention capacity per gram of organic matter is greater for coal than for oil shale. This implies that the capacity of Type III organic matter, in general, is probably greater than that for Type I organic matter. Cheng (2004) reasoned that this speculation is reasonable given that Type III organic matter has a higher gas generative capability than Type I and, therefore, very likely has higher adsorption.
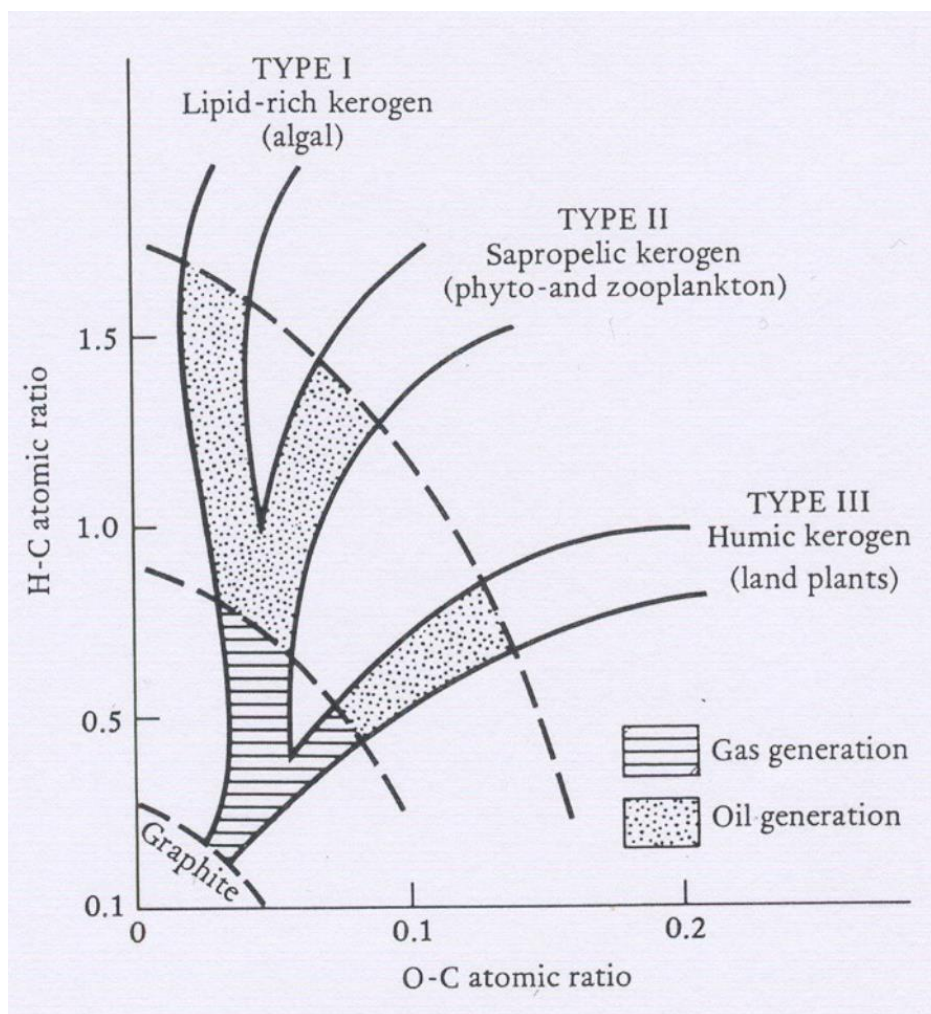
Figure 2.8. Diagram showing the maturation pathway of the three principal types of kerogen. (From Selley, 1985).

2.9 Kerogen maturity of the Ecca Group shales

According to a study conducted by Geel et al. (2013) in the Graystone (Eastern Cape) area of the Karoo Basin the lower Ecca Group has high Tmax values indicating over-maturity. The over-maturity can be attributed to the thermotectonic processes related to the Cape Orogeny overprint on lower Karoo rocks in the study area. It is possible that the maturity of the shales decreases farther north in the Karoo Basin (Geel et al., 2013). The study also observed that the Collingham and Whitehill formations both plot below the Kerogen Type II curve, a response due to thermal degradation. The Prince Albert Formation, on the other hand, falls within the

Kerogen III boundary. Kerogen II is derived from phytoplanktonic organisms and Kerogen III mostly from terrestrial organic matter (Geel et al., 2013).
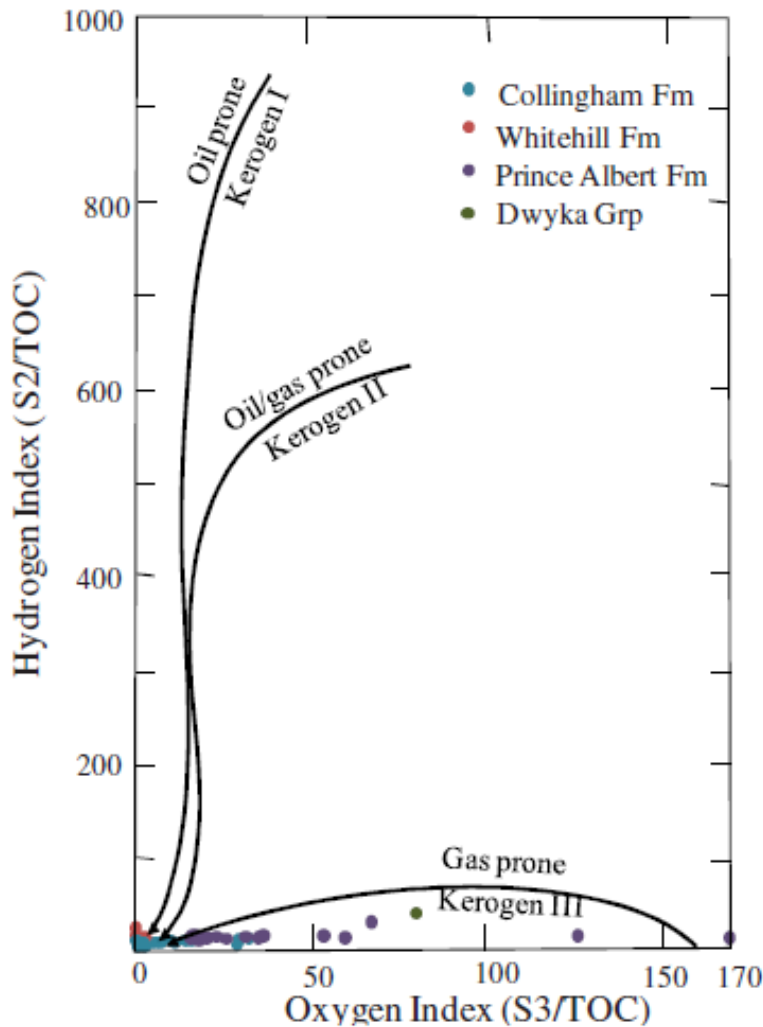
Figure 2.9. Plot of HI vs OI index in a modified Van Krevelam diagram. From Geel et al. (2013). This plot provides an indication of kerogen type. Aquatic organic matter has a high HI content whereas organic matter of terrestrial origin has a low HI, but high OI. The variations of HI values can be indicative of changing depositional settings.

2.10 Previous studies on South African shales

Hydrocarbon exploration of the Karoo Basin was undertaken by Soekor in the 1960s, with some reserves of gas being detected (Vermeulen, 2012). However, the resources were considered unviable at the time and no further exploration has been undertaken in the past 40 years (Vermeulen, 2012).

Currently, the Ecca Group shales of the Karoo Basin are targeted for shale gas exploration by a number of giant energy companies that have applied for exploration rights. The total organic carbon content of these Karoo shales ranges from 3 to 12% (Vermeulen, 2012). The contents of the Whitehill Formation (0.5–14.7% organic carbon content and a thickness of 1–72 m) and the Prince Albert Formation (0.35–12.4% organic carbon content and a thickness of 30–420 m) in the Karoo, obtained from Soekor data, compare favourably to the Marcellus shale (0.3–20% organic carbon content and a thickness of 12–270 m) and the Barnett shale (0.5–13% organic carbon content and a thickness of 15–300 m) in the USA (Vermeulen, 2012). The Marcellus and the Barnett shales have also been proved, through adsorption tests, to have a significant capacity to store CO_2. Table 1 and Figure 2.10 show the TOC values of some of the well-studied shale gas plays from other parts of the world and compare them with those of the Whitehill and Prince Albert formations of the Karoo Basin of South Africa.

Table 1. Table comparing Total Organic Content of shales from well-known shale plays from South Africa, Brazil and the United States (Sources: Kang et al., 2010, Weniger et al., 2010 and Vermeulen, 2012).

Shale or Play	Country/State	Average TOC (weight%)
Barnett	USA	4.00
Marcellus	USA	1–10.00
Haynesville	USA	0–8.00
Horn River	USA	3.00
Woodford	USA	5.00
Whitehill	SA	0.5–14.70
Prince Albert	SA	0.35–12.4
Ponta Grossa	Brazil	0.7–1.30
Irati	Brazil	2.3–26.30
Rio Bonito	Brazil	1.7–43.90
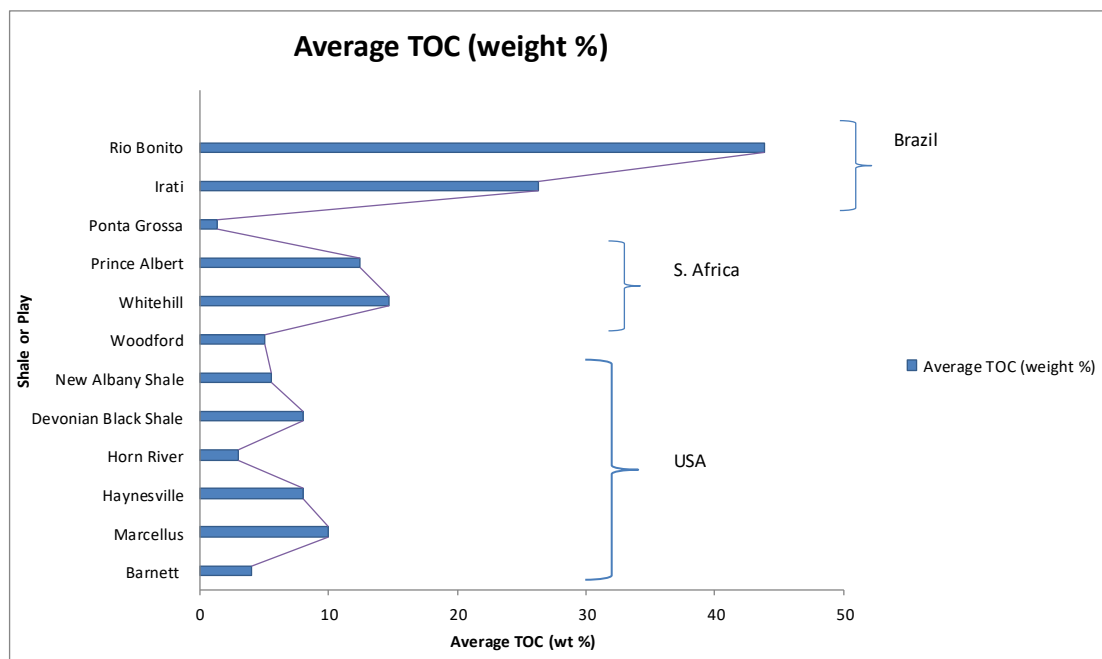
Figure 2.10. Graph showing the comparison of literature values of TOC content of the South African shales and those from the USA and Brazil (Sources: Kang et al., 2010; Weniger et al., 2010; Vermeulen, 2012).

2.11 Coals as analogues

It has been established that coal has quite a significant capacity to adsorb CO_2 (Fiaz et al., 2008). This is largely due to its high TOC content which is significantly higher than that found in shales. This section seeks to explore the various properties in coal that enhance its CO_2 adsorption capacity and to identify similarities with shales. Unlike shales, much research has been done on the coal properties and its CO_2 adsorption mechanisms are well understood. Carbon dioxide adsorption on coals can give valuable clues to the CO_2 adsorption on shales if the similarities in the physico-chemical properties between the two are well understood.

2.11.1 What is coal?

Coal is a combustible sedimentary rock composed of lithified plant debris. This plant debris was originally deposited in a swampy depositional environment (Suárez-Ruiz, 2012). The prolonged burial of the peat at depths of up to several kilometres, compaction, pressure and the influence of elevated temperatures for long periods of time (million years) are known as the coalification process that change peat into coal. Coal did not appear until the Devonian period due to the lack of terrestrial plants, although some organic matter derived from marine algae occurs in Precambrian sedimentary rocks (Suárez-Ruiz, 2012).

The quality of each coal deposit is determined by temperature and pressure and then by the length of time of formation, which is referred to as its 'organic maturity' (World Coal Institute, 2005). The degree of change undergone by plant matter as it matures from peat (plant material) to anthracite (coal) is known as coalification. The coalification process has an important bearing on the physical and chemical properties of coal and affects coal maturity, known as rank (World Coal Institute, 2005).

Low rank coals, such as lignite and sub-bituminous coals are typically softer than other coals, friable materials with a dull, earthy appearance. They are characterised by high moisture levels and low carbon content, and therefore low energy content. Higher ranking coals like anthracite are generally harder and stronger and often have

a black, vitreous lustre. They have a higher carbon content, lower moisture content and produce more energy (World Coal Institute, 2005).

2.11.2 Coal composition

The chemical properties of coal depend upon the proportions of the different constituents present in the parent vegetable mass, the nature and extent of the changes which these constituents have undergone since their deposition and the nature and quantity of the inorganic matter present (Francis, 1961).

Coal is not homogeneous; it is made up of organic and inorganic components (Stach et al., 2008). The building blocks of the carbonaceous component of coal are known as macerals. Macerals are microscopically recognisable components of coal and have different chemical compositions. They are distinguished from each other on the basis of their morphology, hardness, optical properties and chemical characteristics (Stach et al., 2008). There are three coal maceral groups which are vitrinite, inertinite and liptinite. Vitrinite is a product of the decomposition of cellular plant material while inertinite is a product of fossilised charcoal and liptinite comes from decayed leafy matter, spores, pollen and algal matter (Stach et al., 2008).

2.11.3 Mineral and trace element composition of coals

Minerals in coal occur in several forms and are quite variable in physical properties and chemical composition. The most abundant minerals in South African coals are clays, carbonates, sulphides, quartz and glauconite (Weniger et al., 2010). Phosphate minerals such as apatite are present as sub-microscopic grains except in some coals where they occur as discrete microscopic grains. They sometimes occur together with rutile and zircon (Falcon and Snyman, 1986). In a study by Weniger et al. (2010) on samples from the Paraná Basin in Brazil, XRD analysis revealed that the mineral matter is mostly composed of quartz, kaolinite and mica. There are also minor contributions of pyrite, ankerite, calcite, dolomite, albite and alunite. These minerals are of sedimentary and/or diagenetic origin.

Trace elements contribute greatly to the overall geochemistry of coal. More recently trace element composition of coal has been studied due to the growing concern over emissions of environmentally sensitive elements. The US 1990 Clean Air Act Amendments list As, Be, Cd, Co, Cr, Hg, Mn, Ni, Pb, Sb, Se and radionuclides as hazardous air pollutants (HAPs) (Pollock et al., 2000). Other trace elements that are associated with coals are Cu, Mo, V, Zn, Ba, B, Co, U, Th, Br and Cl (Pollock et al., 2000).

2.11.4 Kerogen classification (Type) of coal

Coal is usually classified as Type III kerogen (Suárez-Ruiz, 2012). Kerogen Type III is derived from higher plants and can be associated with terrestrial inputs into lacustrine or marine settings. Type III organic matter is also associated with gas generation.

2.11.5 CO_2 adsorption on coals

Adsorption is a process that occurs when a film of gas or liquid (adsorbate), molecules, adheres to the surface of a solid (adsorbent) (Kirk and Othmer, 1991a).

There are two types of adsorption namely physical and chemical sorption. Physical sorption occurs when non-balanced physical forces appear at the boundary of the

adsorbate and adsorbent. Chemical adsorption, on the other hand, occurs when molecules from adjacent phases form chemical bonds at the interface (Kirk and Othmer, 1991a).

The adsorption of CO_2 onto coal occurs by means of physical adsorption. Gas in bituminous coal is stored mainly as adsorbed molecules on micropore surfaces with diameters less than 2 nm (Fiaz et al., 2008). The volume of gas adsorbed in coal is largely a function of its internal surface area, type of gas, pressure and temperature (Fiaz et al., 2008). Coal can store considerably larger volumes of gas than conventional reservoirs such as sandstone at the same P-T (pressure-temperature) conditions due to its large internal surface areas (Fiaz et al., 2008).

At a given set of P-T conditions, CO_2 adsorption capacity is influenced by coal composition, rank and moisture content (Fiaz et al., 2008). Previous studies have shown that the CO_2 storage capacity is inversely proportional to mineral content and positively correlated with carbon content and coal rank (Fiaz et al., 2008).

2.11.6 Effect of mineral matter on CO_2 adsorption on coals

It has been mentioned in the previous section that mineral matter in coals in mainly composed of clays, carbonates, sulphides, quartz and glauconite. In a study conducted by Weigner et al. (2010) on coal samples from the Paraná Basin, considerable CO_2 sorption capacity (~0.183 mmol/g) with organic contents approaching zero was observed. This could be attributed to the mineral matter. Differences in mineralogical composition of the samples result in different CO_2 sorption capacities. For instance, pure clay minerals (kaolinite, montmorillonite and illite) have a significant sorption capacity for CO_2. Illite is reported to have a higher CO_2 sorption capacity than kaolinite (Weigner, 2010). The higher carbonate content of coals could also contribute to higher CO_2 sorption capacities through carbonate dissolution (Weigner, 2010). Carbon dioxide sorption in coals increases with increasing organic carbon content (Weigner, 2010).

2.11.7 Effect of maceral composition on CO_2 sorption on coals

The effect of maceral composition on CO_2 sorption on coals is attributed to the differences in microporosity of the macerals. Vitrinite is predominantly microporous, whereas inertinite rather meso- to microporous (Weigner, 2010). Adsorption isotherms indicate that in most cases bright (vitrinite-rich) coals have a greater adsorption capacity than their dull (often inertinite-rich) equivalents (Crosdale, 1998).

2.11.8 Effect of maturity on CO_2 sorption on coals

Previous studies have shown that CO_2 sorption capacity decreases with increasing rank (Weigner, 2010). With increasing thermal maturity from medium-volatile bituminous to anthracite rank, the microporosity of coal increases (Weigner, 2010). Since most of the physical adsorption takes place in the micropore structure of coal, the increase in microporosity with increasing rank is also considered to cause an increase in sorption capacity from medium-volatile bituminous coal to anthracite (Weigner, 2010).

2.11.9 Coal occurrences in the Karoo Basin

The Main Karoo Basin hosts the major coal resources of South Africa. Coal seams are present within the Permian Vryheid and Volksrust formations and the Middle Triassic Molteno Formation in the northern part of the basin (Cadle et al., 1993). Vryheid Formation coals are, on average, characterised by much higher contents of inertinite than northern hemisphere coals.

2.11.10 Summary

The adsorption of CO_2 on shales is significantly lower than on coals. The lower porosity and organic carbon content and higher ash content of shales results in reduced gas adsorption capacity in shales compared to coals (Chareonsuppanimit et al., 2012). TOC, as well as porosity, therefore play a critical role in the adsorption capacity in both shales and coals. Mineral matter and maturity are two other properties that have a significant influence on the gas adsorption capacity, both in shales and in coals. Coals have a higher adsorption capacity than shales largely due to their inherently higher organic carbon content compared to shales.

2.12 Adsorption isotherms

Adsorption isotherms are the most commonly used technique to determine the amount of gas a shale sample can hold at a particular temperature and pressure. The word "isotherm" refers to the volume of gas adsorbed on a solid surface as a function of pressure for a specific temperature, gas and solid material (Foo and Hammed, 2010).

A wide variety of equilibrium isotherm models have been developed over the years. These are described by Langmuir, Freundlich, Brunauer-Emmet-Teller, Redlich-Peterson, Dubini-Radushkevich, Temkin, Toth, Koble-Corrigan, Sips, Khan, Hill, Flory-Huggins and Radke-Prausnitz Isotherm (Foo and Hammed, 2010).

The Langmuir adsorption model is the most commonly used to describe the adsorption of gases on a solid.

The model is based on the following assumptions (Saghafi et al., 2007):

a) The surface of the absorbent is uniform.
b) Adsorbed molecules do not interact.
c) The adsorption mechanism remains the same until equilibrium is established, and
d) At maximum adsorption only a monolayer of adsorbate molecules is formed.

Graphically, the Langmuir Isotherm is characterised by a plateau — an equilibrium saturation point where once a molecule occupies a site, no further adsorption can take place (Foo and Hammed, 2010).

The simplified mathematical expression used for the Langmuir model is as follows:

$$N_e = \frac{(p_i - p_{eq})}{g_{sample}}$$

--- eq.1

$$V_{void} = V_{reactor} - V_{sample}$$

2.12.1 Low pressure CO$_2$ adsorption: pore characterisation (BET)

The pore structure is one of the major factors that control the gas capacity of shales and therefore is the key element in their characterisation and the assessment for their gas generating capacity (Cao et al., 2015). Porosity measurements and investigations of pore size distribution are critical in the study of unconventional resources (e.g. shale gas) and contribute to a better understanding of storage and migration pathways of hydrocarbons within fine-grained rocks (Furmann et al., 2014).

It is generally accepted that low pressure adsorption of CO$_2$ is useful for characterising microporosity (pore diameter < 2 nm), while low pressure adsorption of N$_2$ is useful for characterising meso- and macroporosity (Clarkson et al., 2013). Nitrogen cannot access the finest micropores at low temperatures. At -196 °C, N$_2$ lacks the required thermal energy to diffuse through the narrow constricted pore throats. Carbon dioxide, which is used at higher temperature and thus has greater thermal energy, can force through narrow passages and is believed to represent the 'truest' surface area, measuring microporosity and ultra-microporosity (e.g. < 0.5 nm diameter) (Ross et al., 2009).

The pore size terminology of the International Union of Pure and Applied Chemistry (IUPAC) was recommended for the geoscientists working on shales, with micropores

having less than 2 nm, mesopores between 2 and 50 nm, and macropores greater than 50 nm (Tian et al., 2015).

The IUPAC has classified the sorption isotherms into six types, designated I to VI.

The specific surface area (often referred as "BET surface area") can be calculated from the sorption curve based on the sorbed gas volume in a relative pressure (p/p_0) range of 0.05–0.35 using the Brunauer-Emmet-Teller (BET) method. The specific surface area can be defined as the space site where the gas is sorbed onto the surface of solid particles and is therefore an indicator of the sorption capacity of shales (Cao et al., 2015).

2.12.2 High pressure CO_2 adsorption

There are two most commonly used methods for studying gas sorption equilibria at high pressures: 1) the manometric (commonly referred to as the volumetric method) and the 2) gravimetric methods. The experimentally determined quantity (irrespective of the method used) is the "excess sorption" or "Gibbs surface excess". The uptake of gas by the sorbent is determined at constant temperature and as a function of gas pressure (or density) giving the excess sorption isotherm (Gasparik et al., 2014).

The gravimetric method makes use of the direct measurement of mass change of a sample being exposed to sorptive gas at constant temperature at varying pressures. The current gravimetric devices utilise either a high precision microbalance or a magnetic suspension balance for mass measurements down to sub-µg resolution (Gasparik et al., 2014). In the manometric method, on the other hand, the uptake of gas is measured by monitoring the drop in pressure in a fixed known volume containing the adsorbent sample. The measuring device consists of a reference cell (RC) and a sample cell (SC) with calibrated volumes equipped with a high precision pressure sensor kept at constant temperature conditions. The measurement is done by successively transferring the sorptive gas through the reference cell into the sample cell containing the absorbent sample. The excess sorption is then calculated as the difference between the total amount of gas transferred into the sample cell and the unabsorbed gas occupying the void volume of the sample cell (Gasparik et

al., 2014). The diagram below (Figure 2.11) shows a manometric set-up that was adopted for this study.

Unlike in the manometric method, in the gravimetric method the leakage does not affect the measurement accuracy as long as the pressure in the sample cell can be kept constant. However, the accuracy of the gravimetric technique on materials with relatively low sorption capacity (such as shales) is compromised at high pressures (>10 MPa) due to a large contribution from buoyancy, especially for devices limited to small (< 1 g) sample amounts (Gasparik et al., 2014). The gravimetric method is also usually more costly and its equipment requires high level expertise to operate. Therefore, the volumetric technique was chosen for this study.
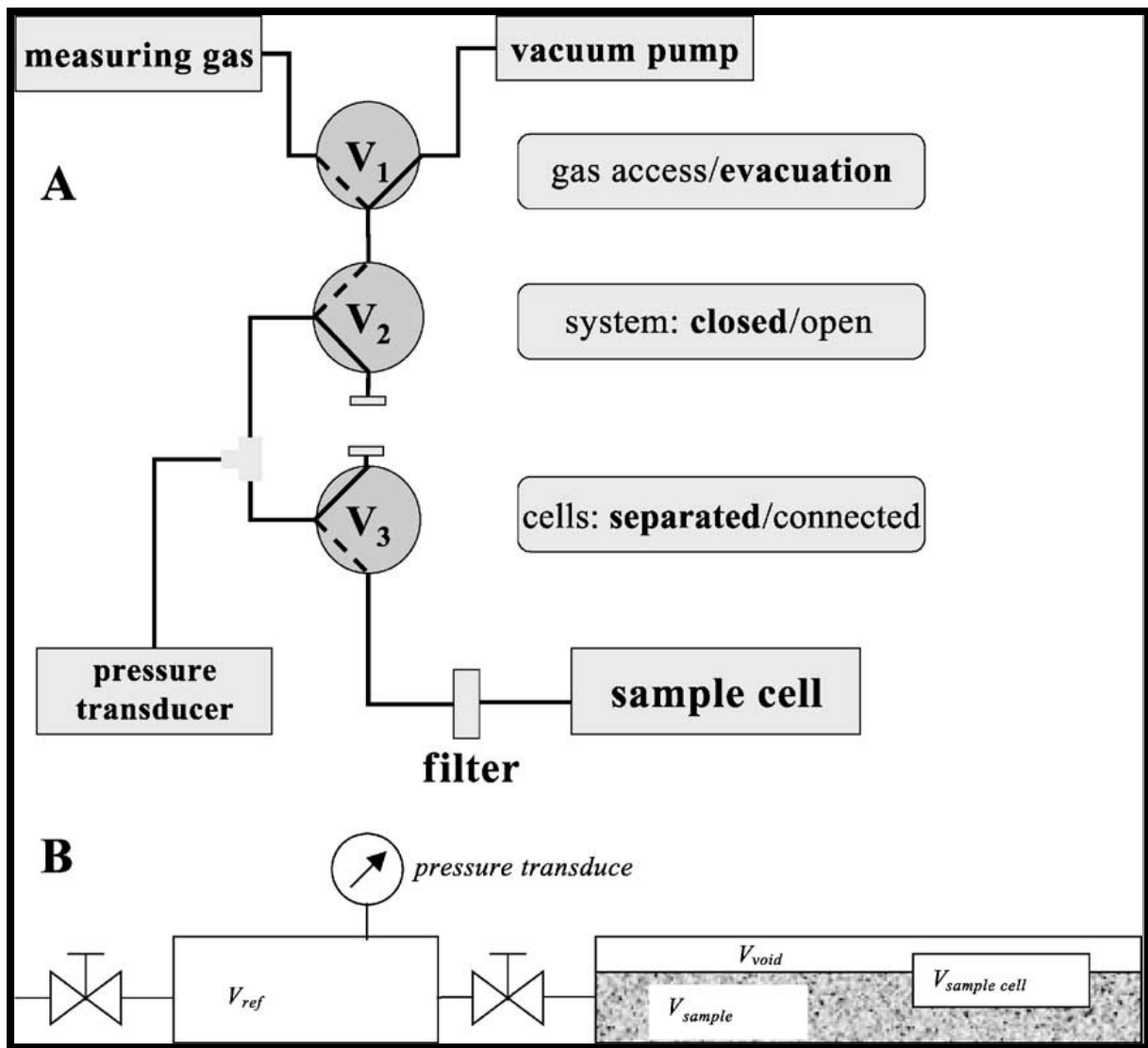
Figure 2.11. Schematic diagram of the experimental set-up for CO_2 adsorption on shale samples. (Source: Krooss et al., 2002).

2.12.3 The establishment of equilibrium

Adsorption equilibrium (the ratio between the adsorbed amount of gas and the amount remaining in the solution) is established when an adsorbate containing phase is in contact with the adsorbent for sufficient time, whereby its adsorbate concentration in the bulk solution is in a dynamic balance with the interface concentration (Foo and Hameed, 2010). The establishment of equilibrium in the

manometric method is inferred by monitoring the changes in pressure. No general criteria or recommendations were found in the literature with respect to equilibrium times. However, Gasparik et al. (2014) argues that insufficient equilibration times will lead to an underestimation of the sorption capacity and possibly some effect on the isotherm shape. For samples with a significant proportion of pores in the nano-scale range, the equilibrium process can be very lengthy and a true equilibrium may never be reached in an experiment due to kinetic restrictions. It is important, however, to define at least a "technical equilibrium" meaning that the measured pressure (or mass) changes should be of the same order of magnitude as the changes due to temperature fluctuations (resolution limit) over a sufficiently long time interval (Gasparik et al., 2014). Powdered samples can be used in sorption experiments to minimise the equilibration time and reduce the duration of the experiments (Amann et al., 2011). Substantially long equilibration times require a very good leak-tightness of the set-up (Gasparik et al., 2014). At low pressures, the equilibration process is considerably longer than at high pressures. Accordingly, the equilibration times should be initially sufficiently long in order to approach the thermodynamic equilibrium as closely as possible, while they can be reduced with the progression of the experiments (depending on the uptake kinetics) in order to minimise the effect of leakage (Gasparik et al., 2014).

2.12.4 The effect of moisture

The moisture content of the samples influences the sorption capacity quite significantly. On the one hand, the CO_2 uptake increases by dissolution of CO_2 in the water, on the other hand, a competitive adsorption between the water molecules and the CO_2 decreases the sorption capacity (Amman et al., 2011). Samples also need to be degassed prior to the experiment to get rid of the moisture and of other volatiles.

2.12.5 The effect of temperature on excess sorption capacity

The maximum sorption capacity decreases with increasing temperature (Li et al., 2010). Li et al. (2010) noted that isotherms recorded at different temperatures converge at elevated pressures (> 20 MPa) and suggest that this indicates that the temperature dependence of the excess sorption isotherms nearly vanishes in this pressure range. In the low pressure range, CO_2 excess sorption isotherms show normal temperature behaviour, i.e. the sorption capacity increases with decreasing temperature. As mentioned earlier, at higher pressures (> 20 MPa) the temperature dependence of excess sorption isotherms decreases to nearly zero, thus higher temperatures will be preferable for storage. In the Li et al. (2010) study on coal, one set of isotherms was measured at 35 °C (308.15 K), which is very close to the critical temperature of CO_2 (T_c = 304.13 K; P_c = 7.38 MPa) and closer to realistic reservoir conditions for coal (P > 8 MPa, T > 35 °C).

2.12.6 Adsorption isotherm models

Sorption isotherms relate to the gas storage capacity of a coal or shale as a function of pressure. The data obtained from sorption isotherms can be used to predict the maximum volume of gas that can be stored in the reservoir rock during injection, or the amount that can be produced from the rock when the pressure is depleted (Godec, 2013). Different isotherms are characteristic of different gases. Adsorption isotherms are presented on a curve as a volume of gas per unit of coal or shale mass, at various pressures (Godec, 2013).

The Langmuir model appears best suitable for the purpose of this study. Unlike other equations used by other researchers, the Langmuir equation uses only two experimental parameters and therefore reduces the processing and computation time (Saghafi, 2010). The Brunauer-Emmett-Teller (BET) model is used in this study for low pressure CO_2 adsorption (Section 4.9). This model assumes monolayer adsorption, whereby adsorption can only occur at a finite (fixed) number of definite localised sites that are identical and equivalent to one another with no lateral interaction and steric hindrance between adsorbed molecules, even on adjacent

sites (Foo and Hameed, 2010). Graphically it is characterised by a plateau built when the equilibrium saturation point is reached; where once a molecule occupies a site no further adsorption can take place (Foo and Hameed, 2010).

CHAPTER THREE: EXPERIMENTAL WORK AND CHARACTERISATION

3.1 Samples

The shale and siltstone samples were sampled from the old Soekor deep boreholes that are archived at the Council for Geoscience's National Core Library situated in Donkerhoek, east of Pretoria. Five boreholes, namely KL 1/65, LA 1/67, SW 1/67, G39974 and BE 1/67 were selected, logged and sampled (Figures 3.1 and 3.2). Six samples were selected for analysis on physico-chemical properties and adsorption (both low and high pressure adsorption) behaviour. Geographical representation, lithology and organic content are three of the key factors taken into account when choosing the samples. The samples were classified according to their level of darkness using the Munsel rock colour chart where N1 is the darkest and N5 the lightest. The darkest samples are deemed to be high in organic content, whereas the lighter (N4–5) are suspected to be the least carbonaceous. The boreholes were drilled more than 40 years ago. As a result, most of them are now weathered and broken into pieces with only small portions of intact core with relatively less weathering (Figures 3.3 and 3.4).
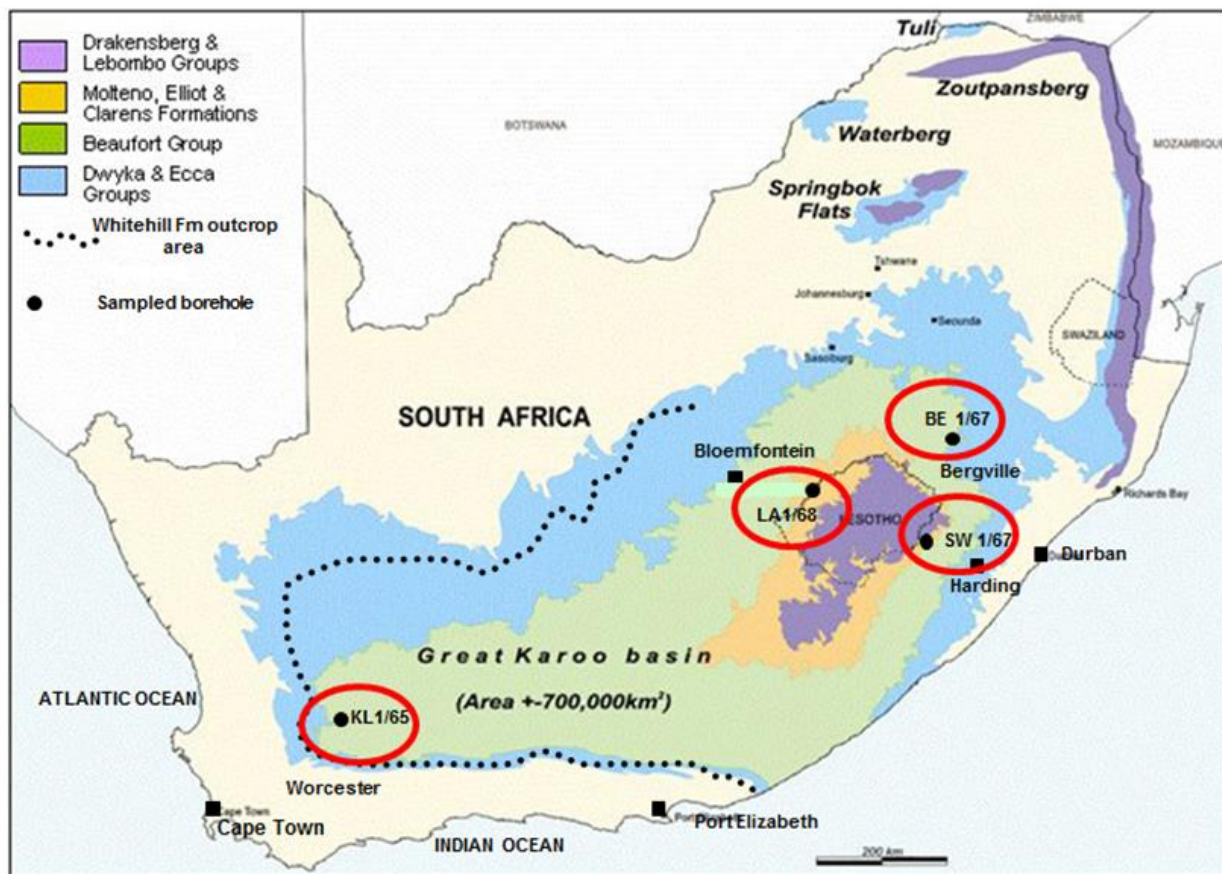
Figure 3.1. Map showing the geographic position of the sampled boreholes. (Adapted from Petroleum Agency SA, 2010).
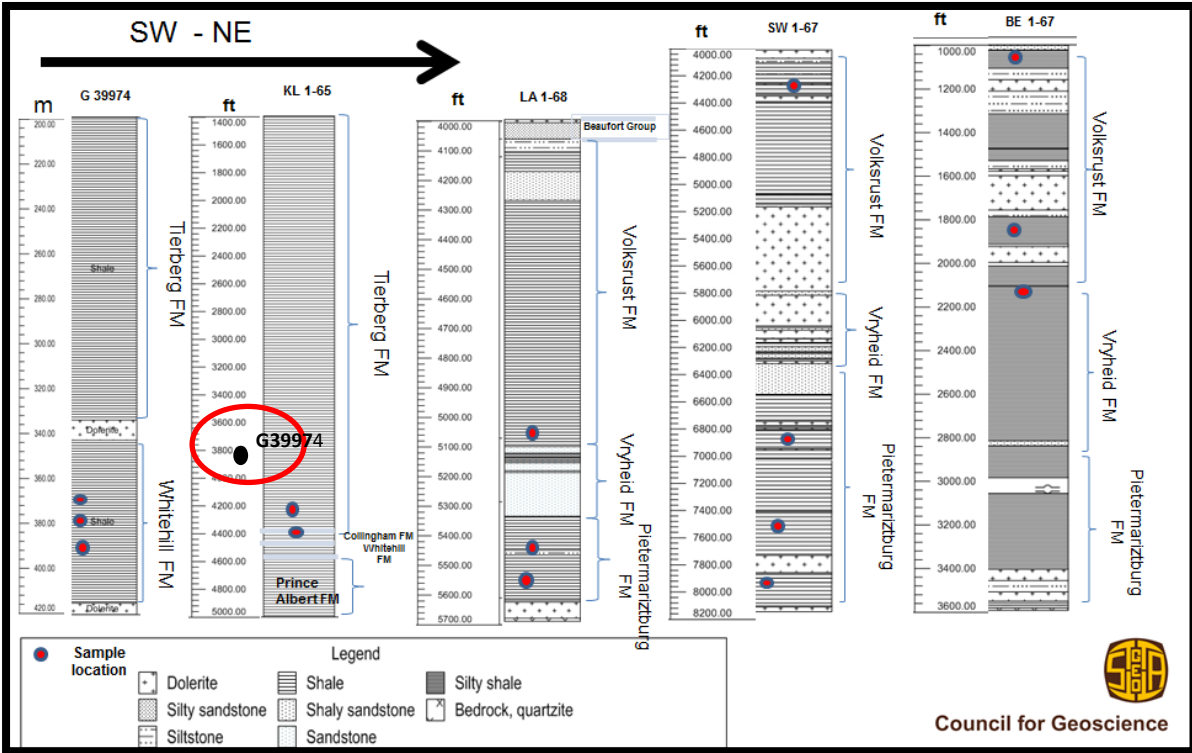
Figure 3.2. Borehole logs for the five sampled boreholes.

Figure 3.3. Core trays laid out at the National Core Library for the sampling phase. The core is mostly broken and disaggregated, but portions of intact core could be found in places.

Figure 3.4. Photograph showing a closer view of the weathered and broken core.

3.2 Lithological description of the boreholes

The lithology intersected by these boreholes is mainly of shales of the Ecca Group. These shales are generally dark-grey to greyish black in colour. Sandstone lenses have also been encountered in the Vryheid and Volksrust formations boreholes situated in the north-eastern Karoo Basin. The sandstone units are mostly interbedded with argillaceous siltstone. The cores also show multiple dolerite intrusions into the Ecca Group shales. These dolerite intrusions have caused a severe thermal alteration resulting in baked mudstones, spotted slate, etc. Calcite and pyrite alteration are also associated with the intrusions (Proedrou, 1971). The shales are mainly micaceous, bioturbated in places with sporadic calcite and pyrite veins. The shales of the Prince Albert and Whitehill formations appear to be of significantly higher carbon content than their light-grey north-eastern counterparts.

3.3 Characterisation of the shale samples

X-ray diffraction (XRD) analysis was used to determine the mineral composition of the shale samples. The elemental concentration and composition were determined by means of X-ray fluorescence (XRF). Total organic carbon (TOC) analysis was also conducted to determine the content of organic carbon in the samples, while the scanning electron microscope (SEM) coupled with an energy dispersive system (EDS) were used to determine the morphology of the grains and mineralogy. The High Pressure Volumetric Adsorption System (VAS) was used to measure the CO_2 adsorption capacity of the shale samples, while BET was used to measure micropore volume and surface area.

3.3.1 X-ray powder diffraction

The mineral composition primarily reflects the depositional environments and digenetic evolution of the shales during their sedimentation and maturation and is an important factor in the physical properties of the shales (Cao et al., 2015).

The samples were prepared according to the standardised PANalytical backloading system, which provides nearly random distribution of the particles.

The samples were analysed using a PANalytical X'Pert Pro powder diffractometer in θ–θ configuration with an X'Celerator detector and variable divergence and fixed receiving slits with Fe filtered Co-Kα radiation (λ=1.789Å). The phases were identified using X'Pert Highscore plus software. The diffraction traces with the identified phases follow below.

The relative phase amounts weight% was estimated using the Rietveld method (Autoquan program). The analyses were performed at the Council for Geoscience Laboratory.

3.3.2 X-ray fluorescence (XRF)

XRF was used to determine the major and trace element composition of the shale samples. The samples were crushed and milled. For major element analysis the milled sample (< 75 μ fraction) was roasted at 1 000 °C for at least three hours to oxidise Fe_2+ and S and to determine the loss of ignition (LOI). Glass disks were prepared by fusing 1.00 g roasted sample and 9.50 g flux consisting of 70.69% $Li_2B_4O_7$, 19.79% $LiBO_2$ and 0.50% LiI at 950 °C. For trace element analysis 12.00 g milled sample and 3.00 g Hoechst wax was mixed and pressed into a powder briquette by a hydraulic press with applied pressure at 25 tons. The glass disks and wax pellets were analysed by a PANalytical Axios X-ray fluorescence spectrometer equipped with a 4 kW Rh tube. The analyses were performed at the Council for Geoscience Laboratory.

3.3.3 Petrography

Petrographic sample preparation and analysis were conducted at the Council for Geoscience with the use of a Leica petrographic microscope with an inbuilt camera and software that enables capturing of photomicrographs. The analyses were conducted under x40 magnification.

3.3.4 Scanning electron microscopy

A SEM/EDS study was carried out at the Council for Geoscience XRD Laboratory on a Leica Stereoscan 440 SEM linked to an OXFORD INCA EDS (Energy Dispersive System). The system is equipped with an Oxford X-Max SDD detector with a 20 mm^2 active area and resolution of ca. 128eV for Mn K-a (5 895 eV) and has the capabilities for secondary, backscattered and cathodoluminescence electron imaging, X-ray EDS microanalysis and X-ray element mapping.

3.3.5 Total organic carbon

TOC analyses were conducted at Mintek by direct combustion, where the CO_3 was leached from the sample portion using diluted HCl. The acid and water are removed by vacuum filtration. The dry residue is mixed with a metal accelerator and combusted using a high frequency combustion furnace and total C — which represents organic carbon — determined from it by combustion.

3.3.6 Vitrinite reflectance — thermal maturity determination

Six block mounts were prepared at the Council for Geoscience Petrography Laboratory and submitted to the Department of Geology at the University of Johannesburg for vitrinite reflectance analysis, conducted by Professor Nicola Wagner. The polished blocks were analysed using a Zeiss Axio Imager petrographic microscope fitted with a Hilgers Fossil system for vitrinite reflectance. As there is no South African standard for vitrinite reflectance determination on dispersed organic shales, ASTM standard D7708-14 applies. The analyses were conducted at a magnification of x500 under reflected light with oil immersion. The number of readings taken is largely based on the amount of suitable carbon material available in the sample. The microscope was calibrated using YAG 0.9 and ST 5.37 calibration standards and cross-checked with internal standards at 0.99 and 1.63. Mean random reflectance values were obtained, as well as representative histograms to determine

reflectance value distribution. Photographs of each sample were taken at a magnification of x500 (scale bar included on image) under reflected light using an oil immersion lens.

3.3.7 Low pressure CO_2 adsorption measurements

Low pressure CO_2 adsorption using BET analysis was performed at the University of North West. This technique is used to measure micropore volume. Prior to CO_2 adsorption, the samples (about 0.20 g each) were degassed under vacuum (10.00 µmHg) in order to eliminate moisture or condensed volatiles, which could prevent the adsorbate accessibility. Degassing of the samples was done at ambient temperature (25 °C) for 48 hours to avoid the release of volatiles. The evacuated samples were analysed at 0 °C in an ice bath. The results were processed using the ASAP 2020 V3.01 software linked to the facility at the University of North West. The ASAP 2020 uses two independent vacuum systems, one for sample analysis and the other for sample preparation. This allows preparation and analysis to proceed simultaneously without the inherent delay found in single vacuum system analysers that must share a vacuum pump.

3.3.8 High pressure CO_2 adsorption measurement

3.3.8.1 Adsorption experimental procedure

The adsorption experiments were conducted at the Illinois State Geological Survey (ISGS) with the set-up shown in Figure 3.5 and the following procedure:
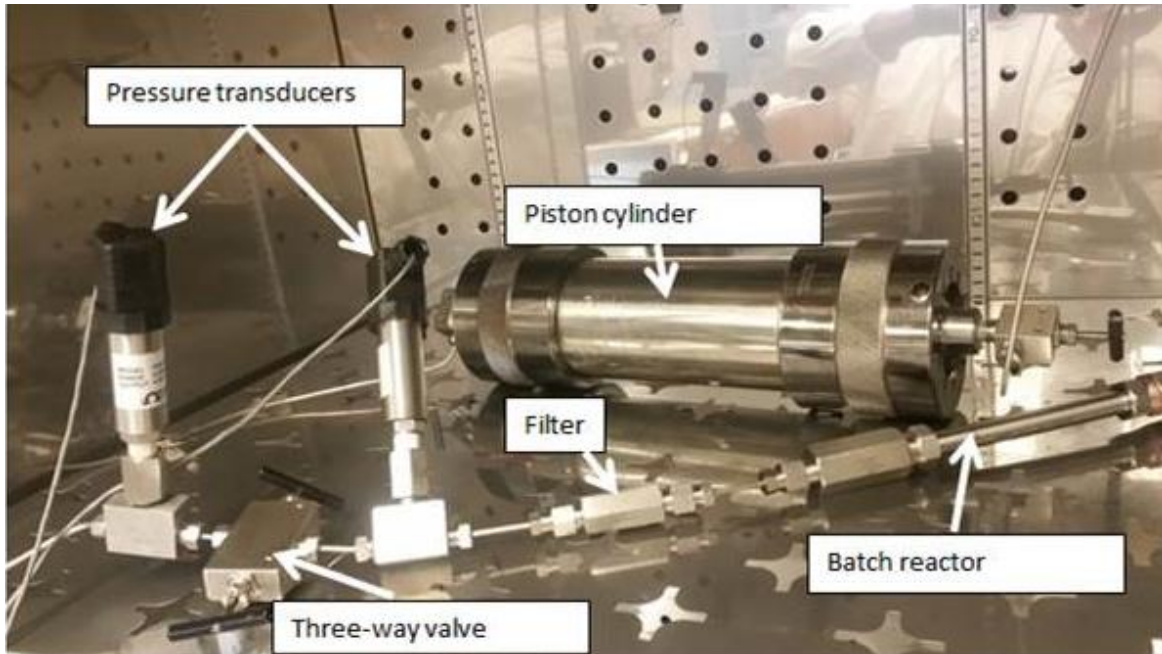
Figure 3.5. Photograph showing the volumetric adsorption system set-up used in this study. This is housed in an oven which maintains the desired temperature during the course of the experiment. There is also an external pump which pumps CO_2 into the piston cylinder and maintains the desired pressure (ISGS).

- It is a requirement in adsorption tests that the samples be degassed before the experiment to remove any surface moisture and any adsorbed gases in the shale samples.
- A known volume of the degassed solid sample is transferred into the batch reactor and the reactor attached to the rest of the assembly.

- The entire system is evacuated to ensure that there are no gases in the system before adsorption and to establish a defined starting point.

- The oven is set to the desired temperature which is held constant for the duration of the experiment.

- The system is then allowed to equilibrate.

- During the experiment, a certain amount of gas is charged into the reference cell.

- Pressure is allowed to equilibrate in the reference cell (this normally takes about 30 seconds).

- The valve separating the reference cell and the sample cell is then opened and CO_2 is admitted into the sample cell.

- The pressure starts to drop in the sample cell and equilibrates after about 30 seconds. Further pressure drop in the sample cell is interpreted as being due to the CO_2 being adsorbed onto the shale sample.

- By measuring the pressures and temperatures before and after gas expansion, the gas molar densities at different stages can be calculated with an appropriate equation of state (EOS) and the amount of gas adsorbed at one pressure level can be determined. The isotherm is obtained by repeating these procedures until the measurement at the highest desired gas pressure is achieved (Xiao-Chun Lu et al., 1994).

CHAPTER FOUR: RESULTS AND DISCUSSION

4.1 Introduction

One of the key objectives of this study is to characterise the physico-chemical properties of the shale and siltstone samples in order to understand their effect on the shale CO_2 sorption behaviour. The following physico-chemical properties were therefore tested:

- Elemental composition (XRF — both major and trace elements)
- Mineralogy (XRD)
- Petrography
- Scanning Electron Microscopy (SEM)
- Total Organic Carbon (TOC)
- Vitrinite Reflectance
- Bulk Density
- Kerogen Maturation
- Low Pressure CO_2 Adsorption (BET), and
- High pressure volumetric adsorption.

The interpretations of each of these properties are discussed individually to allow clarity as to each property's influence on the shales' potential to store CO_2.

4.2 Elemental composition (XRF) results

4.2.1 Major elements (geochemistry)

Major elements concentrations are shown in the table below (Table 2). SiO_2 has the highest concentration across all the samples with an average of 61.41%. This is followed by Al_2O_3 with an average concentration of 18.70%. Fe_2O_3 and K_2O have average concentrations of 6.16% and 2.88%, respectively.

Table 2: The major element concentrations as determined by XRF analysis of the six samples.

Sample Elements	1124'50	5434'20	5560'00	7534'04	389.30	4794.10
SiO2	66.88	60.71	58.35	60.52	55.16	66.81
TiO2	0.65	0.91	0.99	0.95	0.74	0.67
Al2O3	17.24	19.69	21.04	20.19	17.03	17.03
Fe2O3	4.89	5.06	7.07	6.72	6.82	6.38
MnO	0.06	0.05	0.06	0.11	0.08	0.16
MgO	1.64	1.71	2.13	1.42	3.29	1.01
CaO	0.78	0.63	0.24	0.64	0.99	0.14
Na2O	2.31	1.85	2.03	1.15	1.70	0.87
K2O	2.87	2.77	2.68	2.24	3.77	2.95
P2O5	0.17	0.11	0.13	0.34	0.28	0.08
Cr2O3	0.01	0.02	0.03	0.015	0.01	0.01
LOI	2.51	5.54	4.28	6.06	9.35	4.14
Total	100.01	99.04	99.03	100.38	99.22	100.25
H2O-	0.39	1.19	0.85	0.54	0.59	0.54

4.2.2 Major element correlation

The correlations between Al_2O_3, MgO, K_2O and FeO_3 are very poor (Figure 4.1). There is a strong positive correlation between Al_2O_3 and TiO_2 which may demonstrate that Ti originates from a mixed clay assemblage. The poor correlation between Al_2O_3, MgO and K_2O may suggest that these elements are not associated with aluminous clay minerals such as illite.
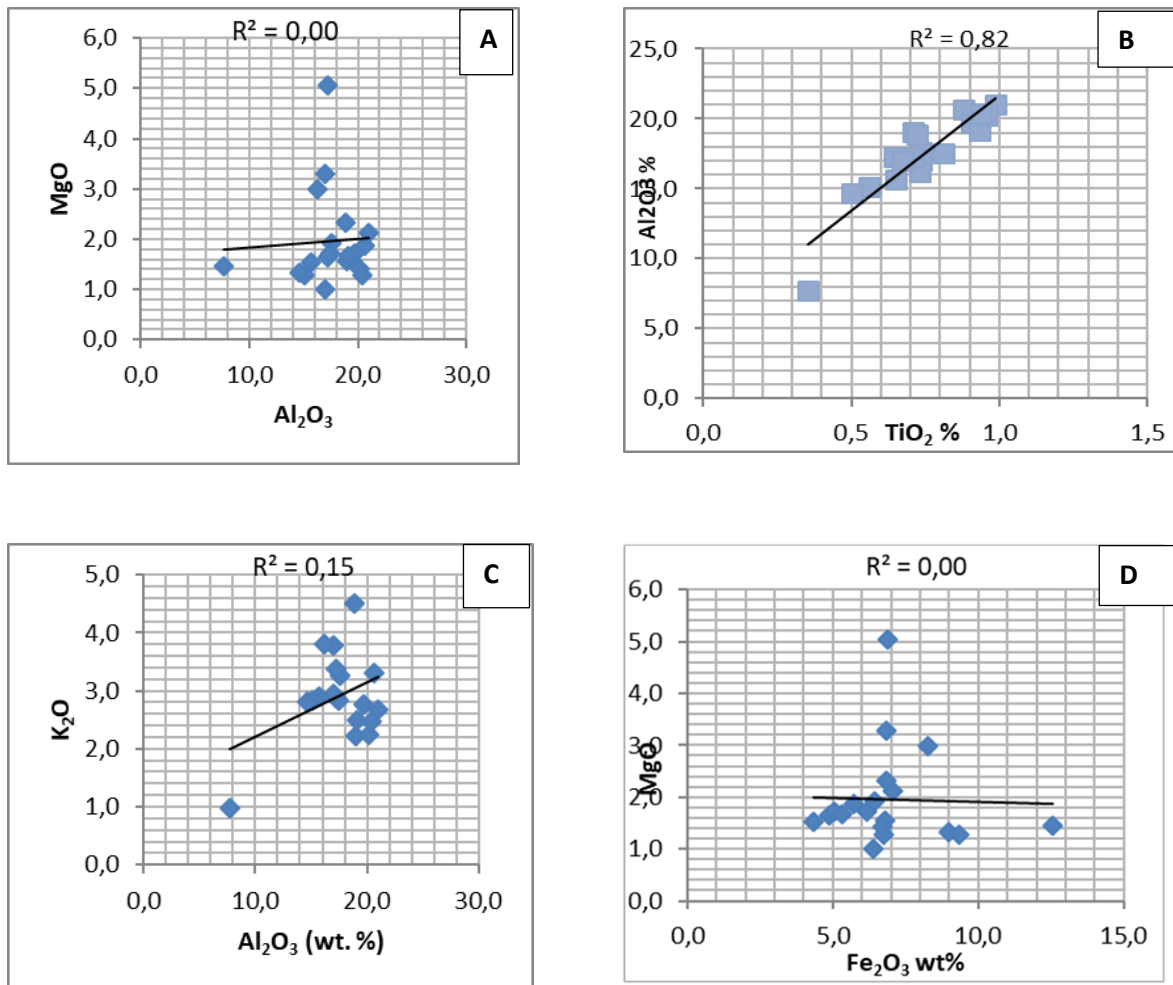
Figure 4.1. Plots showing the correlations between various elements in an attempt to decipher any associations. The following associations are plotted on the graphs: **A:** Al_2O_3 *vs.* MgO; **B**: TiO_2 *vs.* Al_2O_3; **C**: Al_2O_3 *vs.* K_2O; **D**: Fe_2O_3 *vs.* MgO plots.

4.3 Mineralogy (XRD)

Results for XRD analyses for the six samples are recorded in Table 3.

Quartz is a dominant phase in all the samples with an average wt.% of 42.40, and the highest value of 60.29 recorded in sample 4794.10. This is followed by muscovite with an average of 18.34 wt.%. Plagioclase also occurs in significant quantities averaging at 14.00 wt.%, with the highest value of 24.33 wt.% recorded in sample 389.3. Chlorite occurs in all the samples, except for sample 389.30, at an average of 4.71 wt.%. The highest chlorite content of 12.08 wt.% was recorded in sample 1124.50. Biotite occurs in samples 389.30, 4794.10 and 5434.2 with 12.93, 6.33 and 4.56 wt.%, respectively. Microcline occurs in samples 389.3, 5434.2, 5560.0 and 7534.04, at an average of 3.05 wt.%. Sample 389.30 has the highest value of 8.13 wt.%. Kaolinite only occurs in samples 1124.50, 4794.1, 5434.2, 5560 and 7534.04 at an average of 9.01 wt.%. Gypsum is only present in sample 389.3 with 20.42 wt.%. Smectite only occurs in sample 5434.2 with 26.72 wt.%.

Table 3: XRD results as semi-quantitative estimates of the phase abundances expressed in wt.%.

Sample Number	Biotite	Chlorite	Gypsum	Kaolinite	Microcline	Muscovite	Plagioclase	Quartz	Smectite
389.3	12.93	0.00	20.42	0.00	8.13	20.42	24.33	33.59	0.00
1124.5	0.00	12.08	0.00	8.31	0.00	15.62	18.39	45.60	0.00
4794.1	6.33	3.23	0.00	8.63	0.00	10.27	11.25	60.29	0.00
5434.2	4.56	5.39	0.00	9.04	4.64	10.01	8.19	31.45	26.72
5560	0.00	7.61	0.00	13.42	2.69	27.08	14.61	34.58	0.00
7534.04	0.00	0.00	0.00	14.63	2.83	26.66	7.01	48.87	0.00

4.4 Petrography

4.4.1 Sample 1124.50

This sample is a siltstone under the microscope. The sample consists of elongated detrital mica flakes embedded in a matrix that varies from indurated silica cement to clay rich. Most clay minerals present in the sample are diagenetic and might have come from the alteration of feldspars. Angular quartz grains also occur scattered throughout the matrix. The quartz grains are held together by the silica cement. Secondary haematite is also seen occurring in small crystals, although it is not very distinct. The haematite sits in small veins which suggests that there was some fluid movement after lithification. Chlorite was also recorded, which indicates regional low-grade metamorphism. Calcite was also seen filling some small joints. The rock does not appear to be strongly weathered. Compaction is not very pronounced either. The rock is well laminated, with several laminae seen alternating with organic matter. Elongate plant remains are also recorded. No visible porosity is present in the thin section. The elongate plant fragments do not show any preferred orientation, which is interpreted to indicate that compaction was very low. No folding or schistosity was observed. Usually such sediment is strongly compacted. The apparent lack of strong compaction might be due to early silicification.
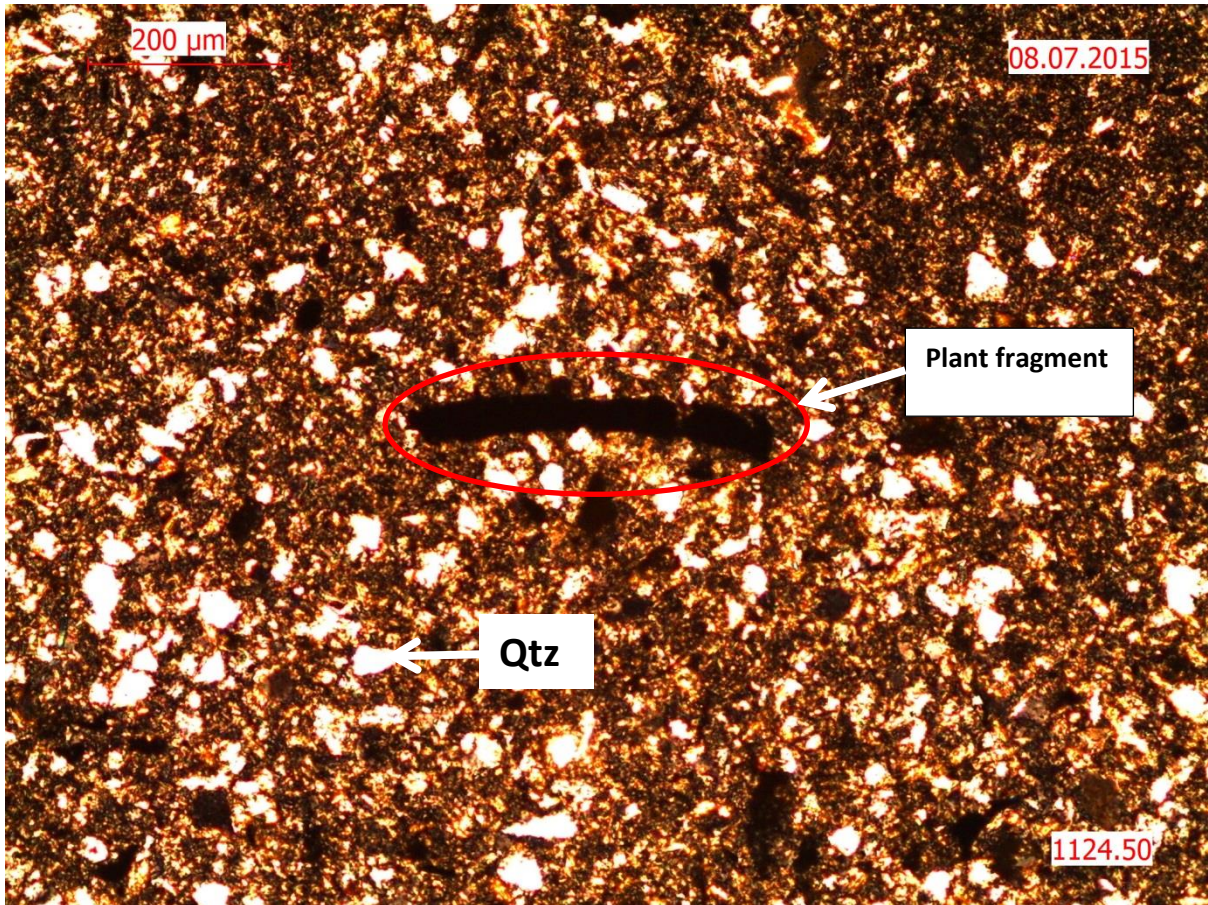
Figure 4.2. Photomicrograph of sample 1124.50, siltstone in cross-polarised light with oil immersion to enhance the field of view. This photomicrograph shows angular quartz grains scattered in a fine-grained matrix that appears to be enriched in clay minerals and organic matter. Note the elongate fragment of what appears to be a plant remain.

4.4.2 Sample 5560

This rock is very similar to sample 1124.50 described above. It is also a siltstone. The rock has abundant clay minerals. A single angular structure interpreted to be a plant fragment was observed under the microscope. The rock shows very low compaction and faint lamination. No porosity or permeability are discernible in the thin section. Small patches of haematite hint towards the presence of iron (Fe) in the diagenetic environment.
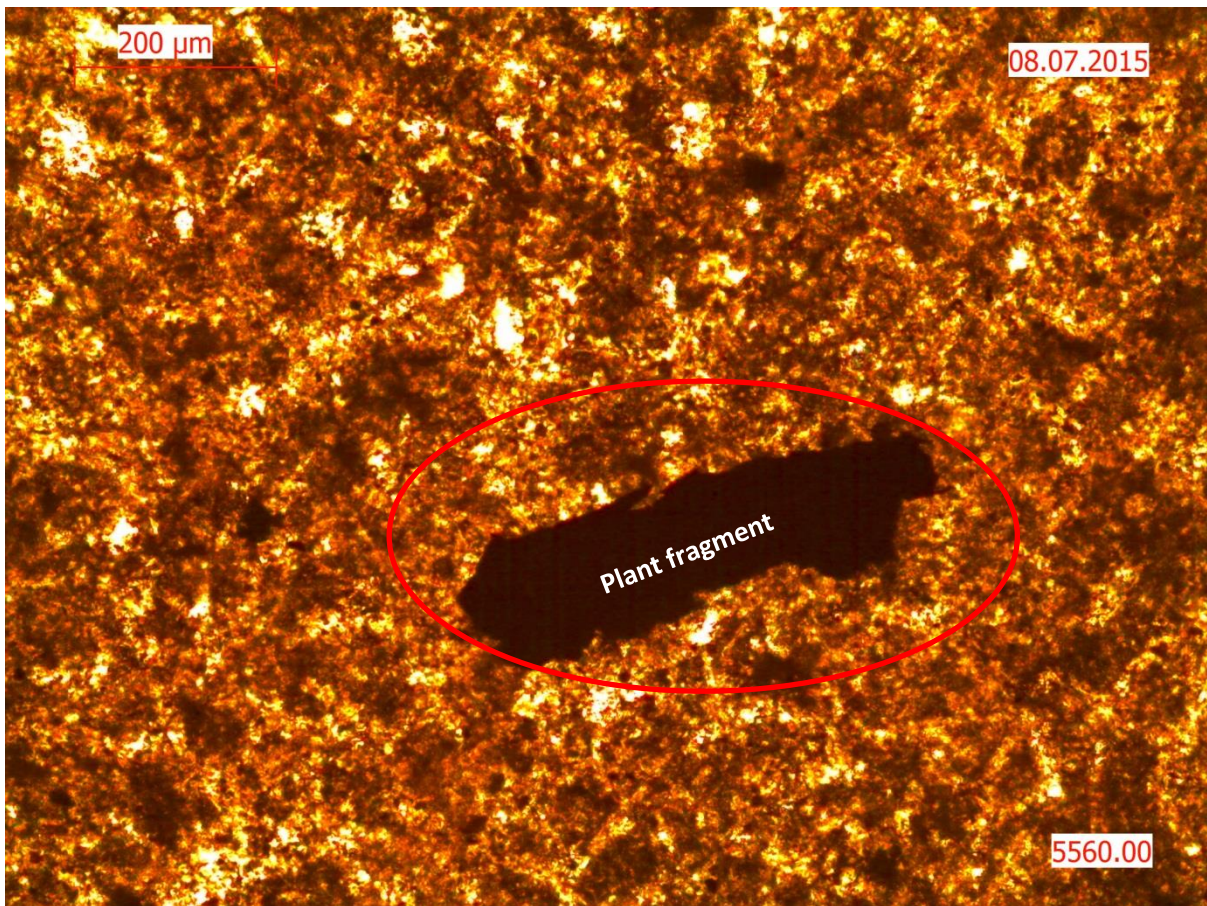
Figure 4.3. Photomicrograph for sample 5560 in cross-polarised light with oil immersion showing a fine-grained clay-rich matrix interspersed with fine-grained anhedral quartz grains and occasional plant fragments.

4.4.3 Sample 5434.2

This is a fine-grained sandstone with abundant large flakes of detrital mica embedded in a clay-rich matrix. The matrix is also enriched in iron (Fe), mostly in the form of goethite. Reddish brown patches of goethite are also scattered throughout the section. The goethite possibly comes from iron that came out of the alteration of biotite. The grains in the studied section are generally angular to sub-rounded, up to very angular in some places. The section consists of about 70% quartz and lithic fragments with quartz cement occurring between the grains. Minor plagioclase grains were also encountered locally exhibiting twinning. Some cavities can be observed

which could amount to less than 3% porosity. The rock also does not appear to be strongly compacted. Chlorite is present, suggesting low-grade metamorphism.
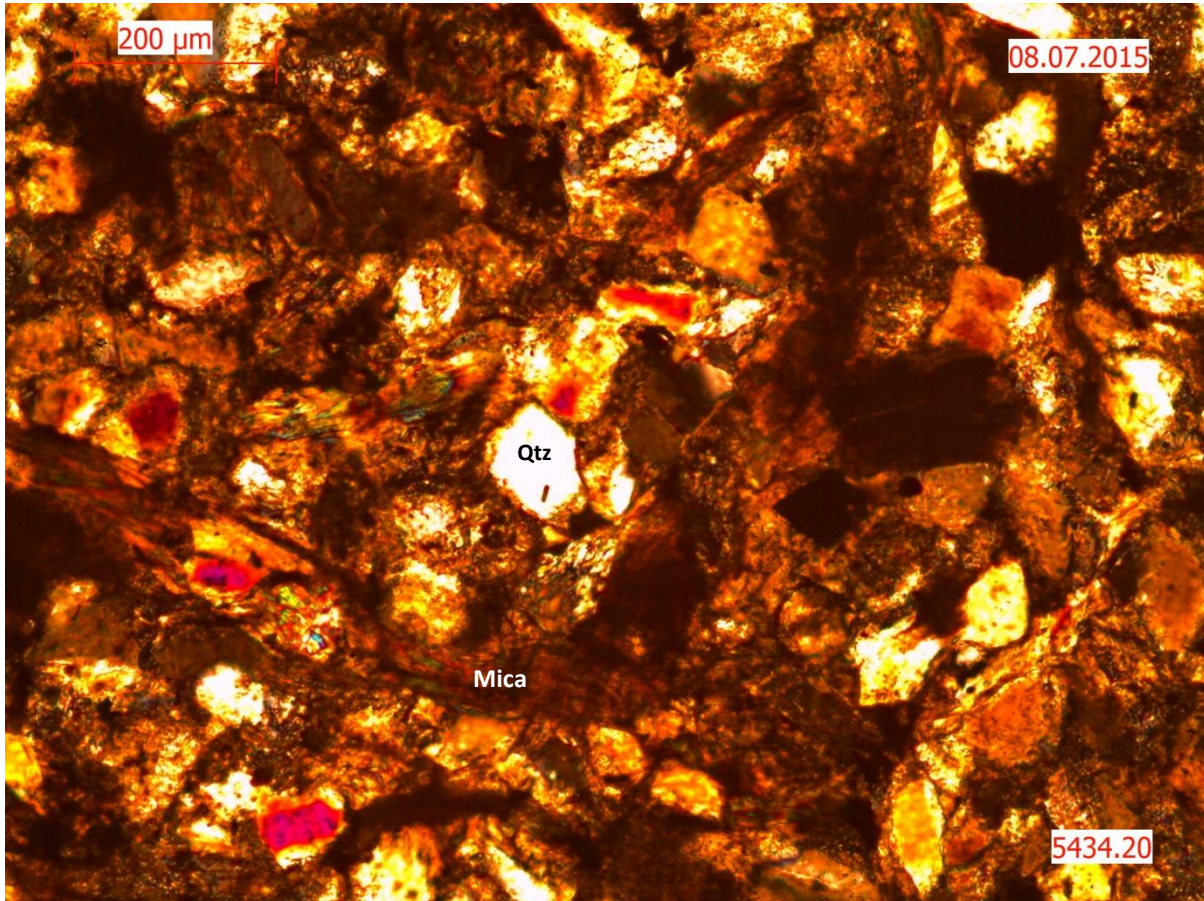
Figure 4.4. Photomicrograph for sample 5434.2 in cross-polarised light with oil immersion. The section shows a fine-grained sandstone dominated by mica flakes interspersed with angular, fine-grained quartz grains.

4.4.4 Sample 4794.10

The organic matter occurs in small fragments. The rock is compacted and finely laminated. Grains of detrital mica also occur scattered throughout the matrix. Silica cementation, which is a product of cementation, can be seen between the clay minerals. The rock shows very low porosity and permeability. The dark matrix appears to consist almost exclusively of organic matter and possibly some minor

clay minerals. Some calcitic veinlets were also encountered. This is an organic carbon-rich shale with very few silt grains present. This is not a black shale, rather a slightly silty shale.
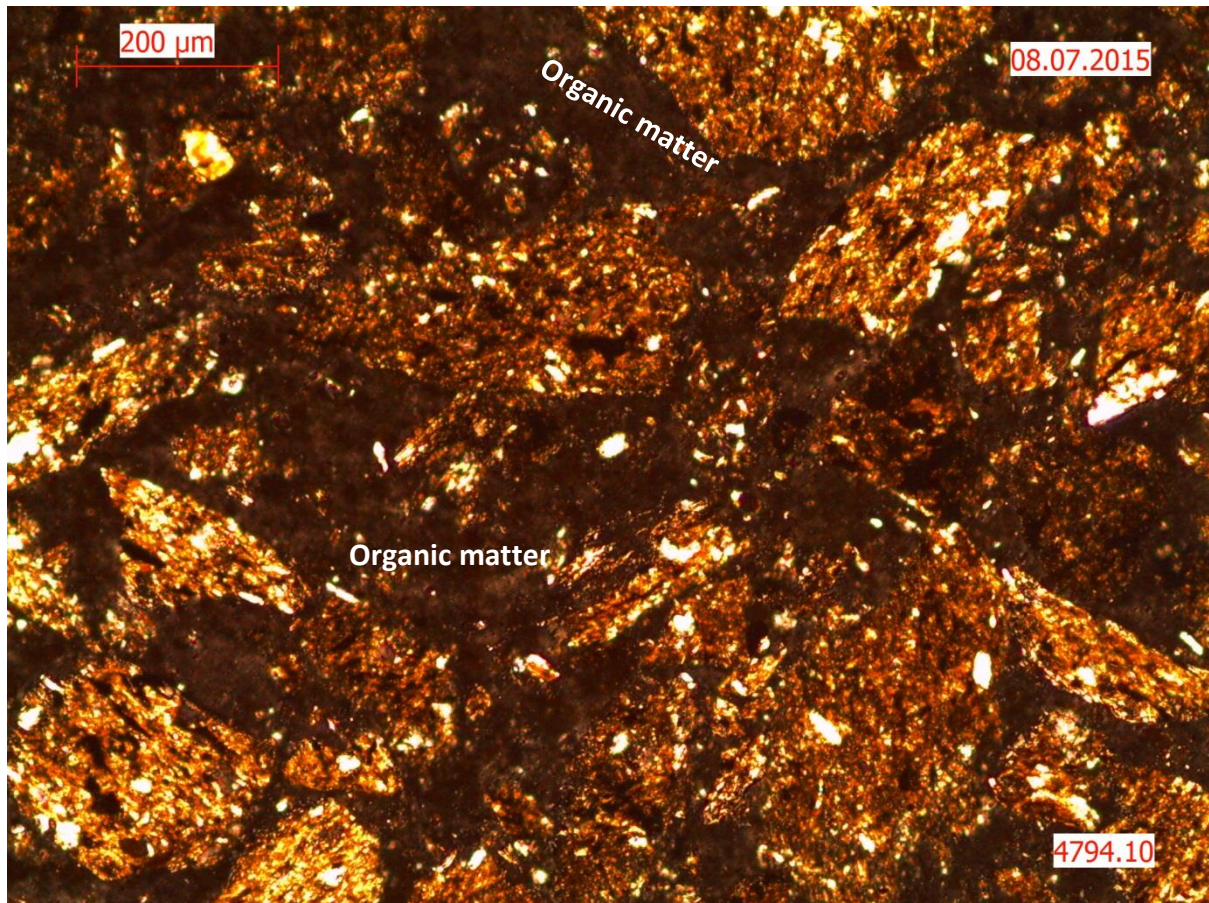
Figure 4.5. Photomicrograph for sample 4794.10 in cross-polarised light with oil immersion. The section shows a fine-grained matrix rich in organic matter — as shown by the dark patches and clay minerals. The matrix is peppered by fine-grained angular to sub-rounded quartz grains.

4.4.5 Sample 7534.04

This is a silty shale. The rock is very rich in organic matter. The matrix is also rich in silica and clay minerals. Detrital mica can be seen occurring throughout the section. A few silt-sized feldspar grains were also encountered. Silica cement is also present as evidence of diagenesis.
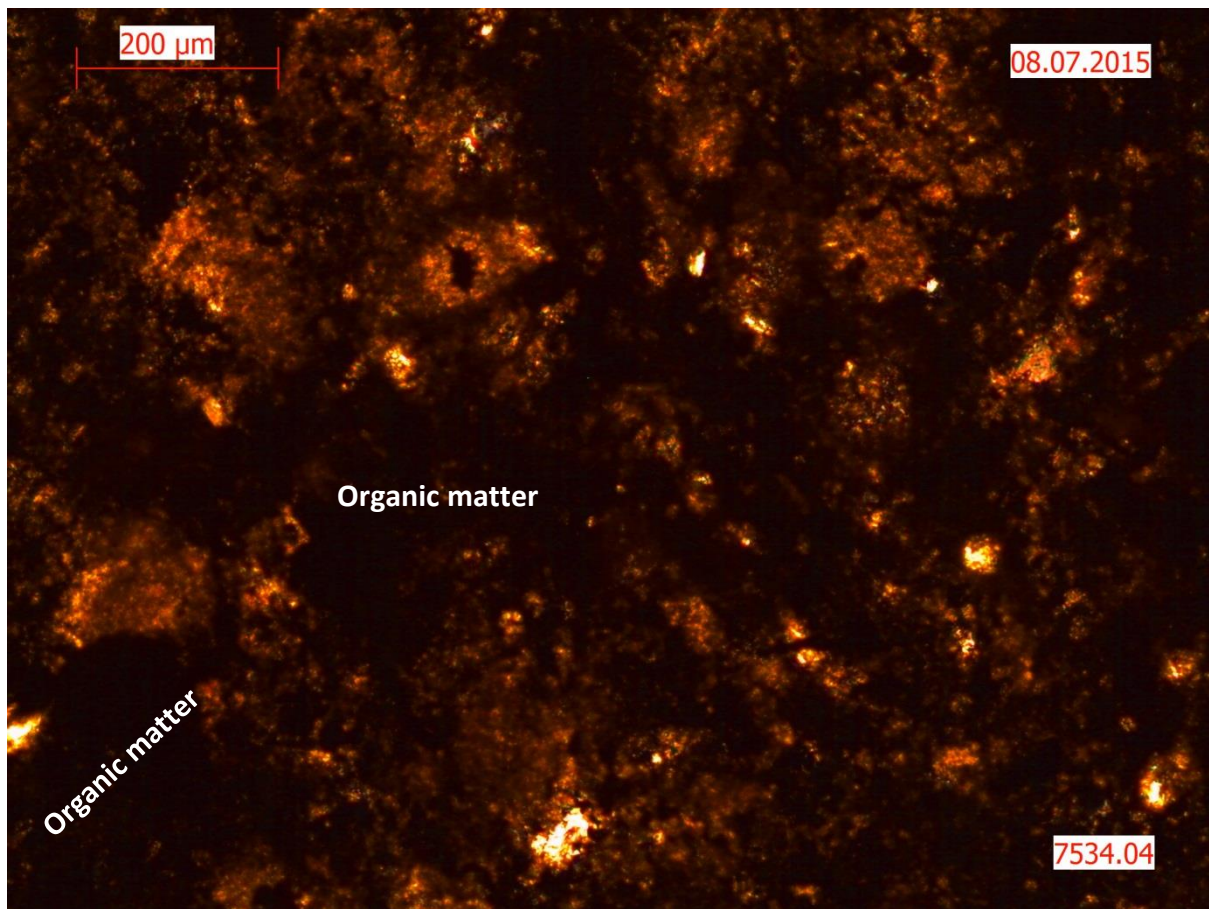
Figure 4.6. Photomicrograph for sample 7534.04 in cross-polarised light with oil immersion. The section is very dark due to the very high organic matter content in the matrix. Oil immersion was used to enhance the view under the microscope, but the dark organic-rich matrix is not translucent. The matrix consists predominantly of organic matter and a small amount of clay minerals. Fine-grained angular quartz grains can be seen scattered sporadically throughout the matrix.

4.4.6 Sample 389.30

This is a black shale with a very high content of organic matter. The organic matter occurs in irregular to oval shape patches with what appears to be a clay-rich matrix filling up the intervening spaces. Fine-grained crystals of detrital mica were also encountered both in the matrix and within the patches of organic matter.

.
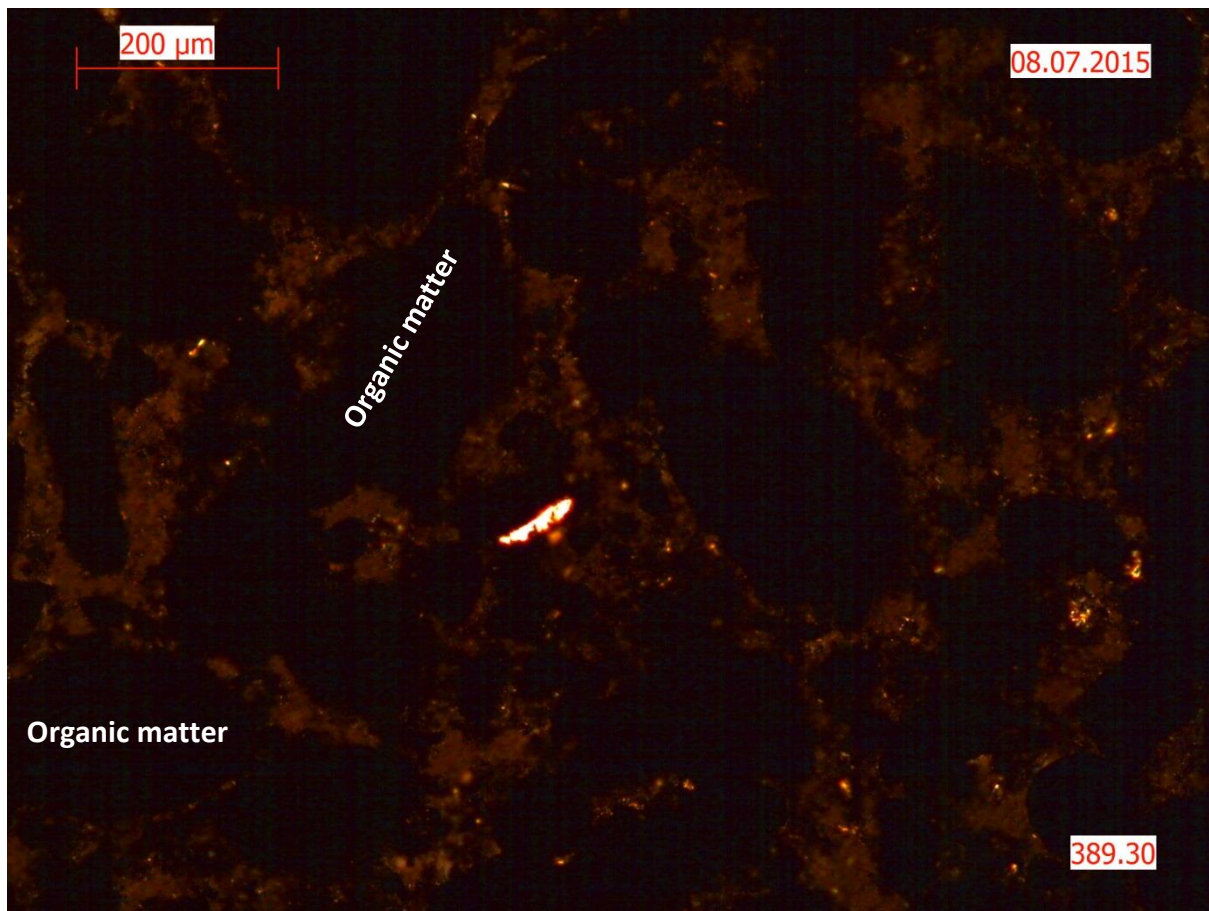
Figure 4.7. Photomicrograph for sample 389.30 in cross-polarised light with oil immersion. The section is very dark due to the high content of organic matter. As a result, other minerals are not clearly discernible. Note the dominant dark patches of organic matter and the sporadic bright spots that are fine-grained detrital mica and quartz. The intervening spaces between the patches of organic matter appear to be filled with clay minerals. The thin section was viewed under the microscope with oil immersion in an attempt to enhance the view.

4.4.7 Summary

The samples are generally siltstones, mudstones and fine-grained sandstones; no pure shales were encountered. Fine-grained and angular to rounded quartz grains are a dominant phase in all the samples. These quartz grains are mostly embedded in a dark to dark-greyish groundmass rich in clays and organic matter. The dark colour of the groundmass is mainly attributed to the organic matter in the shale samples. The organic matter indicates deposition under anoxic (poorly oxygenated) settings. Fine-grained elongate mica detritus or flakes are also a common feature across the samples. The presence of organic matter makes the rocks suitable candidates for adsorption as the CO_2 is trapped through the organic matter known as kerogen. The presence of clays is also expected to enhance the ability to adsorb CO_2 as they have also been found to have CO_2 adsorption capacity (Section 2.8.4). As expected for shales and mudstones, the samples show very little or no porosity and permeability. Presence of chlorite in some of the samples is indicative of low-grade metamorphism, possibly greenschist facies. Signs of diagenesis and compaction were also noted in some of the samples with diagenetic minerals such as haematite, now goethite, and the silica (SiO_2) cements. Patches of silica, calcite and haematite cementation were also encountered in some of the samples.

The samples do not exhibit strong lamination, compaction and induration as expected. This could be the effect of weathering and deterioration of the core in the last 40 years. The clay minerals probably swelled and the core disintegrated.

4.5 Scanning electron microscopy and energy dispersive X-ray analysis

Scanning electron microscopy (SEM) and energy dispersive X-ray analysis (EDX) were used to determine the accessory mineralogy on a selected set of four of the six samples. EDX shows that apart from the dominant quartz observed in petrographic analysis the samples also contain mica, plagioclase rutile and zircon in minute quantities. The SEM image (Figure 4.8 B) also shows a bright spot of Fe-sulphide

which from EDX peaks (S:Fe ration of 2:1) is suspected to be pyrite — most probably chalcopyrite. Of note is also the presence of rutile (Ti-oxide) (Figure 4.9 B), apatite with EDX peaks of Ca, and O, calcite and zircon. The presence of pyrite would suggest reducing (anoxic) conditions during late diagenesis. The reducing conditions at the site of deposition are conducive for the preservation of organic carbon. The sample is therefore expected to have a relatively high TOC.
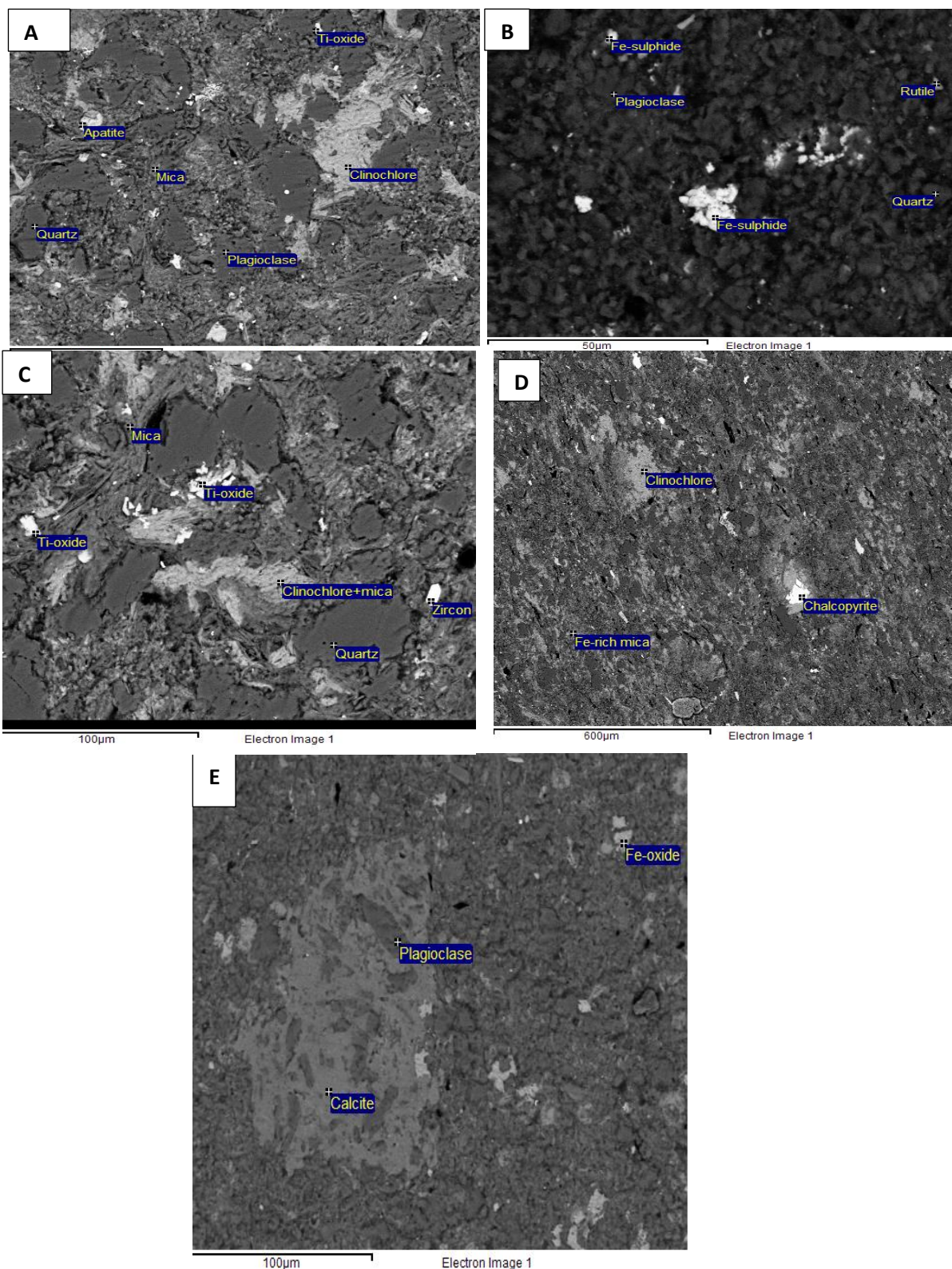
Figure 4.8. Backscatter SEM images of samples 389.30 (A and B), 5560.00 (C), 7534.40 and 4235.74 (D). The images show the mineralogy of the phases picked up from the matrix which is predominantly rich in organic matter and clay minerals.
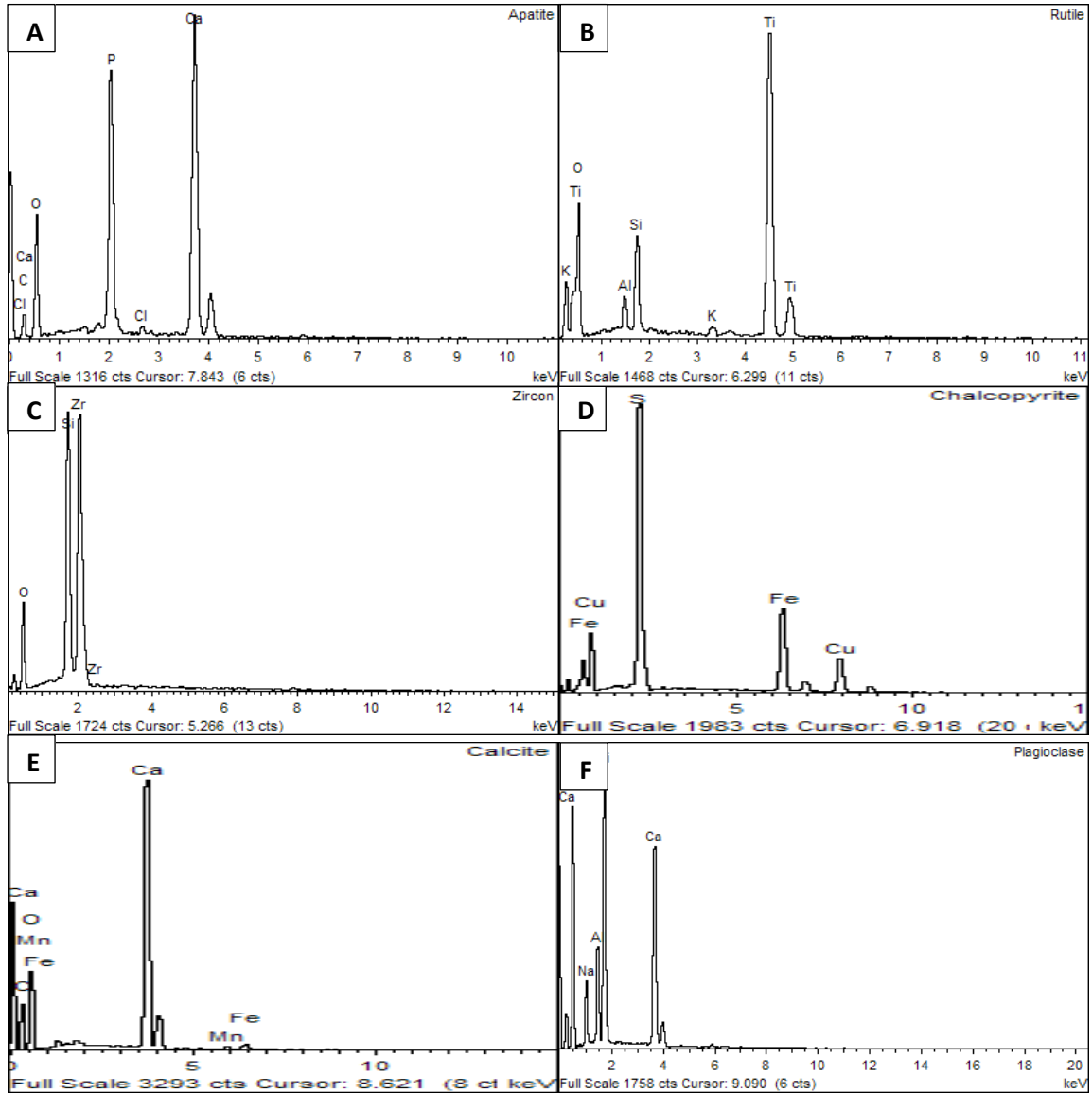
Figure 4.9. Plots showing **EDX** peaks for apatite (A), rutile (B), zircon (C), chalcopyrite (D), calcite (D) and plagioclase (E).

4.6 Total organic carbon

The total amount of organic content in the rock relates to the adsorptive capacity of a shale to hold gas in a matrix, independent of porosity.

The Whitehill Formation measured the highest TOC value of 4.52% as represented by sample 389.3. This is followed by 2.50% from sample 7534.04 of the Pietermaritzburg Formation which is the lowermost unit of the Ecca Group in the north-eastern part of the Karoo Basin. The two other samples from the Pietermaritzburg Formation, 5434.2 and 556, measured 0.77% and < 0.05% TOC, respectively. The Prince Albert Formation, which forms the basal unit of the Ecca Group in the south-western part of the basin, measured 1.17% TOC as represented by sample 4794.1 in Table 3 below. Sample 1124.5 from the Volksrust Formation contained 0.21% TOC.

Table 3. Measured TOC values of the six samples analysed for this study.

Sample Name	TOC (wt.%)	Formation
7534.04	2.50	Pietermaritzburg
4794.1	1.17	Prince Albert
389.3	4.52	Whitehill
5434.2	0.77	Pietermaritzburg
1124.5	0.21	Volksrust
5560	< 0.05	Pietermaritzburg
Average	**1.54**	
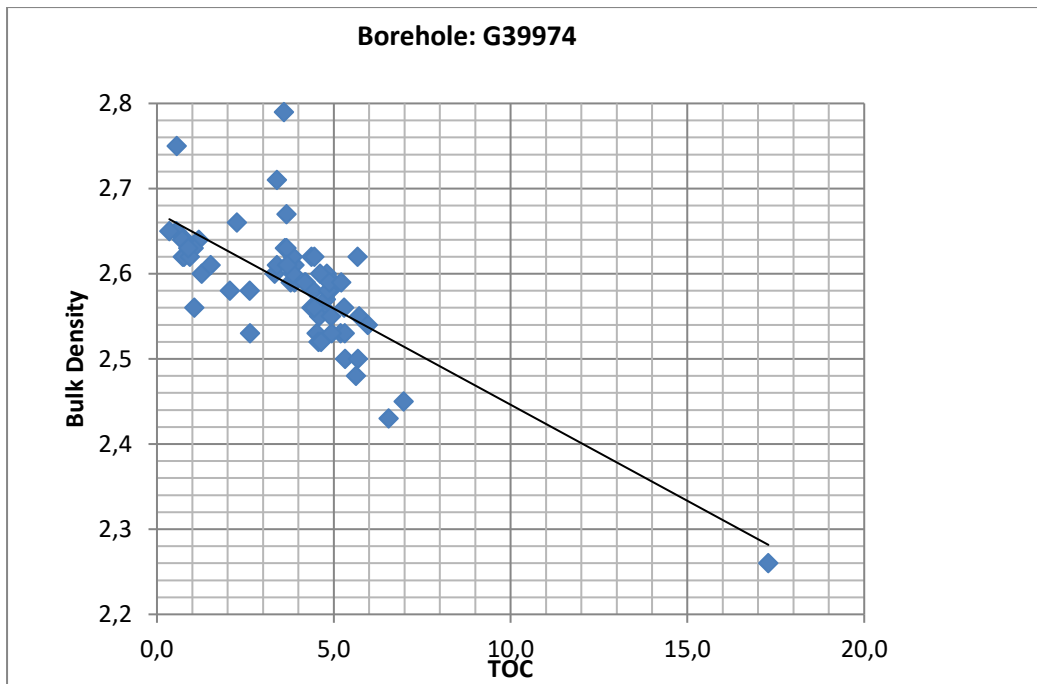
Figure 4.10. TOC vs Bulk Density plot for borehole G39974 from the Karoo Basin. Adopted from Chesapeake Energy (2010).
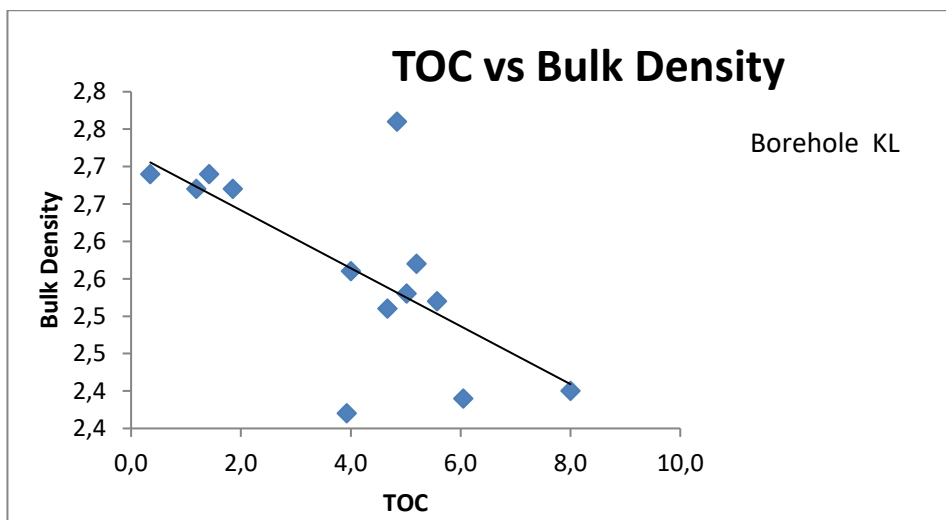
Figure 4.11. TOC vs Bulk Density plot for borehole KL 1/65 from Calvinia in the Karoo Basin. Adopted from Chesapeake Energy (2010).

4.7 Vitrinite reflectance

Vitrinite reflectance (%Ro) is a key diagnostic tool for assessing thermal maturity of organics and is based on measuring the reflectivity (R) of vitrinite through a microscope equipped with an oil immersion objective lens and photometer. Vitrinite is a maceral (plant and animal remains) found in many kerogens (Riley, 2016). As temperature increases, vitrinite undergoes complex, irreversible aromatisation reactions that increase the reflectance. Vitrinite reflectance measurements represent the per cent of light reflectance in oil, designated as %Ro. Values less than 0.6%Ro are considered immature and those over 1.4%Ro are considered overmature (Riley, 2016).

The Whitehill Formation sample, 389.30, contained abundant organic matter, measuring the highest reflectance value of 5.10%. This is followed by sample 4794.10 of the Prince Albert Formation with a measured reflectance value of 4.30%. This is consistent with the total organic content results between these two samples in section 4.6 above. Sample 1124.50 of the Volksrust Formation has a measured reflectance value of 3.35%. The Pietermaritzburg Formation as represented by samples 5434.2, 7534.04 and 5560.00 measures 2.08% and 2.43%, respectively. No organic matter was determined for sample 5560.00, as supported by the TOC.

An extensive amount of pyrite was observed in sample 389.30, far more than any other sample (see Plate 1, Appendix A).

Table 4. Vitrinite reflectance analysis results ($R_0V\%$).

Sample identification		393.3	1124.5	4794.1	5434.2	5560.0	7534.04
Vitrinite Reflectance ($R_0V\%$)	Random	5.10	3.35	2.08	n.d.		2.43
	Std. dev.	0.40	0.25	0.42			0.44
	Min	5.91	5.10	3.40			2.43
	Max	4.13	3.72	1.91			1.53
	n.d. = number of points measured						

4.7.1 Summary

The samples represent different shale and siltstone rocks from different formations of the Ecca Group. The Whitehill Formation has measured the highest reflectance value of 5.10%, followed very closely by the underlying Prince Albert Formation with a reflectance value of 4.30%. This is consistent with the total organic content results which show that the Whitehill and Prince Albert formations contain higher contents of organic matter than their stratigraphic equivalents in the north-eastern part of the Karoo Basin, namely the Pietermaritzburg and Volksrust formations. The Pietermaritzburg Formation is represented by samples 5560.00 (no organic content found), 7534.04 (2.43%) and 5434.20 (2.08%) and the Volksrust Formation is represented by sample 1124.50 with a reflectance value of 3.35%. The presence of a high content of pyrite in sample 389.30 of the Whitehill Formation is indicative of deposition under reducing (anoxic) conditions which are favourable for the preservation of organic matter.

All the six samples measured reflectance values above 1.4%Ro and are therefore classified as overmature. At this stage they likely have less gas generating capacity and therefore less affinity to adsorb CO_2.

4.8 Kerogen maturity

Samples from boreholes BE 1-67, LA 1-67 and SW 1-67 from the north-eastern part of the Karoo Basin were plotted on a HI vs OI index plot (Figure 4.12), which provides an indication of kerogen type. The plot revealed that samples from these boreholes plot predominantly below the Type III kerogen curve. Type III kerogen is gas prone and has the highest gas adsorption capacity compared to kerogen Types I and II due to its gas generative capability (Cheng, 2004). Coal is also classified as Type III kerogen and is known to adsorb CO_2 more (up to 40 times more) than shale. The prevalence of Type III kerogen in the north-eastern part of the Karoo Basin is therefore probably influenced by the presence of coal in the Vryheid and Volksrust formations. The dominance of kerogen Type III in these boreholes also implies that a terrestrial setting was a dominant depositional environment in the north-eastern part of the Karoo Basin, in agreement with McCarthy et al. (2011).
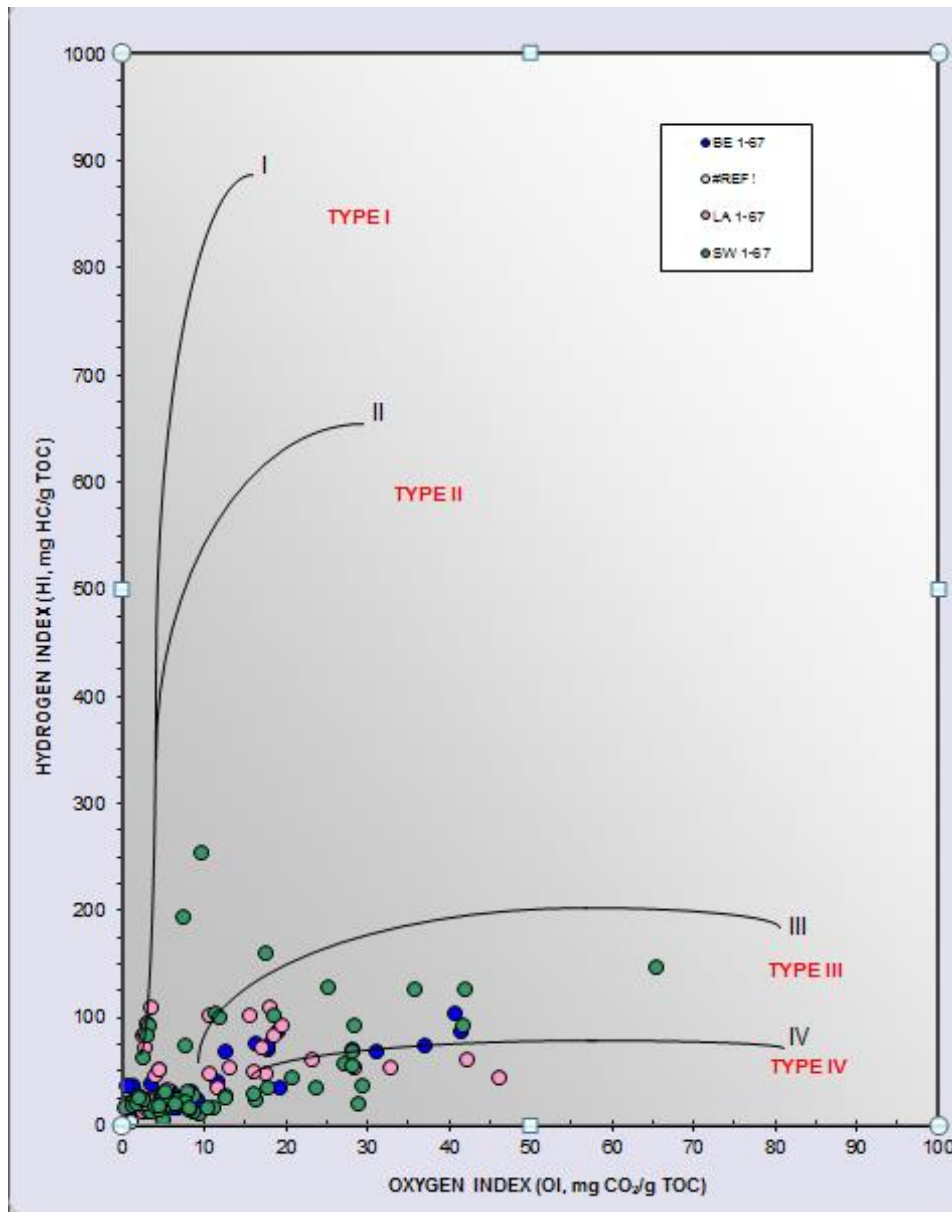
Figure 4.12. Plot of HI vs OI index for samples from boreholes BE 1-67, LA 1-67 and SW 1-67 from the south-western Karoo (analysis conducted by Chesapeake Energy on a different set of samples from the same boreholes sampled for this study). This plot provides an indication of kerogen type. Aquatic organic matter has a high HI content whereas organic matter of terrestrial origin has a low HI, but high OI. The variations of HI values can be indicative of changing depositional settings. Chesapeake Energy (2010).

4.9 Low Pressure CO_2 adsorption: pore characterisation (BET)

The samples exhibit similar isotherm shapes. The sorption isotherms of all six shale samples can be classified as being of Type I (Figure 4.13) (Clarkson et al., 2013). This type of isotherms is indicative of microporous solids (Clarkson et al., 2013). The CO_2 adsorption data were interpreted using the BET model. Sample 389.30 displays the most amount of adsorption, whereas sample 1124.5 displays the least amount of adsorption suggesting little microporosity. Samples 5434.2 and 4794.1 display the same amount of adsorption. TOC content seems to have an influence on the quantity of CO_2 adsorbed. For example, sample 389.3 displays the most amount of CO_2 adsorbed and also has the highest TOC content. Samples 5434.2 and 4794.1 show the same amount of adsorbed CO_2 and have almost the same amounts of TOC. However, sample 5560 shows a departure from this trend as it has the lowest TOC content but does not display the least amount of adsorbed CO_2. The could be the result of other controlling factors in CO_2 adsorption, such as clay content, BET surface area, porosity, bulk density, etc. However, these results sufficiently demonstrate the influence of TOC in the adsorption of CO_2 through the micropores.
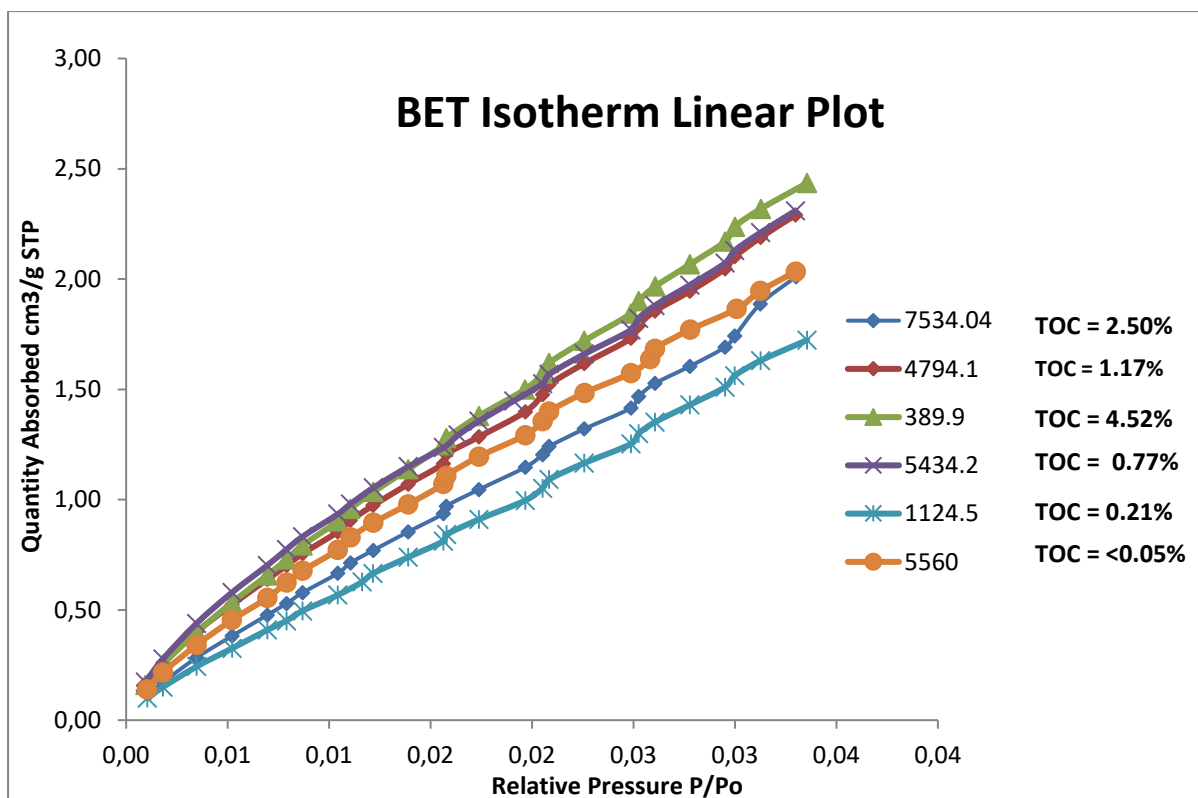
Figure 4.13. Low pressure CO_2 adsorption isotherms for the six studied shale samples, showing the adsorptive capacity of the samples at different pressures.

The specific surface area (often referred to as "BET surface area") was calculated from the sorption curve based on the sorbed gas volume in a relative pressure (p/p_0) range of 0.05–0.35 using the Brunauer-Emmet-Teller (BET) method (Cao et al., 2015). The specific surface area can be defined as the space site where the gas is sorbed onto the surface of solid particles and is therefore an indicator of the sorption capacity of shales (Cao et al., 2015).

The shale samples exhibit a specific surface area of 17.40–21.88 m^2/g, with an average of 19.66 m^2/g (Table 5). This compares quite favourably with the Silurian shales in the Sichuan Basin (China) which exhibit a specific surface area of 17.83–29.49 m^2/g, with an average of 22.18 m^2/g (Cao et al., 2015). Figure 8.11 displays the surface areas of the six shale samples with sample 7534.04 showing the highest BET surface area (21.8822 m^2/g) followed very closely by sample 389.3 (21.6608

m^2/g). Sample 5434.2 shows the lowest surface area (17.3980 m^2/g). The six shale samples do not show a marked difference in specific surface area at all.

Table 5. TOC, porosity and BET surface area measurements of the samples analysed for porosity.

Sample Name	TOC (wt.%)	BET Surface Area (m^2/g)
7534.04	2.50	21.88
4794.1	1.17	18.80
389.3	4.516	21.66
5434.2	0.771	17.39
1124.5	0.207	19.90
5 560	< 0.05	18.29
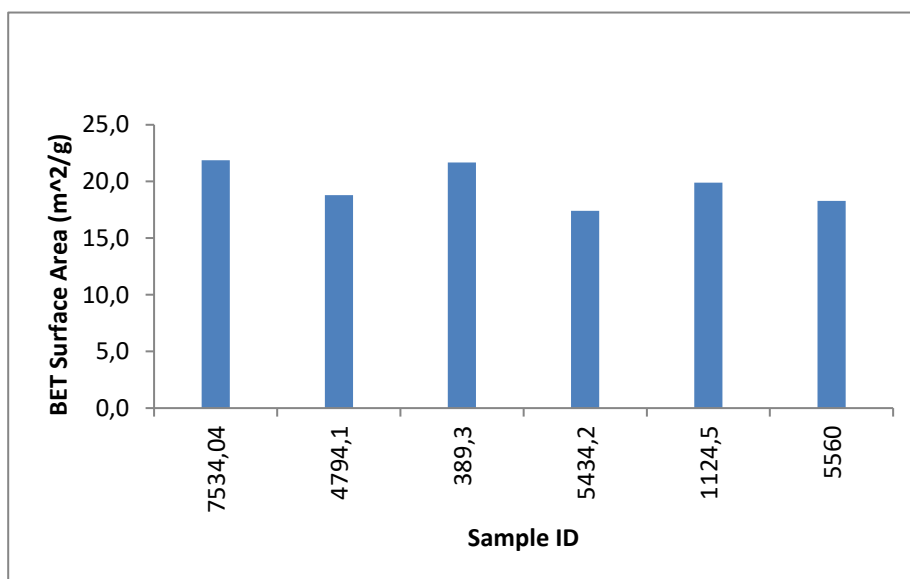
Figure 4.14. Bar graph displaying the BET surface area for the studied shale samples. The BET surface area is measured in m^2/g and is a measure of the space site where the gas is sorbed onto the surface of solid particles.

Figure 4.15 shows a trend of slight increase in BET surface area with increasing TOC content. However, this trend is not very pronounced. The correlation between TOC content and BET surface area also does not appear to be very strong (R^2 = 0.58) showing that TOC is not a dominant contributor in the specific surface area of these shales.
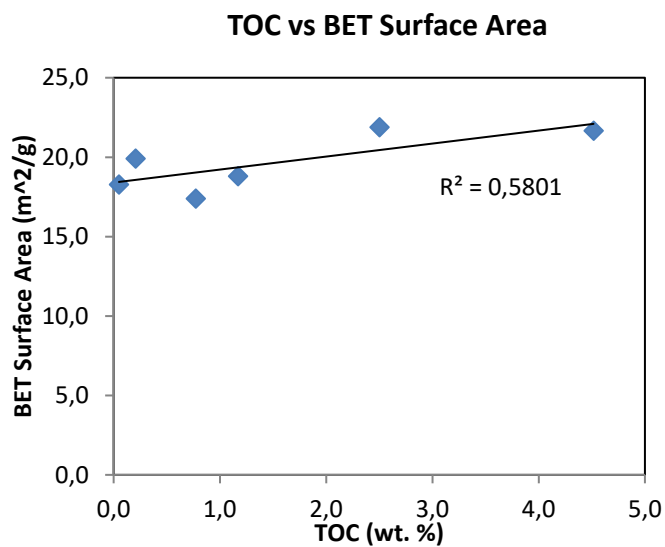
Figure 4.15. Correlation between TOC and BET surface area.

4.10 High pressure adsorption

All the six samples selected for this study, with TOC ranging from < 0.05–4.52%, were studied in the high pressure adsorption experiments at ISGS.

Equilibrium curves from these experiments showed very little adsorption (i.e. no noticeable drop in pressure as would be expected due to CO_2 in the sample cell being adsorbed onto the shale sample). Other experiments in different pressure steps performed on the same samples showed an unprecedented increase in pressure which could be attributed to bound water in the clays competing for space with the CO_2. The increases show no association with any specific physico-chemical properties of the samples and occurred across the different pressure steps (therefore not influenced by pressure). The samples used in this study come from the over 40 years old Soekor drill cores. Given the number of years these samples have been exposed to the atmosphere, they have undergone severe weathering, which left the cores mostly crumbled. The major problem with this is the degree of oxidation and break-down of pyrite, especially with the Whitehill Formation, which may have been responsible for some of the anomalous results. Oxidation has been proved to reduce sorption capacities of coals by as much as 11% (Krooss et al., 2002). It is strongly suspected that the same effect applies to shales.

The negative (-) values seen in Table 6 below are associated with the experiments that showed an unprecedented rise in pressure during the course of the experiment. The cause of this anomalous behaviour and subsequent negative results could not be explained, apart from the assumptions made above about oxidation of pyrite and the possibility of bound water in the clays. However, these assumptions would need to be ascertained by further studies. From the equilibrium curves (see Figure 4.16) it can be seen that equilibrium was achieved in all the experiments and very little to no adsorption can be read on these curves. Sample 1124.5 shows a significant drop in pressure at the end of the experiment which is also shown by the 5.94 mmol/g of CO_2 adsorbed. Sample 389.3 has the highest TOC content and also shows the highest adsorption capacity for CO_2 which is has the highest amount of 32.16 mmol/g.

Table 6. Experimental results for high pressure CO_2 adsorption for the studied samples. Samples 5434.20 and 5560.00 were the two samples randomly chosen for duplicate experiments. All the experiments were run at a constant temperature of 45 °C.

Sample No.	Presure step	P-high (bar)	P-low (bar)	Mass sample (g)	Ne (mmol/g)
389.30	389.30_ 80 bar	80.47	76.13	2.20	3.67
	389.30_ 100 bar	99.84	80.57	2.20	32.16
	389.30_ 120 bar	120.19	119.83	2.20	0.20
1124.50	1124.50_80 bar	79.51	80.30	2.23	-0.80
	1124.50_100 bar	99.48	96.96	2.23	5.94
	1124.50_120 bar	119.93	120.21	2.23	-0.18
4794.10	4794.10_80 bar	80.90	80.27	2.28	0.57
	4794.10_100 bar	100.19	100.26	2.28	-0.13
	4794.10_120 bar	119.50	117.51	2.28	1.12
5434.20	5434_80 bar	80.52	79.66	2.19	0.92
	5434_100 bar	100.19	104.28	2.19	-7.57
	5434_120 bar	120.11	116.95	2.19	2.09
	5434 Duplicate_80 bar	80.72	81.50	2.19	-0.86
	5434 Duplicate_100 bar	101.93	103.32	2.19	-2.49
	5434 Duplicate_120 bar	119.43	122.63	2.19	-1.91
5560.00	5560_80 bar	80.12	79.99	2.23	0.11
	5560_100 bar	100.62	100.67	2.23	-0.09
	5560_120 bar	119.50	119.45	2.23	0.03
	5560 Duplicate_ 80 bar	79.99	79.94	2.23	0.05
	5560 Duplicate_100 bar	100.57	100.92	2.23	-0.64
	5560 Duplicate_120 bar	120.36	118.85	2.23	0.83
7534.04	7534.04_80 bar	80.87	81.35	2.20	-0.46
	7534.04_100 bar	100.79	101.43	2.20	-1.14
	7534.04_120 bar	120.99	120.89	2.20	0.06
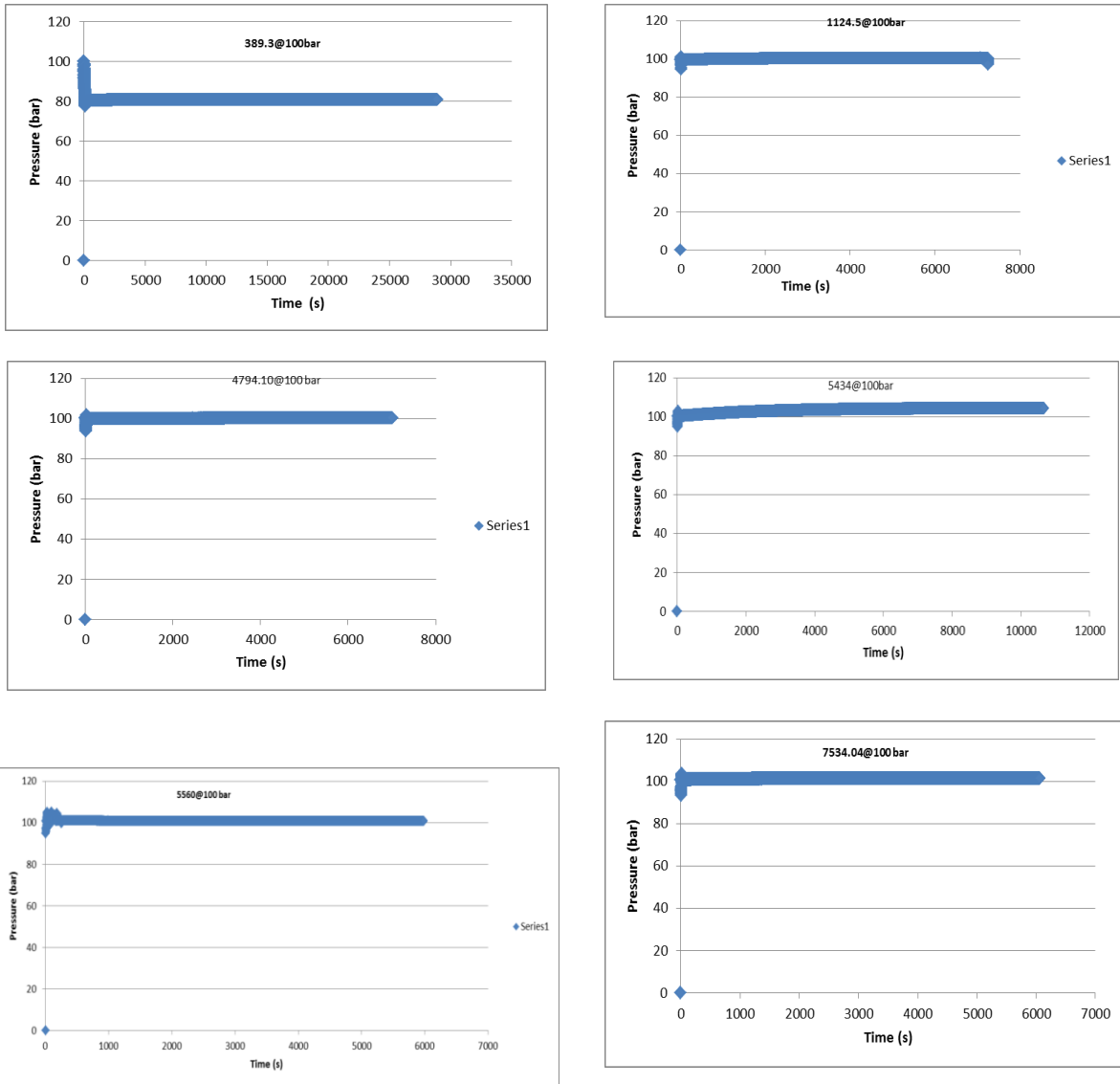
Figure 4.16. Equilibrium curves for all the six samples tested for high pressure CO_2 adsorption. The curves show no drop of pressure during the course of the experiments, which would suggest CO_2 being adsorbed onto the sample and thereby dropping the pressure in the sample cell. All the curves are taken at the pressure of 100 bar and 100 $^{\circ}$C temperature.

CHAPTER FIVE: SUMMARY OF RESULTS AND CONCLUSION

This study was undertaken to characterise the carbonaceous shales, siltstones and mudstones of the Ecca Group in the context of the geological storage of CO_2. The selected samples were analysed for their physico-chemical properties such as mineralogy, elemental composition, petrography, SEM-EDX, total organic carbon (TOC), thermal maturity (vitrinite reflectance), kerogen type, low pressure adsorption and high pressure CO_2 adsorption. This is in an attempt to establish whether the carbonaceous Ecca Group rocks can serve as additional storage reservoir for CO_2 in South Africa.

X-Ray diffraction analysis revealed that the samples have a high content of quartz and this is further supported by XRF and petrography studies. Chlorite and kaolinite are the predominant clay minerals in the samples with smectite only present in sample 5434.2. Clay minerals such as chlorite and kaolinite have micropore structures capable of sorbing gas and therefore, their presence increases the potential to adsorb CO_2. Presence of clays also improves the micropore volume of the shales (Ross and Bustin, 2009). Therefore, the significant presence of chlorite and kaolinite will serve to enhance the shales' ability to store CO_2.

The petrographic examination of the same samples revealed that they are predominantly silty shales and mudstones with some dark shales and fine-grained sandstones. The dark carbonaceous shales are mostly of the Whitehill and Prince Albert formations, with the Whitehill shales showing the highest content of organic matter. As expected from shales, siltstones and mudstones, they are of very poor porosity and permeability as seen under the petrographic microscope. This is further reduced by the abundant silica cementation.

The thin sections generally show a dark to dark-greyish groundmass rich in clays and organic matter, to which the dark-coloured appearance in the sections is attributed. The organic matter indicates diagenesis under anoxic (poorly oxygenated) settings. Fine-grained elongate mica crystals are also a common feature across the samples.

The presence of organic matter makes the rocks suitable candidates for adsorption as the CO_2 is trapped through the organic matter known as kerogen. The presence of pyrite in some of the Whitehill samples as revealed by SEM/EDS also suggests reducing (anoxic) conditions, which are good for the preservation of organic matter and therefore potentially higher affinity to adsorb CO_2. These conditions seem to prevail in the Whitehill and Prince Albert formations and could therefore be targeted for CO_2 adsorption.

TOC measurements from a sample from the Whitehill formation from borehole G39974 gave a measured value of 4.52 wt.% while a sample from the underlying Prince Albert Formation from borehole KL 1-65 measure a value of 1.17 wt.%. In the north-eastern part of the Karoo Basin, two sample from the Pietermaritzburg Formation, a north-eastern stratigraphic equivalent of the Whitehill Formation which pinches out in this part of the basin intersected by boreholes SW 1-67 and LA 1-68, measured 2.50 wt.% and 0.77 wt.%. Sample 1124.5 from the Volksrust Formation intersected by borehole BE 1-67 measured 0.21 wt.%. TOC values of greater than 1.0% are considered good source rock for generating hydrocarbon potential and therefore likely to have a strong affinity for adsorbing significant amounts of CO_2 (Riley, 2016). At 4 wt.%, the Whitehill Formation has the highest organic content and could be targeted for CO_2 adsorption. However, the maturity studies (vitrinite reflectance) determined that all the six samples measured reflectance values above 1.4%Ro and are therefore classified as overmature. This is in agreement with the Geel et al. (2013) study in the Graystone, Eastern Cape, area of the Karoo Basin (Section 2.9), where samples from the lower Ecca Group were found to be overmature. At this stage they likely have a reduced gas generating capacity and therefore a reduced affinity to adsorb CO_2.

Samples from boreholes BE 1-67, LA 1-67 and SW 1-67 from the north-eastern part of the Karoo Basin were plotted on a HI vs OI index plot which revealed that samples from these boreholes are predominantly below the Type III kerogen curve. Type III kerogen is gas prone and has the highest gas adsorption capacity compared to kerogen Types I and II due to its gas generative capability (Cheng, 2004). Coal is classified as Type III kerogen and is known to adsorb CO_2 up to 40 times more than shales (Chareonsuppanimit et al., 2012). The prevalence of Type III kerogen in the north-eastern part of the Karoo Basin is therefore probably influenced by the

presence of coal in the Vryheid and Volksrust formations. The dominance of kerogen Type III in these boreholes also implies that a terrestrial setting was a dominant depositional environment in the north-eastern part of the Karoo Basin (McCarthy et al., 2011).

During low pressure CO_2 adsorption (BET analysis) all the samples displayed similar isotherm shapes. Sample 389.3 from the Whitehill Formation, with the highest TOC, showed the highest quantity of adsorbed CO_2. There is a distinct trend of adsorption capacity increasing with TOC. However, sample 5560 from the Pietermaritzburg Formation shows a departure from this trend as it has the lowest TOC content, but does not display the least amount of adsorbed CO_2. This could be explained by other controlling factors in CO_2 adsorption such as clay content, BET, surface area, porosity, bulk density, etc.

The shale samples exhibit a specific surface area of 17.40–21.88 m^2/g, with an average of 19.66 m^2/g. This compares quite favourably with the gas-bearing Silurian shales in the Sichuan Basin (China) which exhibit a specific surface area of 17.83–29.49 m^2/g, with an average of 22.18 m^2/g (Cao et al., 2015). There is also a trend of surface area increasing with TOC, affirming the influence of organic matter on the surface area.

Equilibrium curves from the high pressure volumetric adsorption experiments showed very little adsorption (i.e. no noticeable drop in pressure as would be expected due to CO_2 in the sample cell being adsorbed onto the shale sample). Other experiments in different pressure steps performed on the same samples showed an unprecedented increase in pressure which could be attributed to bound water in the clays competing for space with the CO_2. This erroneous behaviour of these experiments have largely made the high pressure CO_2 adsorption results inconclusive. The condition of the core could also be the reason for the anomalous behaviour of the experiments, particularly the degree of oxidation and the subsequent breakdown of pyrite.

5.1 Conclusions

This study has demonstrated that the samples from the carbonaceous Ecca Group rocks compare quite favourably, in terms of other physico-chemical properties, to those from other parts of the world, such as the USA and Brazil, which have successfully stored significant amounts of CO_2 in their organic matter. The shales and siltstones of the Whitehill and Prince Albert formations should be particularly targeted due to their high total organic content. The only concern would be the over-maturity of these rocks which could reduce, but not thwart, their affinity for CO_2 adsorption. Additionally, fresh samples are needed to ascertain the CO_2 sorption behaviour of these rocks in order to be able to conclusively deduce their capacity for CO_2 storage and how that capacity can best be optimised.

5.2 Limitations and recommendations

The samples used in this study were obtained from the old Soekor boreholes which were drilled over 40 years ago. The samples have been exposed to the atmosphere for decades and have undergone significant weathering and chemical alterations that could have caused some of the erroneous behaviour in the adsorption experiments and a significant negative impact on the samples' capacity to adsorb CO_2 during the experiments. It is recommended therefore that the high pressure adsorption experiments be repeated on fresh core samples in order to conclusively establish the sorption behaviour of these shales and siltstones and give meaningful advice to the decision-makers on whether or not these shales and siltstones have a role to play in carbon capture and storage endeavours in the country. Fresh samples of the Whitehill and Prince Albert formations could be obtained from the two experimental deep boreholes drilled by KARIN (Karoo Research Initiative) under DST-NRF-CIMERA in 2016 as well as the upcoming 3 500 m deep borehole to be drilled by the Council for Geoscience in the near future, likely 2020.

Sufficient time is also needed for the adsorption experiments since shale samples take much longer to reach equilibrium compared to coals. It can take up to 72 hours for a single sample to rich reach equilibrium and in some cases equilibrium is never achieved. Adsorption experiments therefore need a minimum of six months to

complete successfully. This requires that the workers have an instrument to which they have unlimited access for a duration long enough to successfully complete the experiments. In this study, the only instrument that was available for the experiments was in the United States of America and it was only available to the author for three weeks. This was a limiting factor for this study. As part of capacity building, South Africa should consider recapitalising its own laboratories for these experiments to be able to fully understand the CO_2 sorption behaviour of shales in the context of CO_2 geo-sequestration.

Inter-laboratory comparisons are also recommended, where possible, to ascertain the repeatability of the isotherms and fine-tune the experimental procedure for high pressure adsorption experiments. The author noted that there is no standardised operating procedure for gas adsorption experiments. Even the international round robin tests in the literature reported significant discrepancies in their results owing to their different set-ups and operating procedures. It would be good if such international inter-laboratory tests focused their efforts into validating the methodology for gas adsorption studies. Currently, the experimental procedures differ quite markedly from one operator to another.

The set-up used for this study also had a few shortcomings that could be sources of error. It is manually operated and requires the operator to open the oven and connect the vacuum to the system at the beginning of each pressure step. The opening and closing of the oven could affect the temperature stability of the system and therefore that of the sample cell. It is critically important that the sample temperature must be stable over the whole experiment time period. An automated system is recommended to eliminate such sources of error. An automated system would also significantly eliminate random errors due to the operator.

Gas leakages are a common problem in volumetric set-ups, particularly at very high pressures. Our set-up also experienced a spate of leakages that forced many of our experiments to be re-done. The small leaks that cannot be easily detected are a major concern as they can lead to erroneous interpretation as they can easily be assumed to be an intended result of the experiment — i.e. pressure dropping due to CO_2 being adsorbed onto the sample. Instrument designs therefore need to be

improved to tackle the unacceptably common phenomena of gas leakages in high pressure adsorption experiments.

REFERENCES

Aarnes, I., Svensen, H., Polteau, S. and Planke, S. (2011). Contact Metamorphic Devolatization of Shales in the Karoo Basin, South Africa, and the Effects of Multiple Sill Intrusions. Chemical Geology, 281, pp. 181–194.

Almashramah, Y.A.A. (2011). Maturity of Kerogen, Petroleum Generation and the Application of Fossils and Organic Matter for Paleotemperature Measurements. Master's Thesis in Geology. Lund University, Department of Earth and Ecosystem Sciences, No. 274.

Ammann, A., Waschbusch, M., Bertier, P., Busch, A., Krooss B.M. and Littke, R. (2011). Sealing Rock Characteristics under the Influence of CO_2. Energy Procedia, 4, pp. 5170–5177.

Beck, B., Surridge, T., Liebenberg, J. and Gilder, A. (2011). The Current Status of CCS Development in South Africa. GHGT-10. Energy Procedia, 4, pp. 6157–6162.

Bhebhe, S. (2008). The Effect of Coal Composition on Carbon Dioxide Adsorption. MSc Dissertation. University of the Witwatersrand, pp. 1–151.

Busch, A., Alles, S., Gensterblum, S.Y., Prinz, D., Dewhurst, D.N., Raven, M.D., Stanjek, H. and Krooss, B.M. (2008). Carbon Dioxide Storage Potential of Shales. International Journal of Greenhouse Gas Control, 2, pp. 297–308.

Busch, A., Alles, S., Krooss, B.M., Stanjek, H. and Dewhurst, D. (2009). Effects of Physical Sorption and Chemical Reactions of CO_2 in Shaly Caprocks. GHGT-9. Energy Procedia, 1, pp. 3229–3235.

Cadle, A.B., Cairncross, B., Christie, A.D.M. and Roberts, D.L. (1993). The Karoo Basin of South Africa: type basin for the coal-bearing deposits of Southern Africa. International Journal of Coal Geology, Volume 23, pp. 117–157.

Cairncross, B., Beukes, N.J., Coetzee, L.L. and Rehfeld, U. (2005). The Bivalve Megademus from Permian Volksrust Shale Formation (Karoo Supergroup), Northeast Karoo Basin, South Africa: Implications for Late Permian Basin Development. South African Journal of Geology, 108, pp. 547–556.

Cao, T., Song, Z., Wang, S., Cao, X., Li, Y. and Xia, J. (2015). Characterizing the Pore Structure in the Silurian and Permian Shales of the Sichuan Basin, China. Marine and Petroleum Geology, 61, pp. 140–150.

Chareonsuppanimit, P., Mohammad, S.A., Robinson Jr, R.L. and Gasem, K.A.M. (2012). High-pressure Adsorption of Gases on Shales: Measurements and Modelling. International Journal of Coal Geology, 95, pp. 34–46.

Cheng, A. and Huang, W. (2004). Selective Adsorption of Hydrocarbon Gases on Clays and Organic Matter. Organic Geochemistry, 35, pp. 413–423.

Chesapeake International Exploration, Sasol Petroleum International, and Statoil ASA, (2010). Technical Progress Report No. 2.

Clarkson, C.R., Solano, N., Bustin, R.M., Bustin, A.M.M., Chalmers, G.R.L., He, L., Melnichenko, Y.B., Radlinski, A.P. and Blach, T.P. (2013). Pore Structure Characterization of North American Shale Gas Reservoirs Using USANS/SANS, Gas Adsorption, and Mercury Intrusion. Fuel, 103, pp. 606–616.

Cloete, M. (2010). Atlas on Geological Storage of Carbon Dioxide in South Africa. Council for Geoscience.

Cole, D.I. (2010). Report of the Geology of the Ecca Group   With Emphasis on the Central and Southwestern Parts of the Main Karoo Basin and Previous Hydrocarbon Investigations Relevant to the Present Shale Gas Investigation and Sampling Programme. Work Assignment 3. Council for Geoscience.

Cole, D.I. (2005). Prince Albert Formation. pp. 8–33, In: Johnson, M.R. (Ed.). Catalogue of South African Lithostratigraphic Units. South African Committee for Stratigraphy, Volume, 8, Government Printer, Pretoria, pp. 43.

Cole, D.I. and McLachlan, I.R. (1994). Oil Shale Potential and Depositional Environment of the Whitehill Formation in the Karoo Basin. Publication (unedited), Geological Survey of South Africa, Library book no. 553.283COL (Volume I Text; Volume II Tables and Appendixes).

Cole, D.I. (1991a). Depositional Environment of the Dwyka Group in the Boshof-Hertzogville Area, Orange Free State. South African Journal of Geology, 94, pp. 272–287.

Cole, D.I. (1991b). Whitehill Formation. Catalogue of South African Lithostratigraphic Units. 1st Edition, pp. 3–51.

Cole, D.I. and McLachlan, I.R. (1991). Oil Potential of the Permian Whitehill Shale Formation in the Main Karoo Basin, South Africa. Gondwana Seven Proceedings. pp. 379–390.

Crosdale, P.J., Beamish, B.B. and Valix, M. (1998). Coalbed Methane Sorption Related to Coal Composition. International Journal of Coal Geology, 35, pp. 147–158.

Engelbrecht, A., Golding, A., Hietkamp, S. and Scholes, B. (2004). The Potential for Sequestration of Carbon Dioxide in South Africa. CSIR, pp. 1–6.

Falcon, R.M.S. and Snyman, P. (1986). An Introduction to Coal Petrography: Atlas of Petrographic Constituents in the Bituminous Coals of Southern Africa. The Geological Society of South Africa. Review Paper Number 2.

Fiaz, M.M., Saghafi, A., Barclay, S.A., Stalker, L., Sherwood, N.R. and Whitford, D.J. (2008). Evaluating Geological Sequestration of CO_2 in Bituminous Coals: The

Southern Sydney Basin, Australia as a Natural Analogue. International Journal of Greenhouse Gas Control, I, p. 223–235.

Foo, K.Y. and Hameed, B.H. (2010). Insights into the Modelling of Adsorption Isotherms Systems. Chemical Engineering Journal, 156, pp. 2–10.

Francis, W. (1961). Coal: Its Formation and Composition. Edward Arnold Publishers LTD., Second edition, pp. 1–806.

Furmann, A., Mastalerz, M., Schimmelmann, A., Perdersen, P.K. and Bish, D. (2014). Relationships Between Porosity, Organic Matter, and Mineral Matter in Mature Organic-rich Marine Mudstones of the Belle Fourche and Second White Specs Formations in Alberta, Canada. Marine and Petroleum Geology, 54, pp. 65–81.

Gasperik, M., Rexer, T.F.T., Aplin, A.C., Billemont, P., De Weireld, G., Gensterblum, Y., Henry, M., Kroos, B.M., Liu, S., Ma, X., Sakurovs, R., Song, Z., Staib, G., Thomas, K.M., Wang, S. and Zhang, T. (2014). First International Inter-laboratory Comparison of High-pressure CH_4, CO_2 and C_2H_4 Sorption Isotherms on Carbonaceous Shales. International Journal of Coal Geology, 132, pp. 131–146.

Geel, C., Schulz, H., Booth, P., De Wit, M. and Horsfield, B. (2013). Shale Gas Characteristics of Permian Black Shales in South Africa: Results from Recent Drilling in the Ecca Group (Eastern Cape). European Geosciences Union General Assembly 2013, EGU, Division Energy, Resources and the Environment, ERE, Energy Procedia, 40, pp. 256–265.

Global Energy Technology Strategy Program (GTSP). (2006). Carbon Dioxide Capture and Geologic Storage: A Core Element of a Global Energy Technology Strategy to Address Climate Change.

Godec, M., Koperna, G., Petrusak, R. and Oudinot, A. (2012). Assessment of Factors Influencing CO_2 Storage Capacity and Injectivity in Eastern U.S. Gas Shales. GHGT-11. NETL Shale Study Abstract.

Godec, M., Koperna, G., Petrusak, R. and Oudinot, A. (2013). Potential for Enhanced Gas Recovery and CO_2 Storage in the Marcellus Shale in the Eastern United States. International Journal of Coal Geology, 118, pp. 95–104.

Herzog, H. and Golomb, D. (2004). Carbon Capture and Storage from Fossil Fuel Use. Massachusetts Institute of Technology. Article number: NRGY: 00422.

International Risk Governance Council. (2008). Regulation of Carbon Capture and Storage.

Intergovernmental Panel on Climate Change (IPCC). (2005). Carbon Dioxide Capture and Storage. WMO. UNEP.

International Risk Governance Council (IRGC). (2007). Climate Change 2007: Synthesis Report.

Johnson, M.R., Van Vuuren, C.J., Hegenberger, W.F., Key, R. and Shoko, U. (1996). Stratigraphy of the Karoo Supergroup in Southern Africa: an overview. Journal of African Earth Sciences, Vol. 23, No. 1, pp. 3–15.

Johnson, M.R., Anhaeusser, C.R. and Thomas, R.J. (2006). The Geology of South Africa. The Geological Society of South Africa and the Council for Geoscience, pp. 1–691.

Kang, S.M., Fathi, E., Ambrose, R.J., Akkutlu, I.Y. and Sigal, R.F. (2010). Carbon Dioxide Storage Capacity of Organic-rich Shales. SPE International. SPE 134583.

Kiratu, S. (2010). South Africa's Energy Security in the Context of Climate Change Mitigation. Trade Knowledge Network. Series on Trade and Energy Security — Policy Report 4.

Kirk, R.E. and Othmer, D.F. (1991a). Encyclopedia of Chemical Technology Vol. 1, pp. 493–524, 4th Edition, J. Wiley, New York.

Krooss, B.M., Van Bergen, F., Gensterblum, Y., Siemons, N., Pagnier, H.J.M. and David, P. (2002). High-Pressure Methane and Carbon Dioxide Adsorption on Dry and Moisture-equilibrated Pennsylvanian Coals. International Journal of Coal Geology, 51, pp. 69–92.

Li, D., Liu, Q., Weigner, P., Gensterblum, Y., Busch, A. and Krooss, B.M. (2010). High-pressure Sorption Isotherms and Sorption Kinetics of CH_4 and CO_2 on Coals. Fuel, 89, pp. 569–580.

Lu, X., Li, F.C. and Watson, A.T. (1993). Adsorption Measurements in Devonian Shales. SCA Conference Paper Number 9302.

Maillol, J.M. (2001). Overview of Physical Properties of Earth Materials. GOPH365.

McCarthy, K., Niemann, M., Palmowski, D., Peters, K. and Stankiewicz, A. (2011). Basic Petroleum Geochemistry for Source Rock Evaluation. Oilfield Review 2011:23, No. 2.

Nuttal, B.C., James, A., Eble, A., Cortland, F. and Bustin, R.M. (2004). Poster 106: CO_2 Sequestration in Gas Shales of Kentucky.

Proedrou, P. (1971). Northwestern Section of the Karoo Basin: Area Leased to B.J.H. Du Preez Oil Exploration. Provisional Stratigraphic Report.

Petroleum Agency SA (PASA). (2011). Petroleum Potential of the Karoo Basin.

Pollock, S.M., Goodarzi, F. and Riediger, C.L. (2000). Mineralogical and Elemental Variation of Coal from Alberta, Canada: an Example from the No. 2 Seam, Genesee Mine. International Journal of Coal Geology, 43, pp. 259–286.

Riley, R.A. (2016). Mapping Source Rock and Thermal Maturity of the Devonian Shale Interval in Eastern Ohio. Open-File Report 2016-3. Columbus 2016.

Ross, D.J.K. and Bustin, R.M. (2009). The Importance of Shale Composition and Pore Structure upon Gas Storage Potential of Shale Gas Reservoirs. Marine and Petroleum Geology, 26, pp. 916–927.

Rowsell, D.M. and De Swardt, A.M.J. (1976). Diagenesis in Cape and Karoo Sediments, South Africa, and its Bearing on their Hydrocarbon Potential. Transactions, Geological Society of South Africa, 79, pp. 81–145.

Saghafi, A., Faiz, M. and Roberts, D. (2007). CO_2 Storage and Gas Diffusivity Properties of Coals from Sydney Basin, Australia. International Journal of Coal Geology, 70, pp. 240–254.

Saghafi, A. (2010). Potential for ECBM and CO_2 storage in mixed gas Australia coals. International Journal of Coal Geology, 82, pp. 240–251.

Schwarzkopf, T.A. (1992). Source Rock Potential (TOC+ Hydrogen Index). Evaluation by Integration Well Log and Geochemical Data. Organic Geochemistry, 19, Nos 4–6, pp. 545–555.

Selly, R.C. (1985). Elements of Petroleum Geology. Library of Congress Cataloging in Publication Data. W.H. Freeman and Company, pp. 1–526.

Stach, E., Mackowsky, M., Teichmuller, M., Taylor, G.H., Chandra, D. and Teichmuller, R. (1982). Coal Petrology, 2nd Edition. Gebruder Borntraeger, Berlin.

Suárez-Ruiz, I. (2012). Organic Petrology: An Overview. Instituto Nacional del Carbon (INCAR-CSIC) Oviedo. www.interhopen.com. Accessed in March 2014.

Surridge, A.D. and Cloete, M. (2009). Carbon Capture and Storage in South Africa. Energy Procedia, 1, pp. 2741–2744.

SOEE5730. (2007). Fluid Properties in the Subsurface. Hydrocarbon_props.

SPE Annual Technical Conference and Exhibition. Florence, Italy. 19–22 September 2010.

Tian, H., Pan, L., Zhang, T., Xiao, X., Meng, Z. and Huang, B. (2015). Pore Characterization of Organic-rich Lower Cambrian Shales in Qiannan Depression of Guizhou Province, Southwestern China. Marine and Petroleum Geology, 62, pp. 28–43.

Vandenbrouke, M. and Largeau, C. (2007). Kerogen Origin, Evolution and Structure. Organic Geochemistry, 38, pp. 719–833.

Vermeulen, P.D. (2012). A South African Perspective on Shale Gas Hydraulic Fracturing. International Mine Water Association. Annual Conference 2012.

Weniger, P., Kalkreuth, W., Busch, A. and Krooss, B.M. (2010). High-pressure Methane and Carbon Dioxide Sorption on Coal and Shale Samples from the Parana Basin, Brazil. International Journal of Coal Geology, 84, pp. 190–205.

World Coal Institute. (2005). The Coal Resource: A Comprehensive Overview of Coal. www. worldcoal.org. Accessed in September 2014.

World Meteorological Organisation (WMO). (2011). WMO Greenhouse Gas Bulletin: The State of Greenhouse Gases in the Atmosphere Based on Global Observations through 2010. No. 7.

Lu, X., Li, F. and Watson, A.T. (1995). Adsorption measurements in Devonian shales. Fuel, Vol. 74, No. 4, pp. 599–603.

APPENDIX A: VITRINITE REFLECTANCE MICROGRAPHS

All photographs were taken at a magnification of x500 (scale bar is included on image) under reflected light using an oil immersion lens.
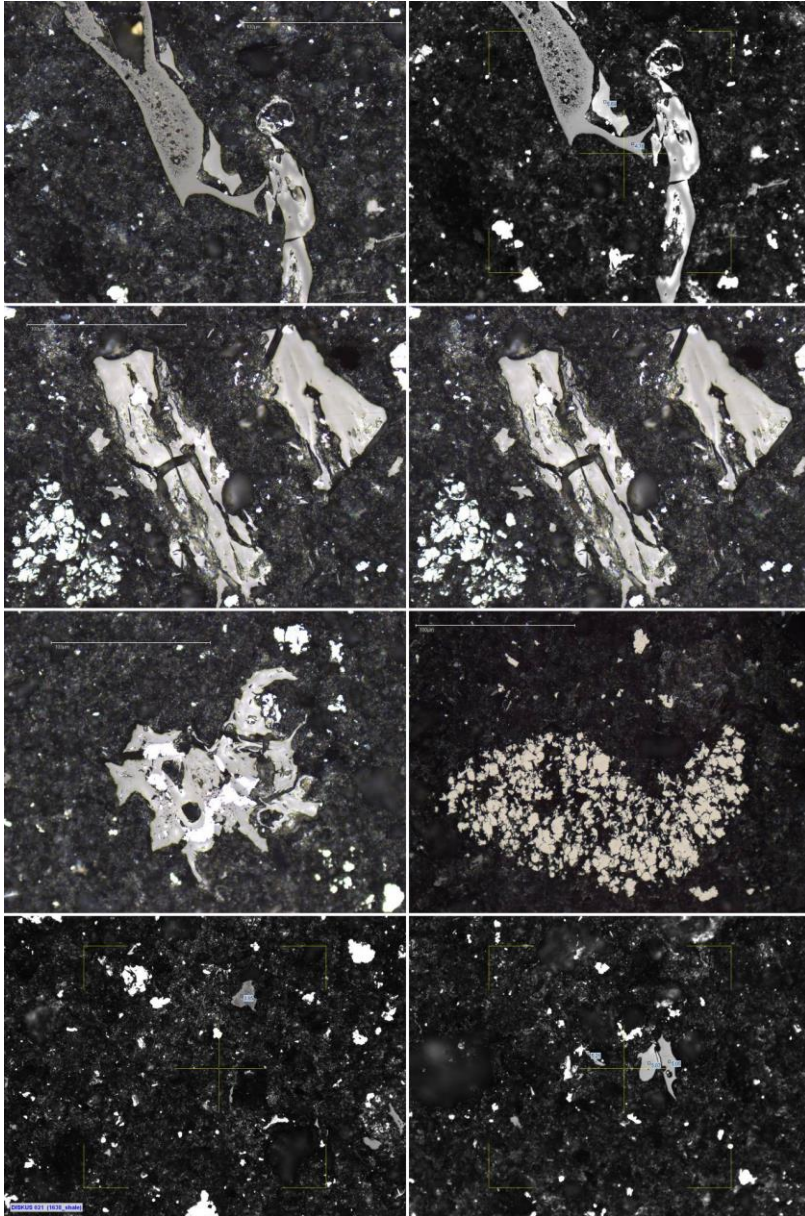

Plate 1: Sample 1638 (389.3) Whitehill black shale. Type and distribution of organic matter, some being large pieces, as well as extensive pyrite (very bright components). Some images include the actual reflectance data; top L colour image; top R B&W image with reflectance values. Scale bar = 100 microns.
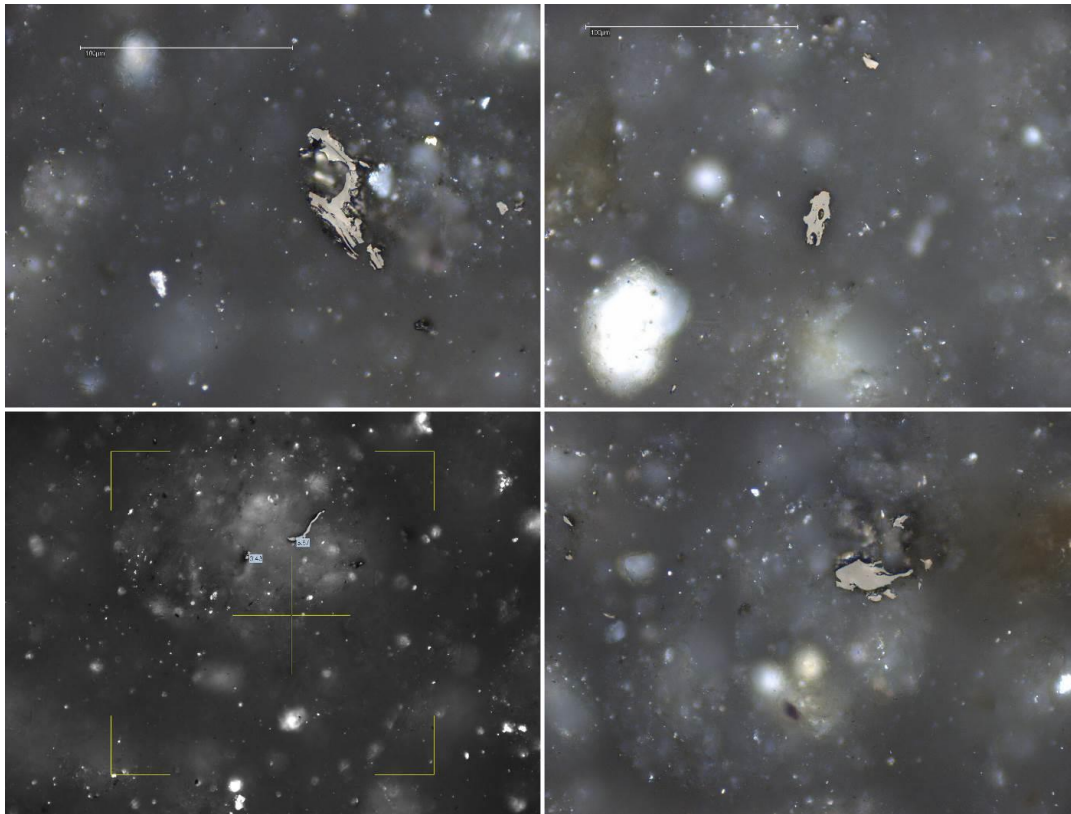
Plate 2: Sample 1639 (1124.5) Volksrust siltstone. Limited organic matter determined; no structure visible. Scale bar = 100 microns.
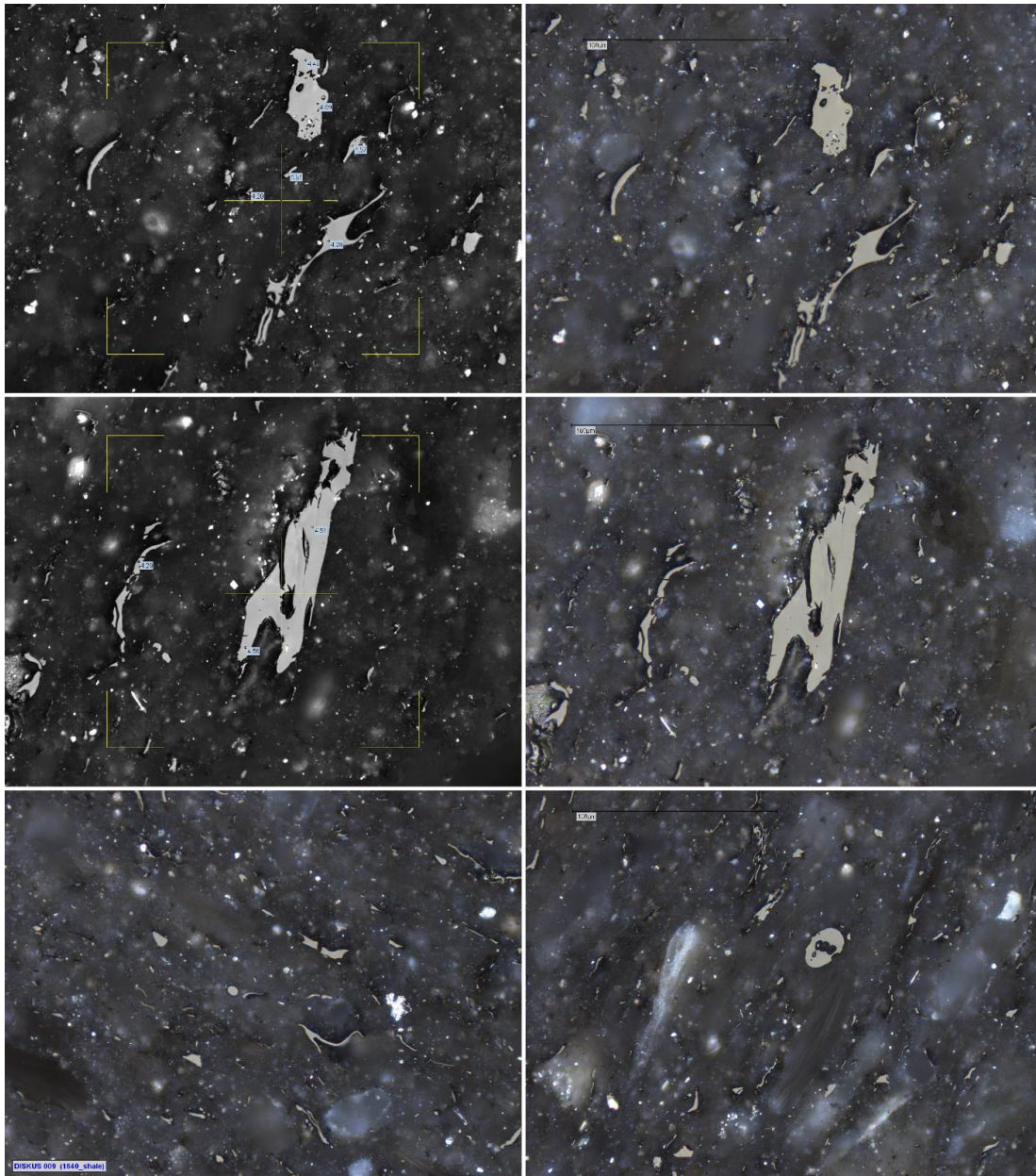
Plate 3: Sample 1640 (4794.1) Prince Albert shale. Type and distribution of organic matter, some being fairly large pieces; limited pyrite. Structure/orientation is apparent. Some images include the actual reflectance data; top L B&W image with reflectance values; top R colour image. Scale bar = 100 microns.
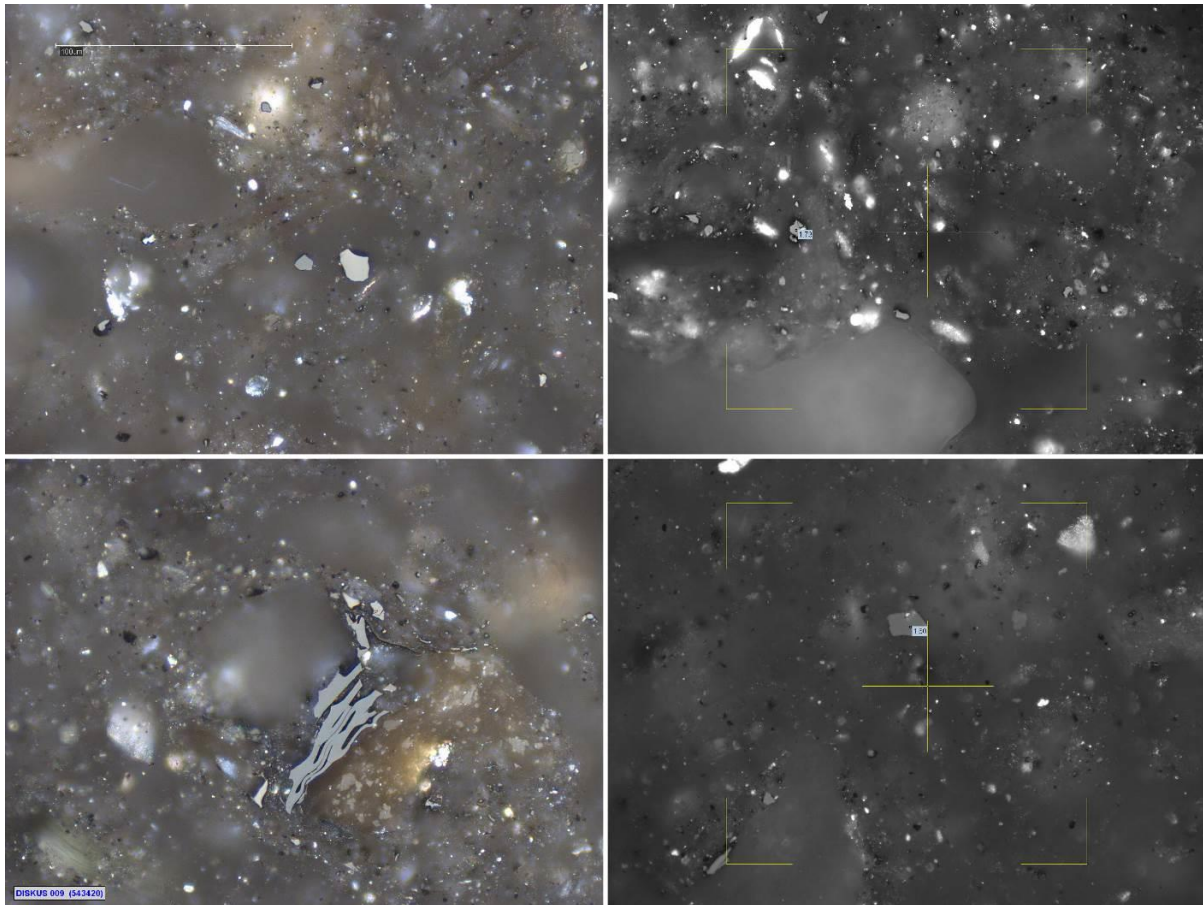
Plate 4: Sample 1641 (5434.2) Pietermaritzburg fine-grained sandstone. Type and distribution of organic matter, most particles being very small. Some images include the actual reflectance data; e.g. top and bottom R. Two populations determined — note difference in shade of grey of particles in top L image. Scale bar = 100 microns.
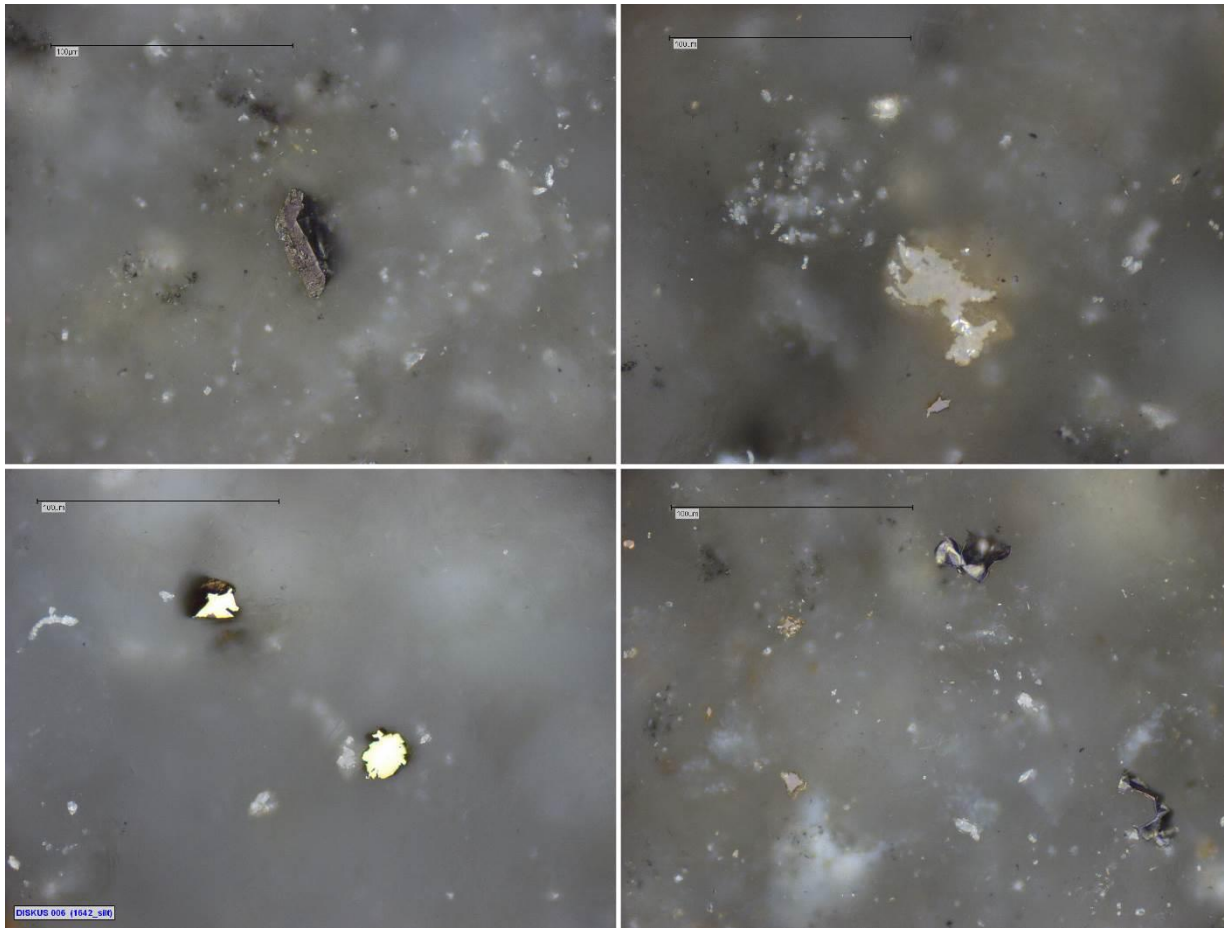
Plate 5: Sample 1642 (5560) Pietermaritzburg siltstone. No organic matter determined; no structure visible. Images show various mineral inclusions. Scale bar = 100 microns.
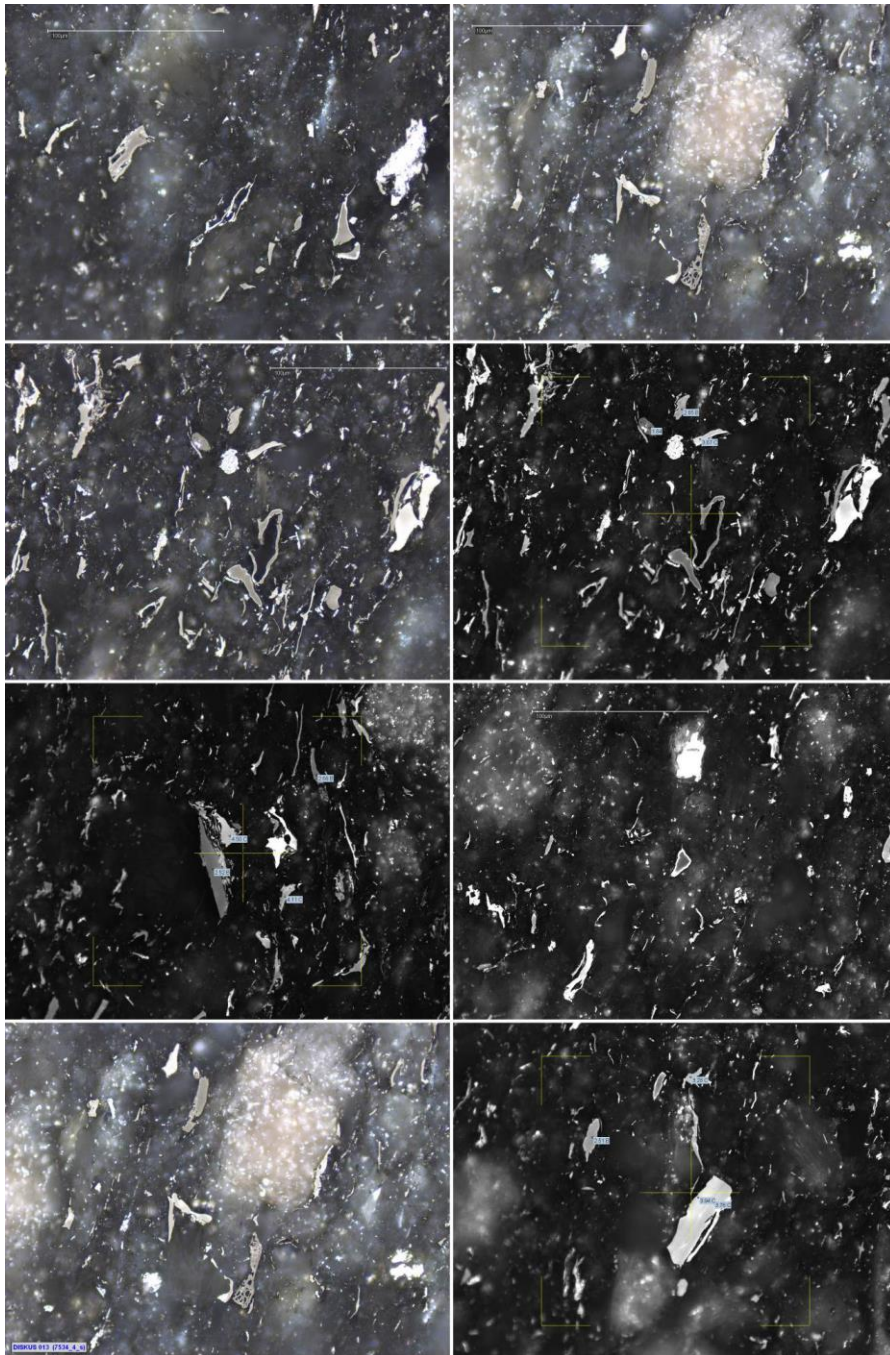
Plate 6: Sample 1643 (7534.03) Pietermaritzburg silty shale. Type and distribution of organic matter, many particles possibly being degraded vitrinite, visible with zonation around particle. Very wide range of reflectance values. Scale bar = 100 microns.